

# First M87 Event Horizon Telescope Results: The Shadow of the Supermassive Black Hole

Yosuke Mizuno

Institute for Theoretical Physics  
Goethe University Frankfurt

on behalf of Event Horizon Telescope collaboration

# First Image of a Black Hole





(News paper)

Cover page all over  
the world!



## Event Horizon Telescope



Event  
Horizon  
Telescope

# The Black Hole Shadow in M 87

## Cover Pages



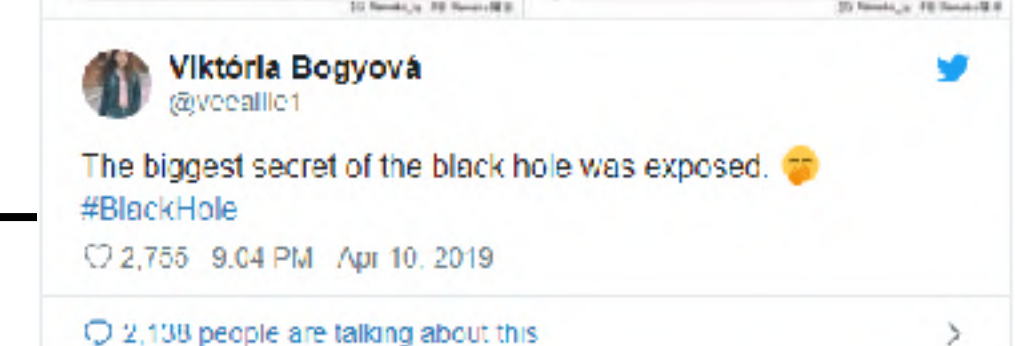
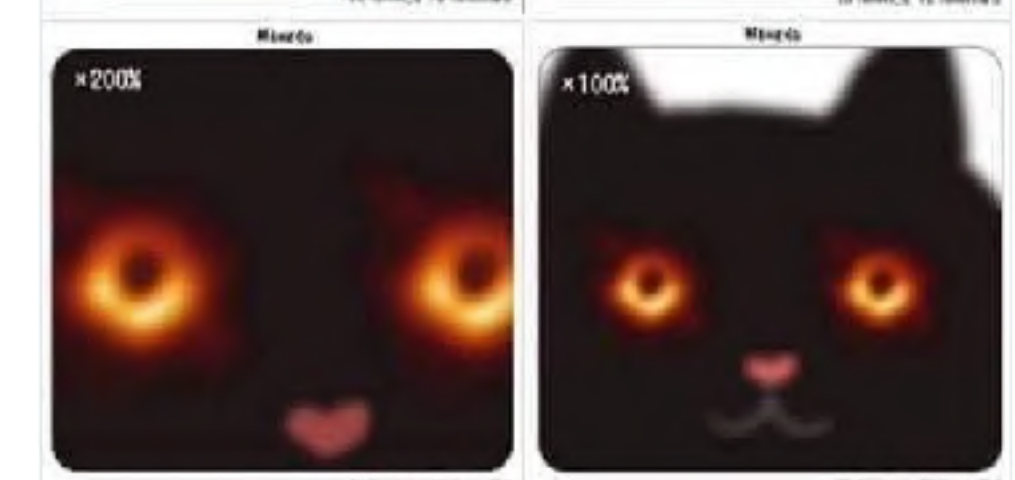
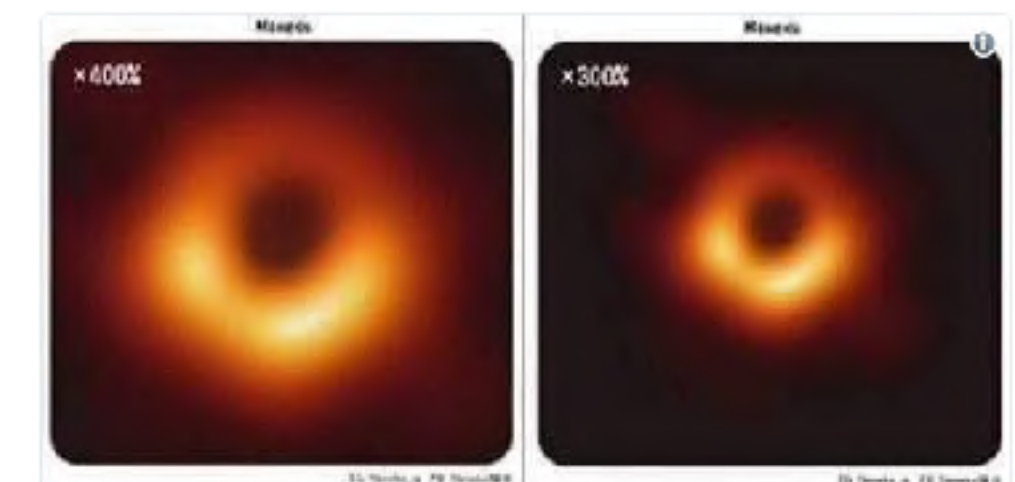
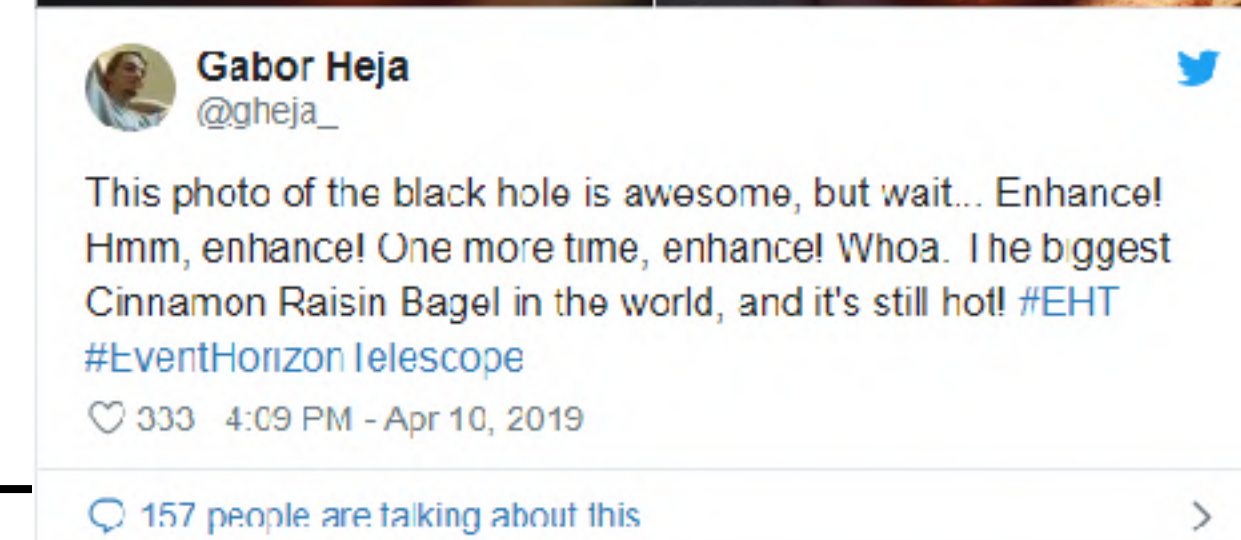
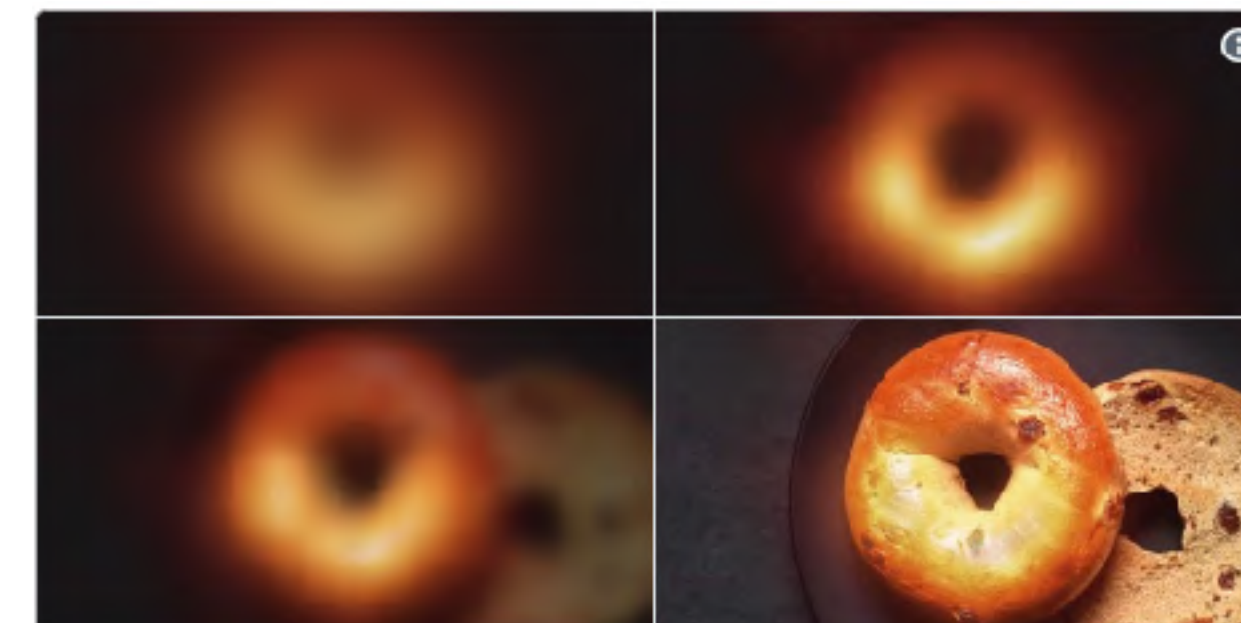


# Social Media Reaction (Twitter)

hashtag of EHT is 1st of trends



ME AFTER BUYING  
THE IPHONE XS





# The First M87 EHT Results: Six ApJ Letters

---

17P Paper I: The Shadow of the Supermassive Black Hole (Summary Paper)

Coordinators: G. Bower, H. Falcke & D. Psaltis

28P Paper II: Array and Instrumentation (Instrumentation Paper)

Coordinators: S. Doeleman, V. Fish & R. Tilanus

32P Paper III: Data Processing and Calibration (Calibration Paper)

Coordinators: L. Blackburn, S. Issaoun & M. Wielgus

52P Paper IV: Imaging of the Central Black Hole in M87 (Imaging Paper)

Coordinators: [K. Akiyama](#), K. Bouman, A. Chael, J. Gomez & M. Johnson

31P Paper V: Physical Origin of the Asymmetric Ring (Theory Paper)

Coordinators: C. Gammie, [Y. Mizuno](#), H.-Y. Pu

44P Paper VI: The Shadow and Mass of the Central Black Hole (Modeling Paper)

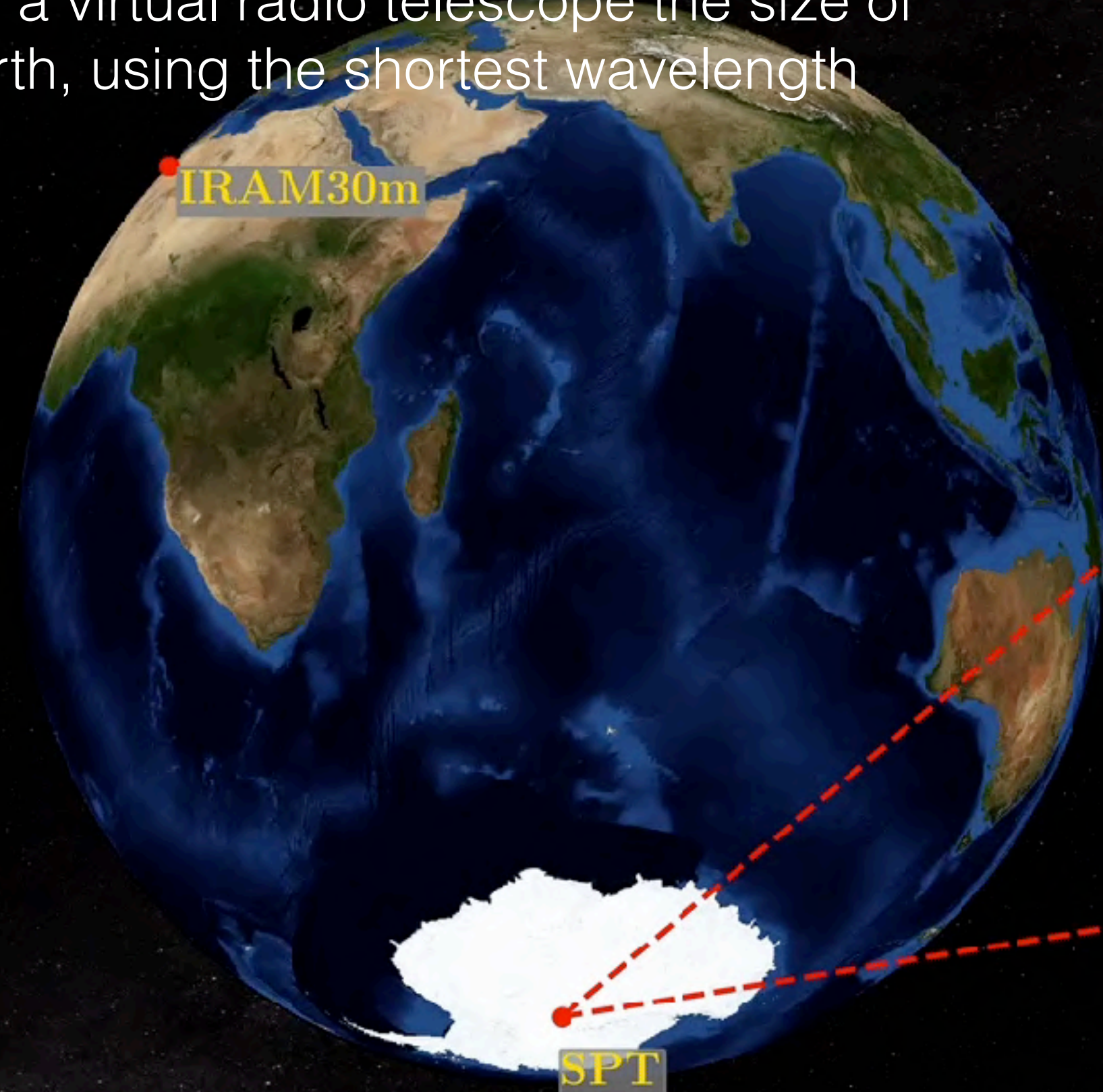
Coordinators: [K. Asada](#), A. Broderick, J. Dexter, F. Ozel





# Event Horizon Telescope Collaboration

Create a virtual radio telescope the size of the earth, using the shortest wavelength



South Pole Telescope (SPT)



Country : Antarctica

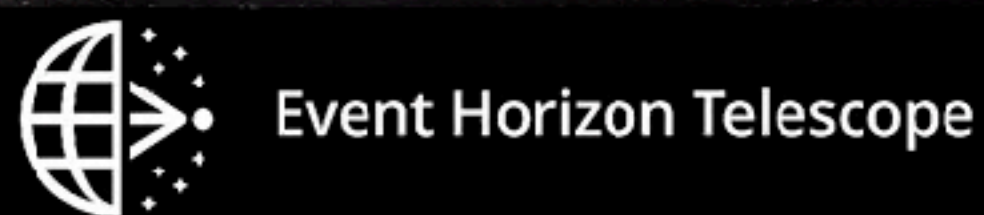
Coordinates : 90°S 0°E

Diameter of telescope : 10 m

$\lambda = 1.3 \text{ mm}$  ( $\nu = 230 \text{ GHz}$ )

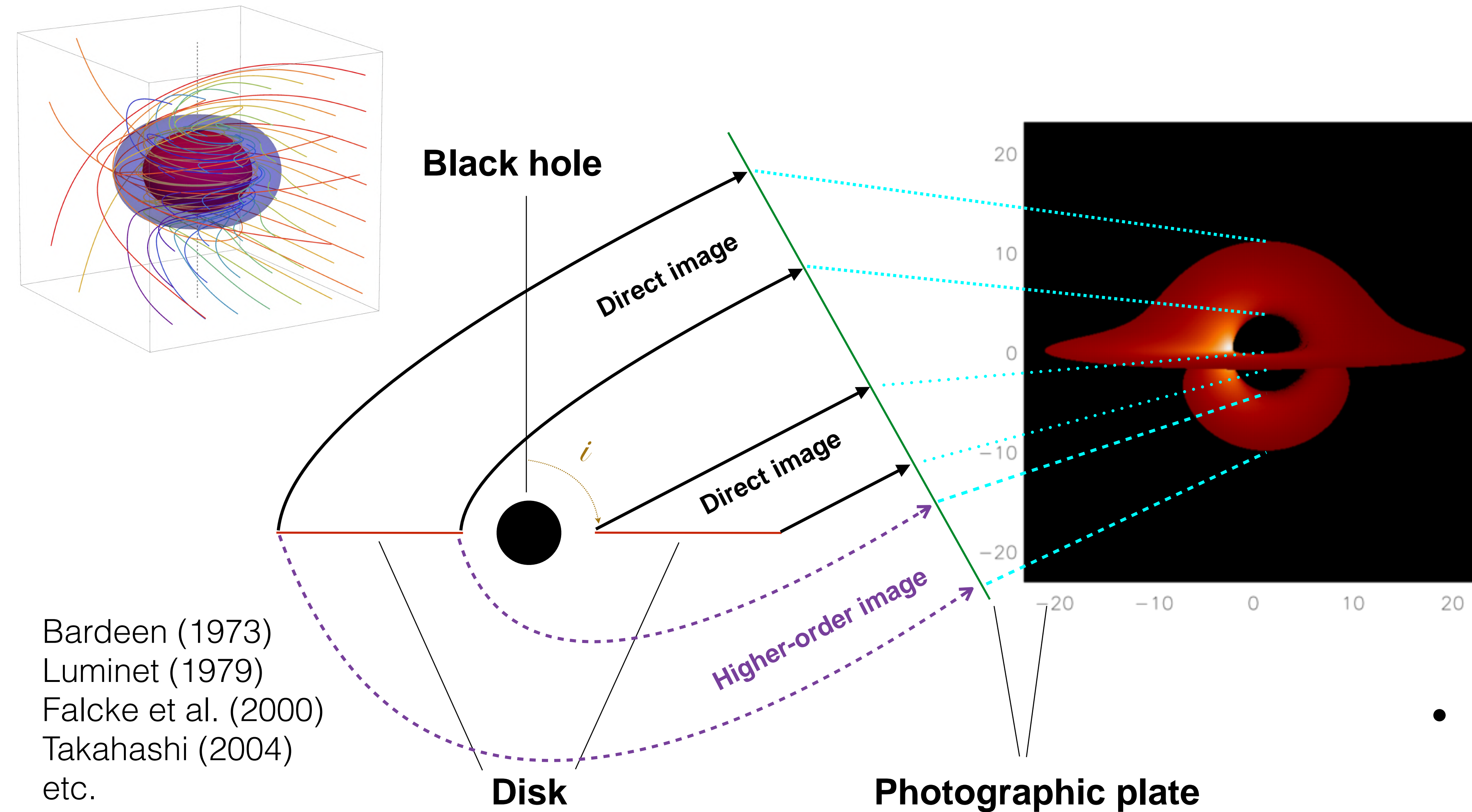
$D \sim 10,000 \text{ km} \Rightarrow \lambda/D \sim 25 \text{ } \mu\text{as}$

© C. M. Fromm & L. Rezzolla





# Strong GR: Black Hole Shadow



Shadow diameter:

Non-spinning ( $a=0$ )

$$D_{\text{sh}} \sim 5.2 * R_g$$

Spinning ( $a=1$ )

$$D_{\text{sh}} \sim 4.8 * R_g$$

Bardeen (1973)  
Luminet (1979)  
Falcke et al. (2000)  
Takahashi (2004)  
etc.

- Shadow size and shape encodes GR (e.g., Johannsen & Psaltis 2010)



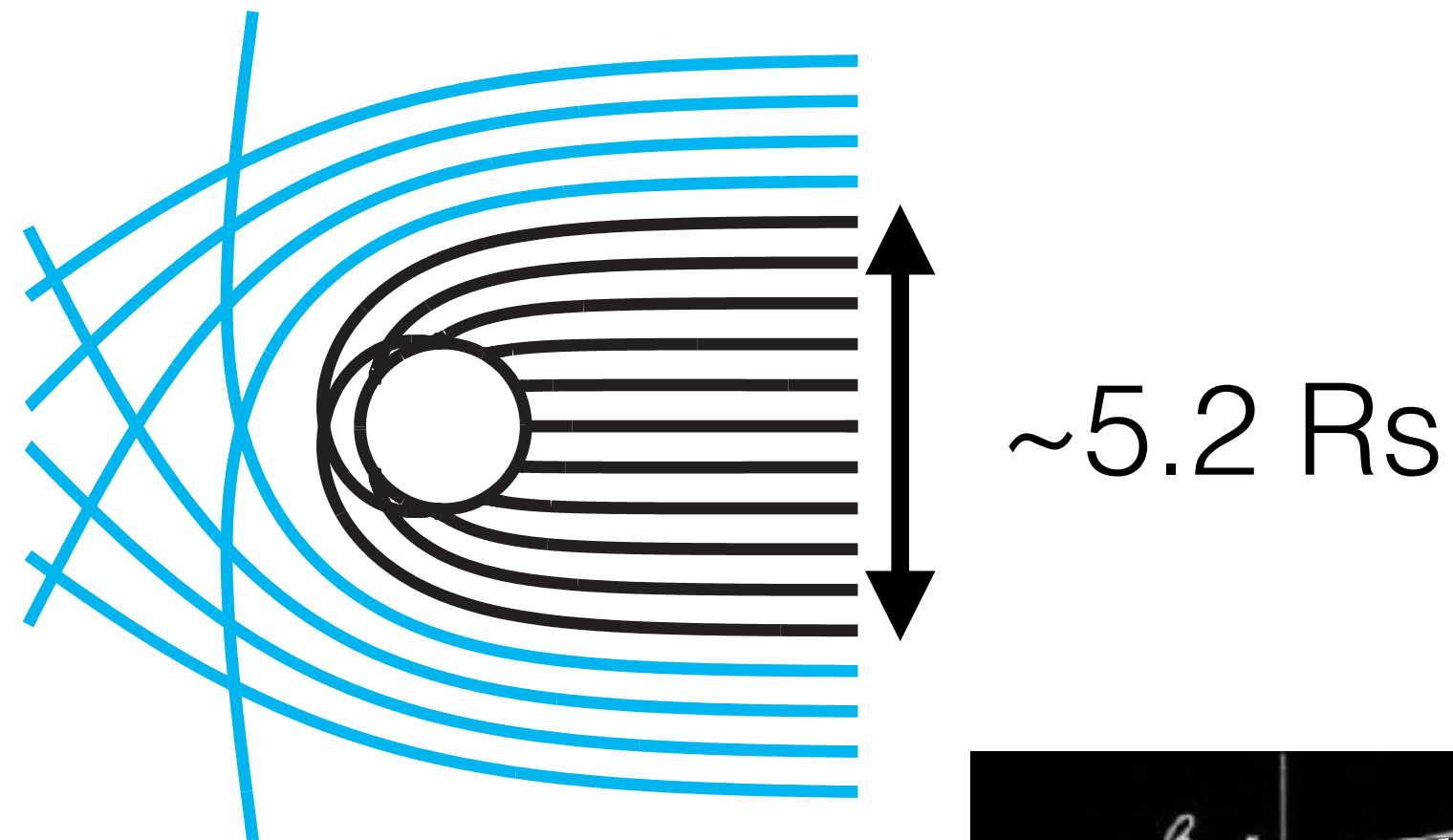
Event Horizon Telescope



# The Shadow of a Black Hole

Non-spinning Black Hole

*top view*



Maximumly Rotating Black Hole

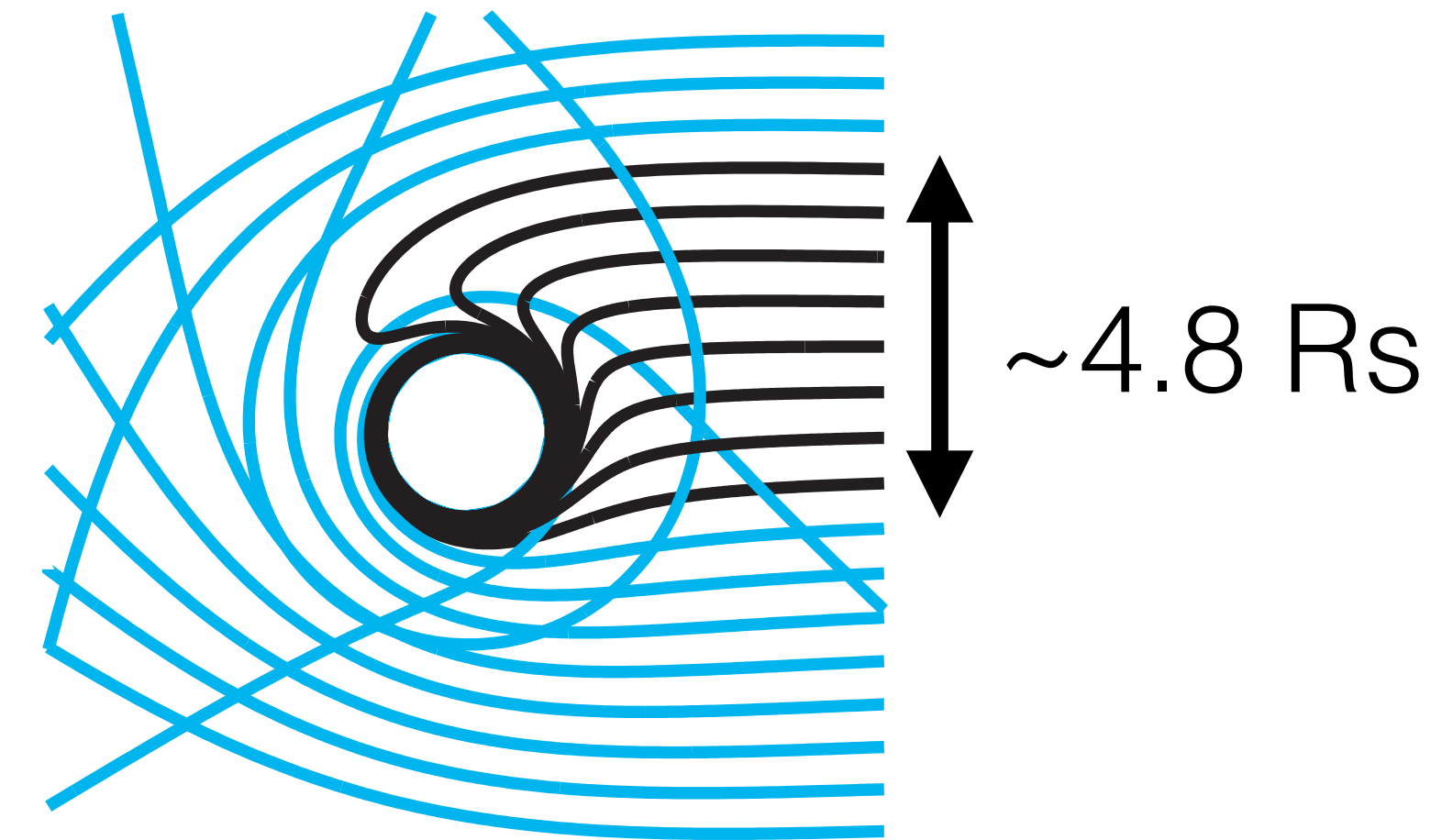
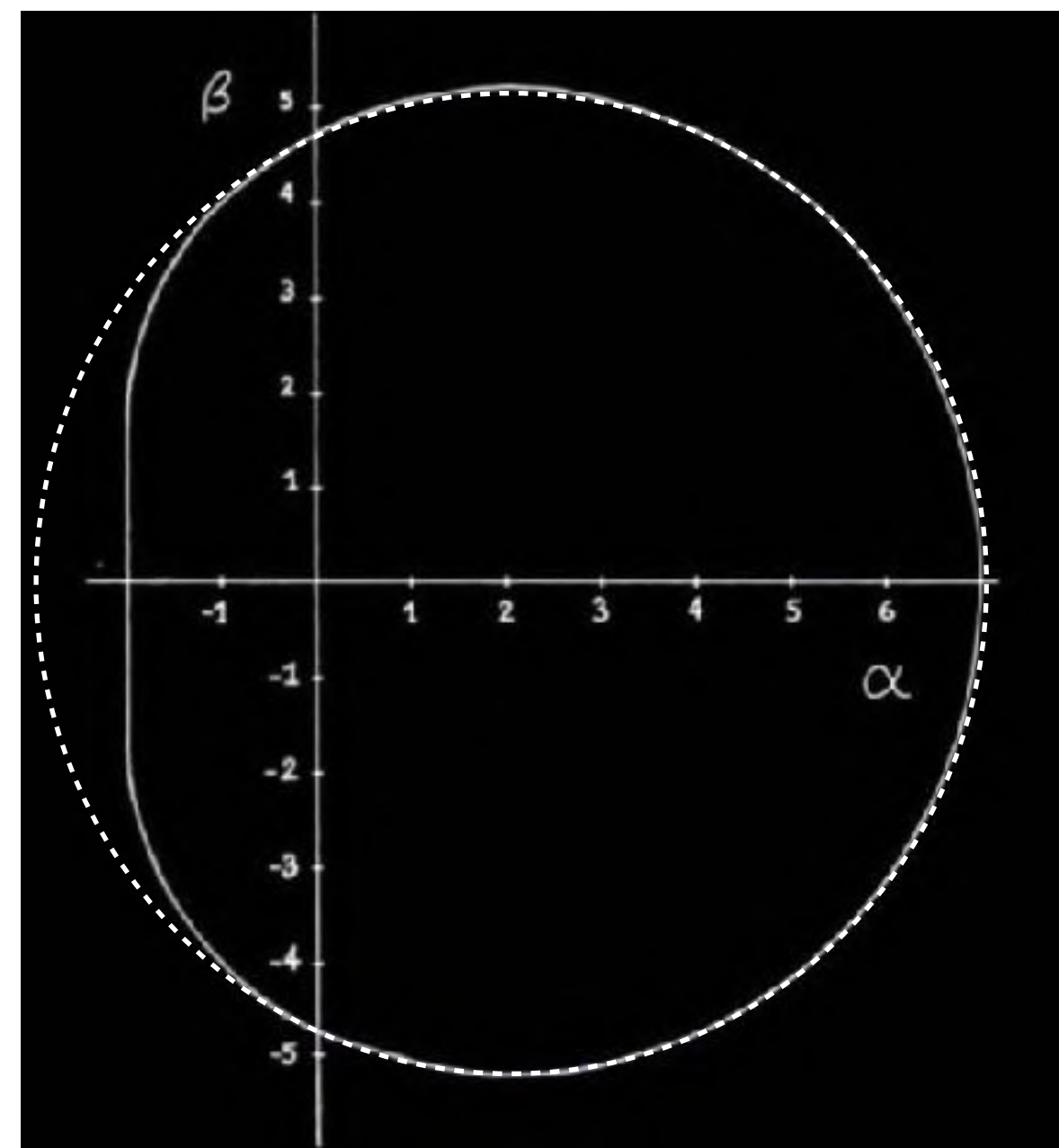


(Figure credit: Hung-Yi Pu )



$i=90$  deg

Black Holes cast shadows

(Bardeen 1973; Falcke et al. 2000)

with a radius that changes

only by 4% with the spin

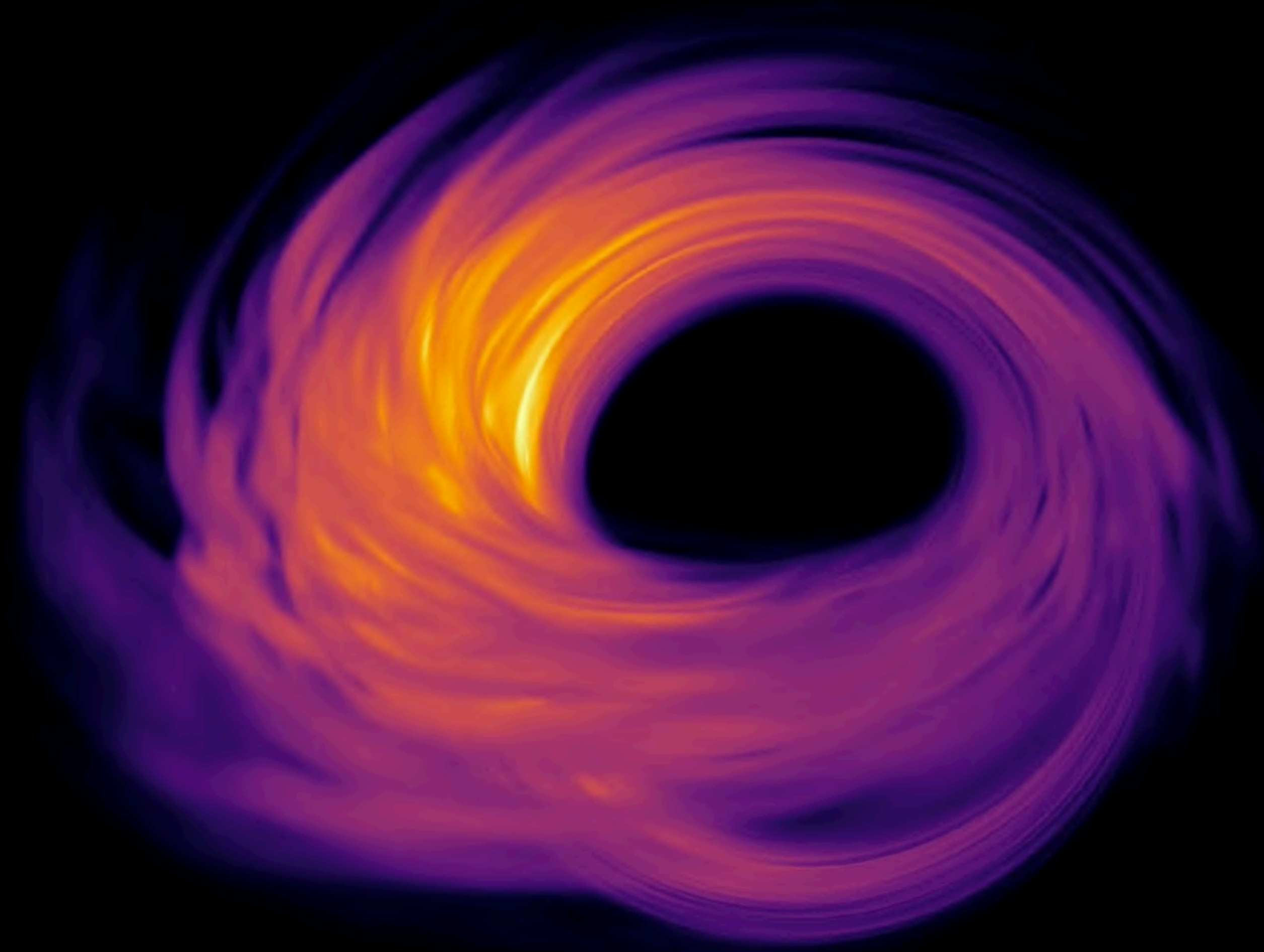
(Johannsen & Psaltis 2010)



Event Horizon Telescope



# *Shadow of Black Hole*



Snapshot image of GRMHD simulation  
of Kerr BH with  $a=0.94$

Changing viewing angle (theta & phi)

Movie: Z. Younsi



# Black Holes with the Largest Angular Sizes

| Source | BH Mass<br>( $M_{\text{solar}}$ )                                  | Distance<br>(Mpc) | 1 $R_s$<br>( $\mu\text{as}$ ) |
|--------|--|-------------------|-------------------------------|
| Sgr A* | $4 \times 10^6$  | 0,008             | 10                            |
| M87    | <del><math>3.3 - 6.2 \times 10^9</math></del><br>$6.5 \times 10^9$ | 16,8              | <del>3.6 - 7.3</del><br>7.6   |
| M104   | $1 \times 10^9$  | 10                | 2                             |
| Cen A  | $5 \times 10^7$  | 4                 | 0,25                          |





# Event Horizon Telescope 2017

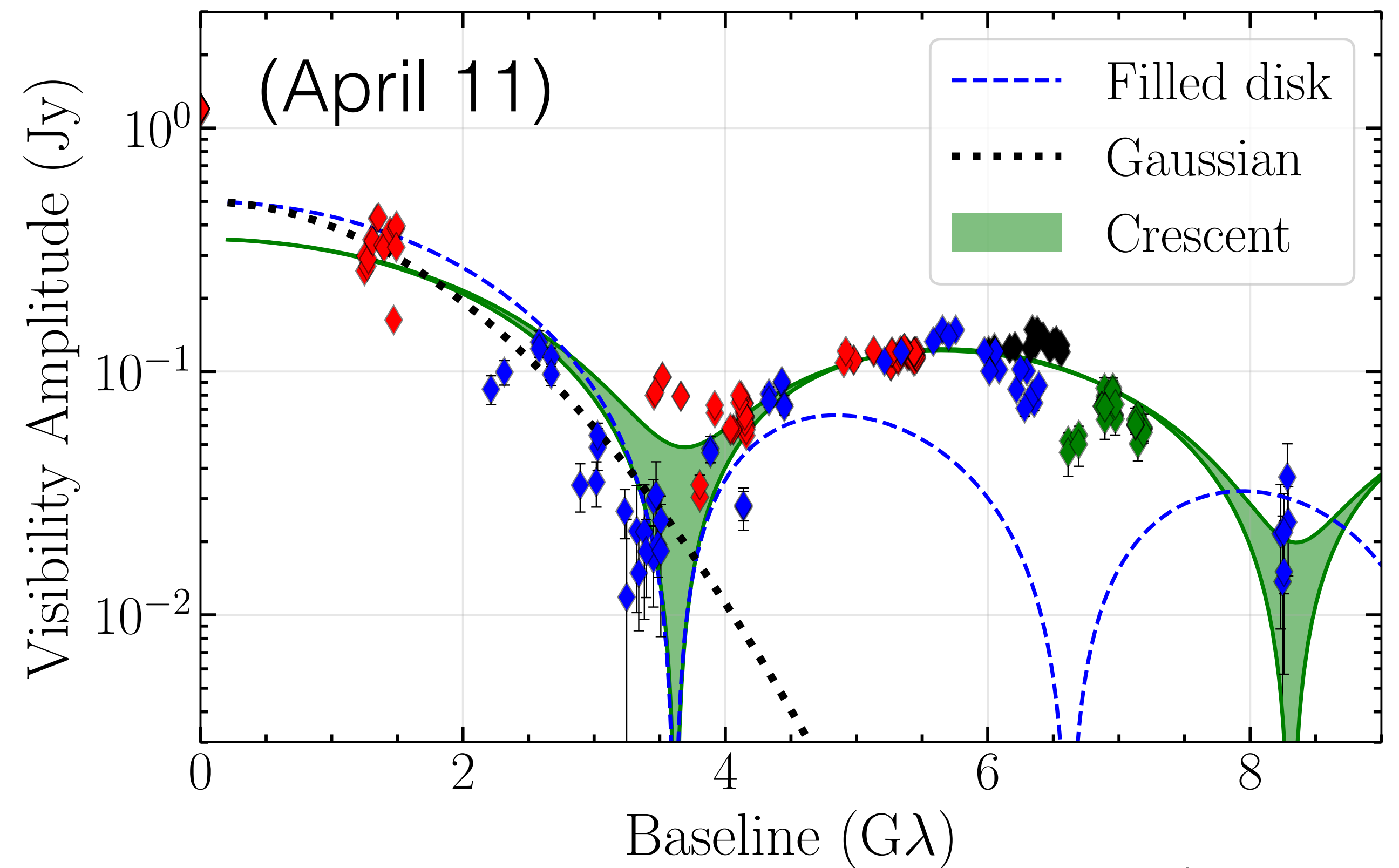
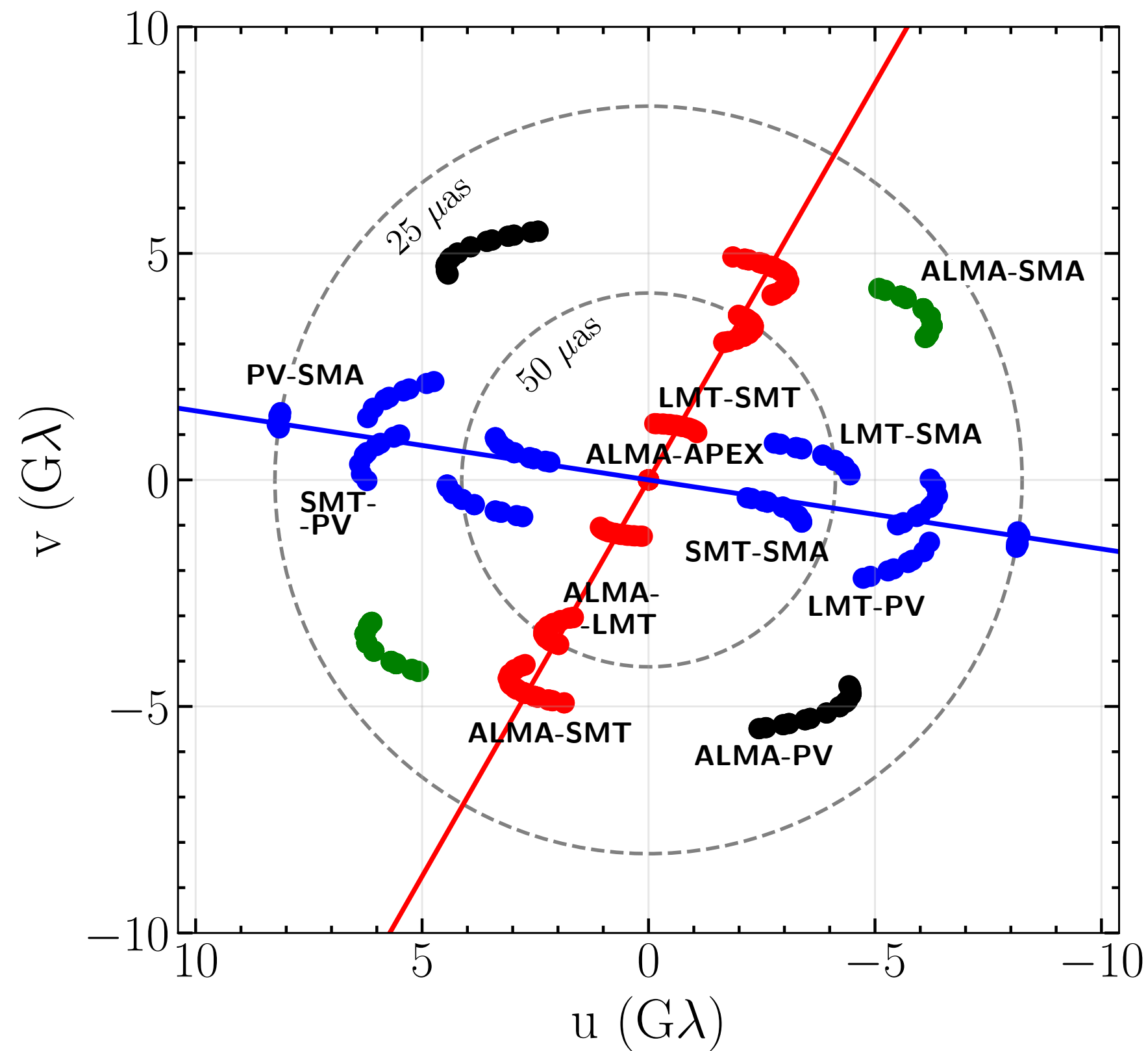




# Calibrated data sets (before imaging)

EHT 2017 M87 data look consistent with an asymmetric ring (“crescent”)

Fourier domain



(Paper VI)





# Fantastic Four: Black Hole Image Hunters

## Team 1

### Americas

US & Chile

(SAO, U. Arizona, U. Concepcion)

Leader: K. Bouman & A. Chael

new method

(regularised max likelihood)

## Team 2

### Global

US, Japan, Netherland

(MIT, NAOJ, Hiroshima U., Radboud U.)

Leader: K. Akiyama & S. Issaoun

## Team 4

### East Asians

Korea, Japan & Taiwan

(ASIAA, KASI, NAOJ)

Leader: S. Koyama

traditional method

(CLEAN + self-cal)

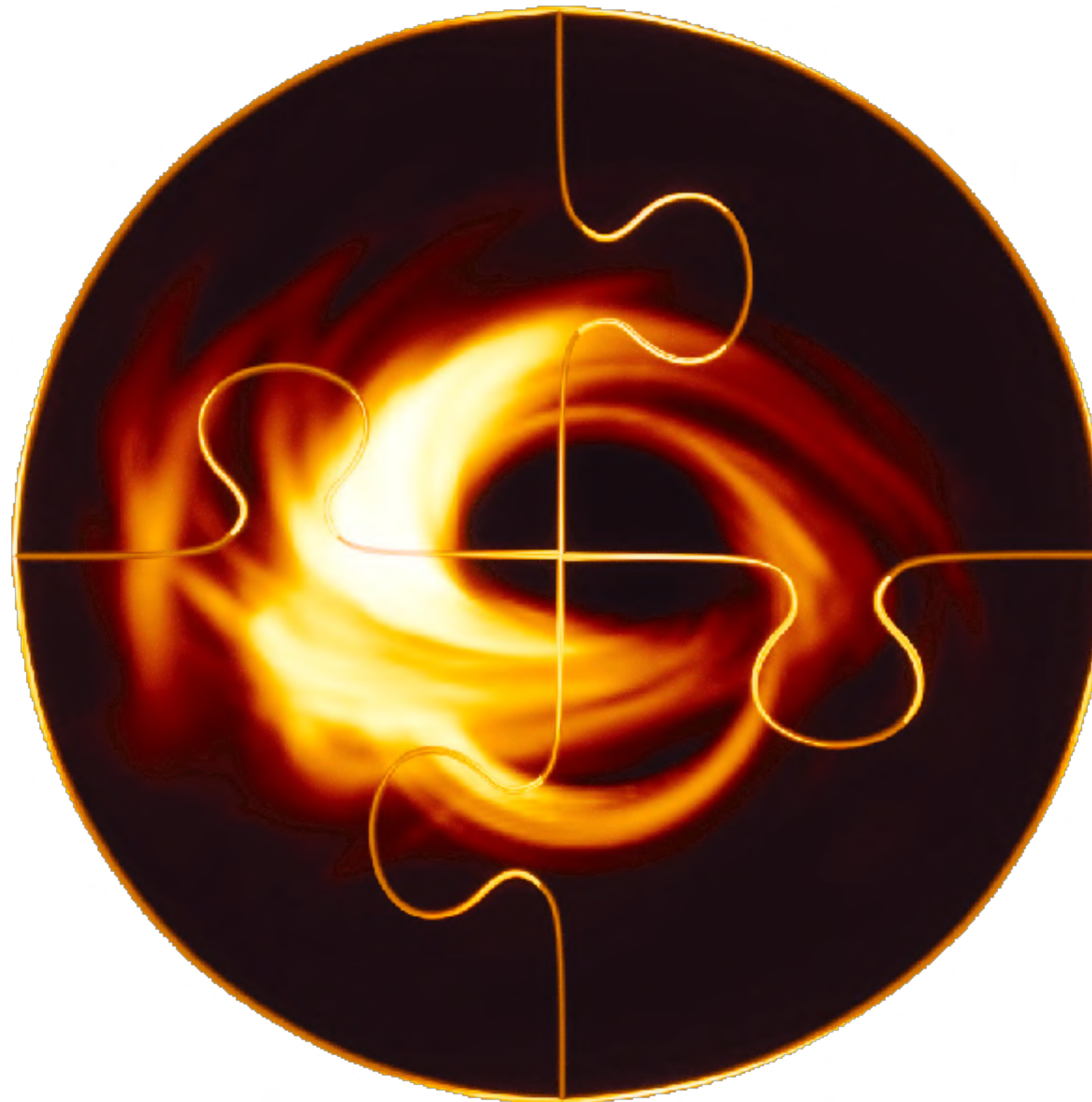
## Team 3

### Cross Atlantic

US, Spain, Germany, Finland

(Boston U, MPIfR, IAA, Aalto, GU)

Leader: A. Marscher



Event Horizon Telescope



# Fantastic Four: Black Hole Image Hunters

## Team 1

### Americas

US & Chile

(SAO, U. Arizona, U. Concepcion)

Leader: K. Bouman & A. Chael

new method

(regularised max likelihood)

## Team 2

### Global

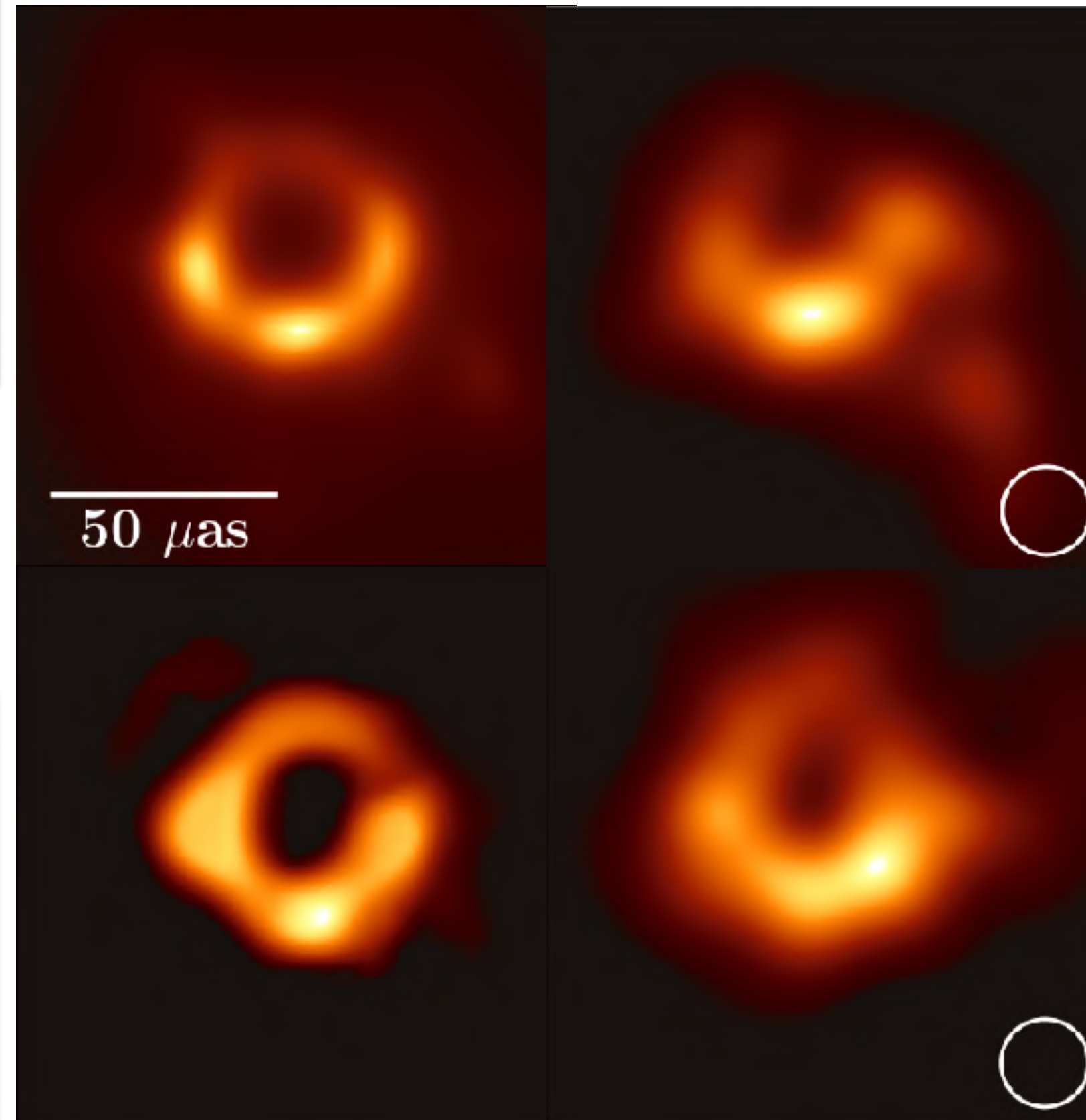
US, Japan, Netherland

(MIT, [NAOJ](#), [Hiroshima U.](#), Radboud U.)

Leader: [K. Akiyama](#) & S. Issaoun

## The First EHT Images of M87

July 24, 2018



## Team 4

### East Asians

Korea, Japan & Taiwan

([ASIAA](#), KASI, [NAOJ](#))

Leader: [S. Koyama](#)

traditional method

(CLEAN + self-cal)

## Team 3

### Cross Atlantic

US, Spain, Germany, Finland

(Boston U, MPIfR, IAA, Aalto, [GU](#))

Leader: A. Marscher

Each team blindly reconstructed images

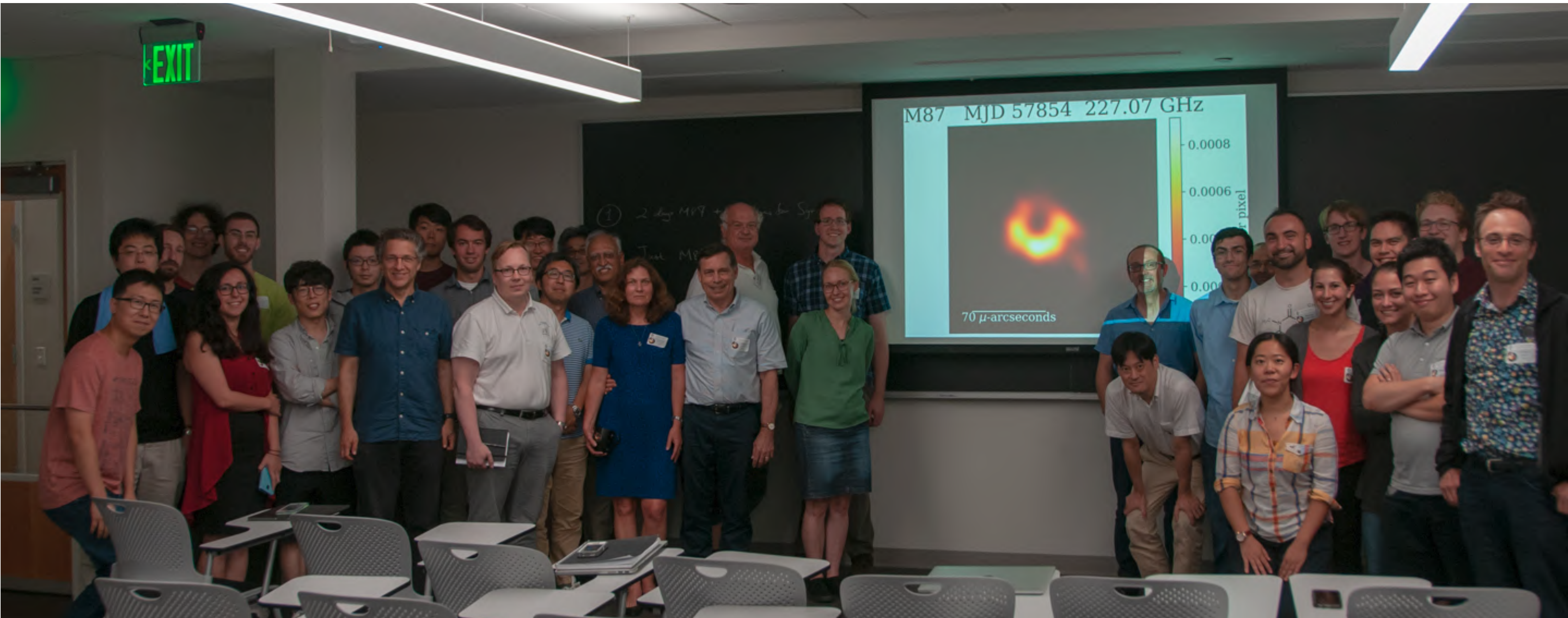
Goal: Assess human bias



Event Horizon Telescope

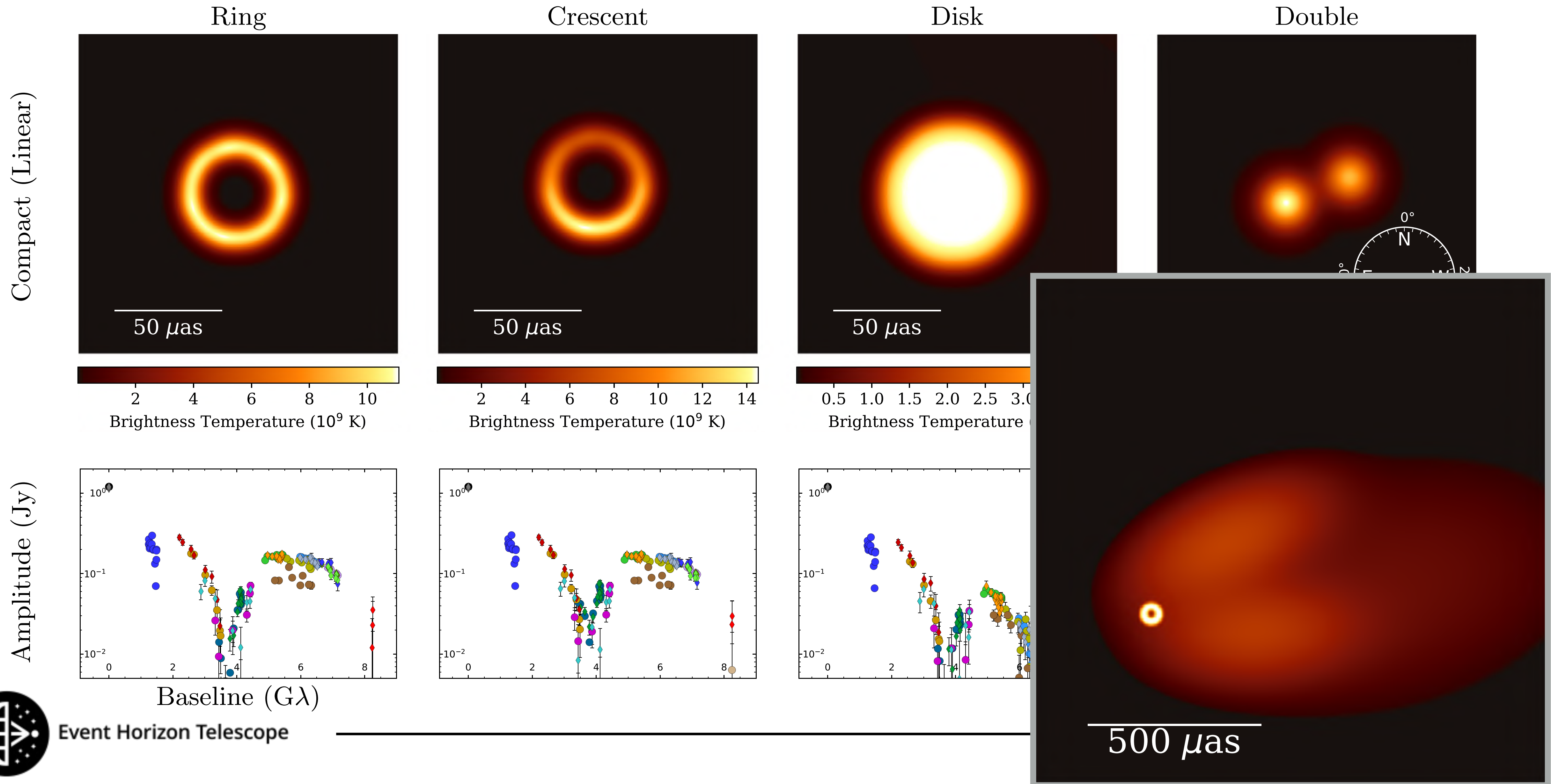


# The First EHT Images of M87 (July 24, 2018)



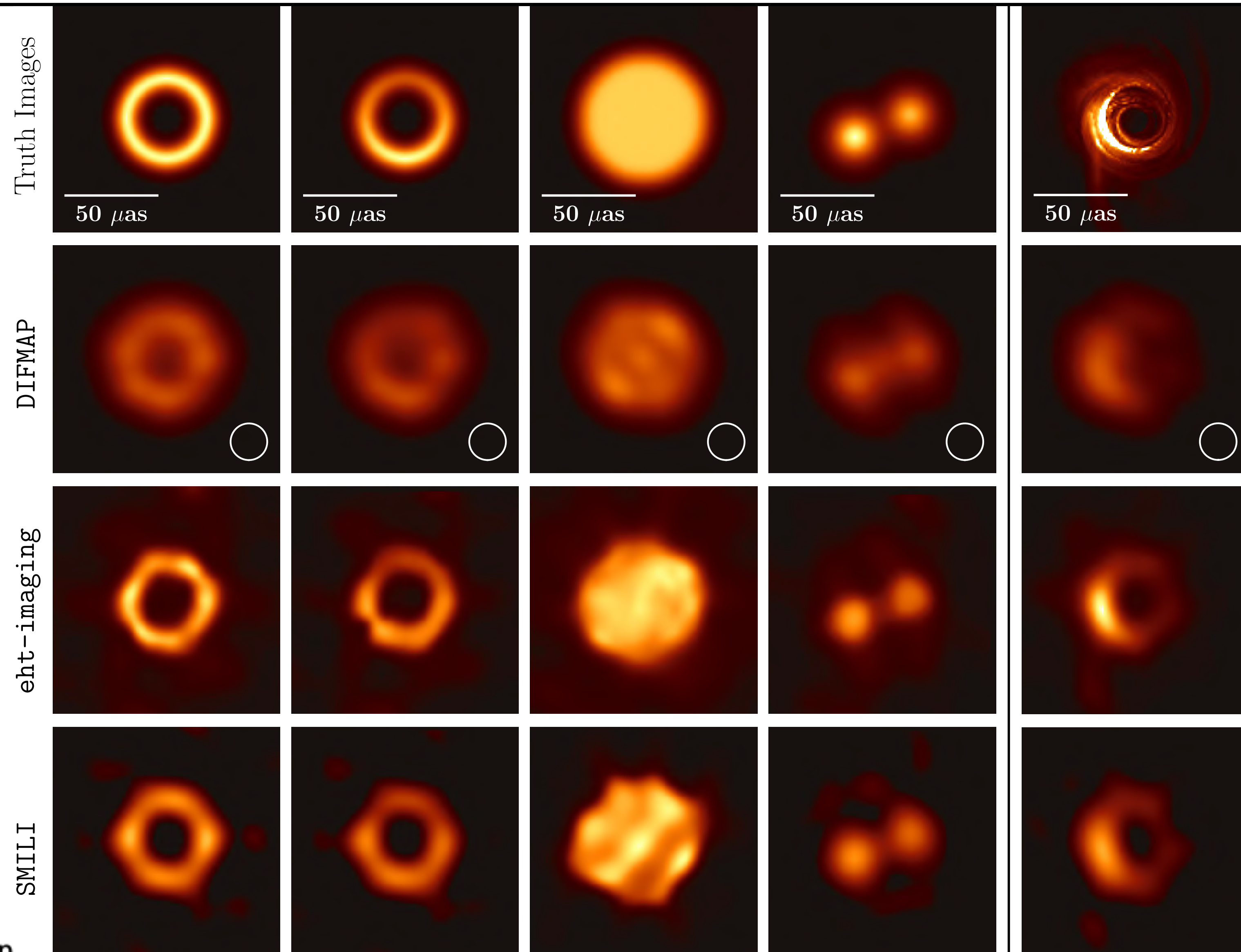


# Models with Different Morphologies but Similar Visibility Amplitudes





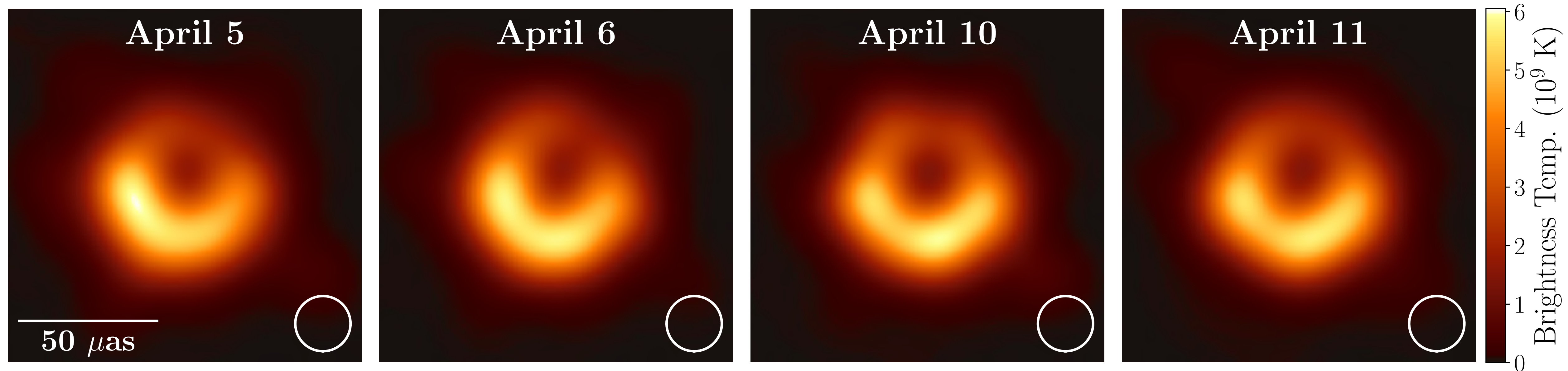
# Fiducial Synthetic Data Images





# Averaged Images

EHT 2017 M87 reconstructed averaged images look like asymmetric rings



No significant changes are observed during the 6-day span of the 2017 EHT campaign



# Theoretical Modeling Pipeline

---

What ingredients do we need for realistic theoretical model of BH Shadow?

1. Plasma dynamics (accretion flow & jet) around the black hole
2. Radiation process
3. BH Spacetime
4. VLBI array configuration and schedule (for EHT 2017 observation)

*computational infrastructure*

GRMHD **simulations** in arbitrary spacetimes (**BHAC**)  $\Rightarrow$  ray-traced, deconvolved **images** (**BHOSS**)  $\Rightarrow$  comparison with **observations** (**GENA**)



# What about the parameter space?

## GRMHD

- Black Hole spin  $-1 < a^* < 1$
- Accretion type (SANE or MAD depends on magnetic flux)

*Simulation Library*  
**>15 GRMHD runs**

**SANE**: Standard and Normal Evolution  
**MAD**: Magnetically Arrested Disk

4 GRMHD codes (**BHAC**, iham, KORAL, H-AMR)

## GRRT

- Black Hole mass
- Accretion rate
- Radiation microphysics (thermal synchrotron, eDF: R-beta model)
- Orientation towards the observer (inclination and jet position angle)

3 GRRT codes (**BHOSS**, ipole, Raptor)

*Image Library*  
**>60,000 images**

$$\frac{T_i}{T_e} = R_{\text{high}} \frac{\beta_p^2}{1 + \beta_p^2} + \frac{1}{1 + \beta_p^2}$$

Electrons colder at high plasma beta (disk), warmer at low plasma beta (jet)

## Prior knowledge from observations

- BH mass: 6.2e9 or 3.5e9 Msun
- Inclination angle: 17 or 163 deg with jet position angle 288 deg

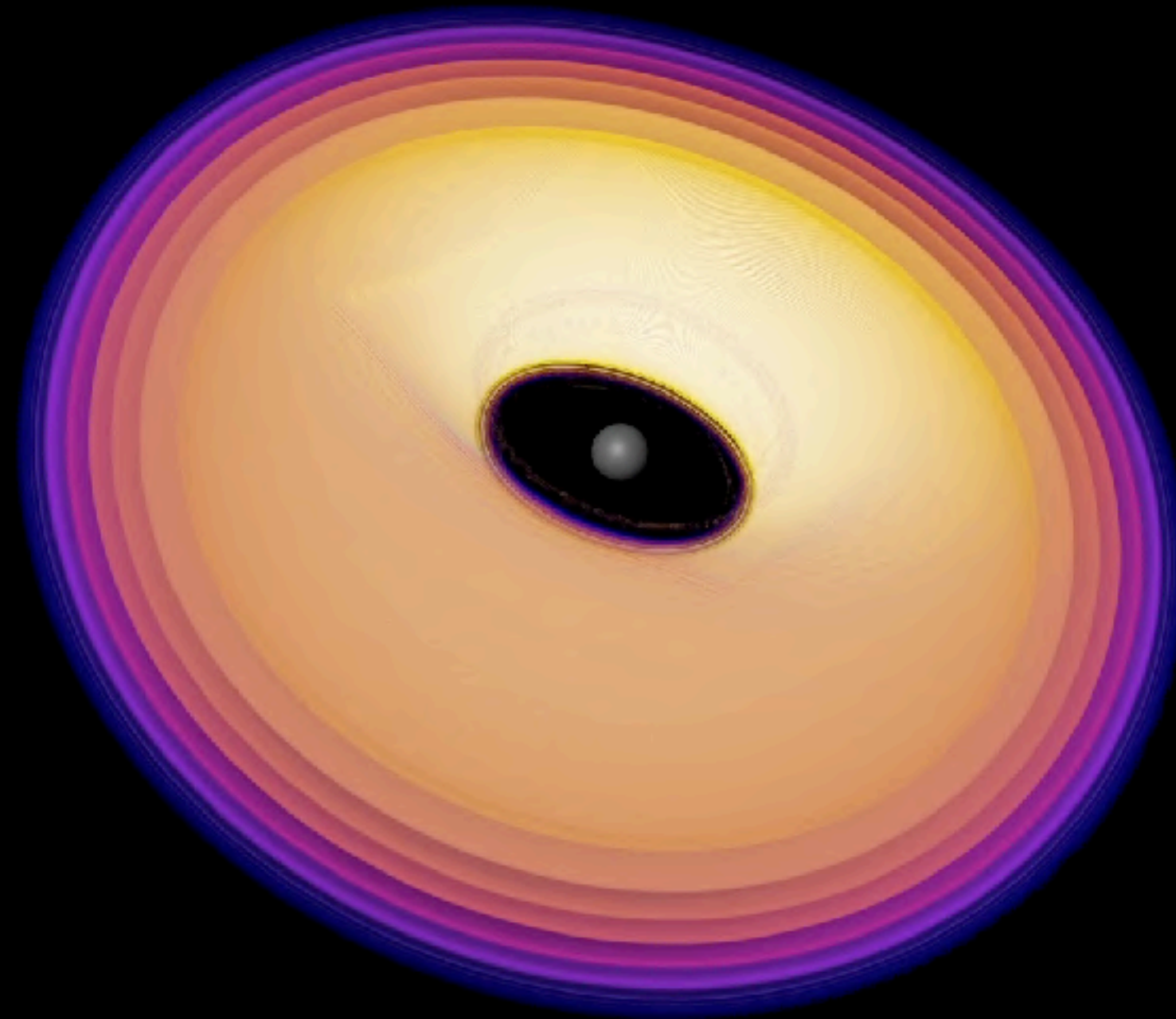




# GRMHD Simulations

- Model the accretion flow (RIAF) onto a black hole
- Torus in hydrodynamical equilibrium with poloidal B-field
- Monitor accretion rate and evolve until quasi-steady state

Kerr black hole with  $a=0.94$ ,  
SANE model



Credit: L.Weih, L. Rezzolla,  
Frankfurt BHCam team

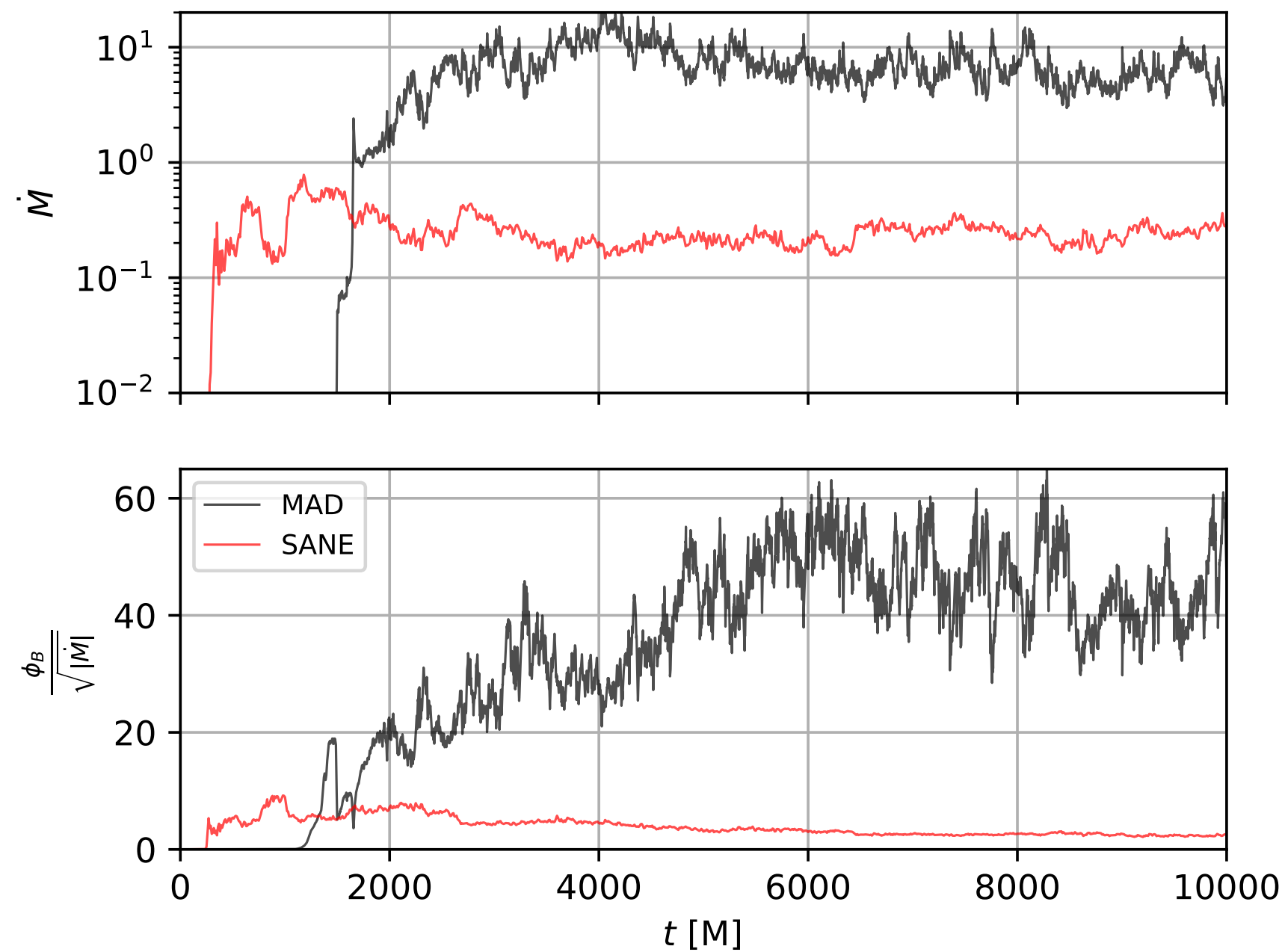


# MAD vs SANE (GRMHD Simulations)

RIAF model, two extreme situation

3D GRMHD simulations  
with  $a=0.94$

Kerr BH  $a=0.9375$

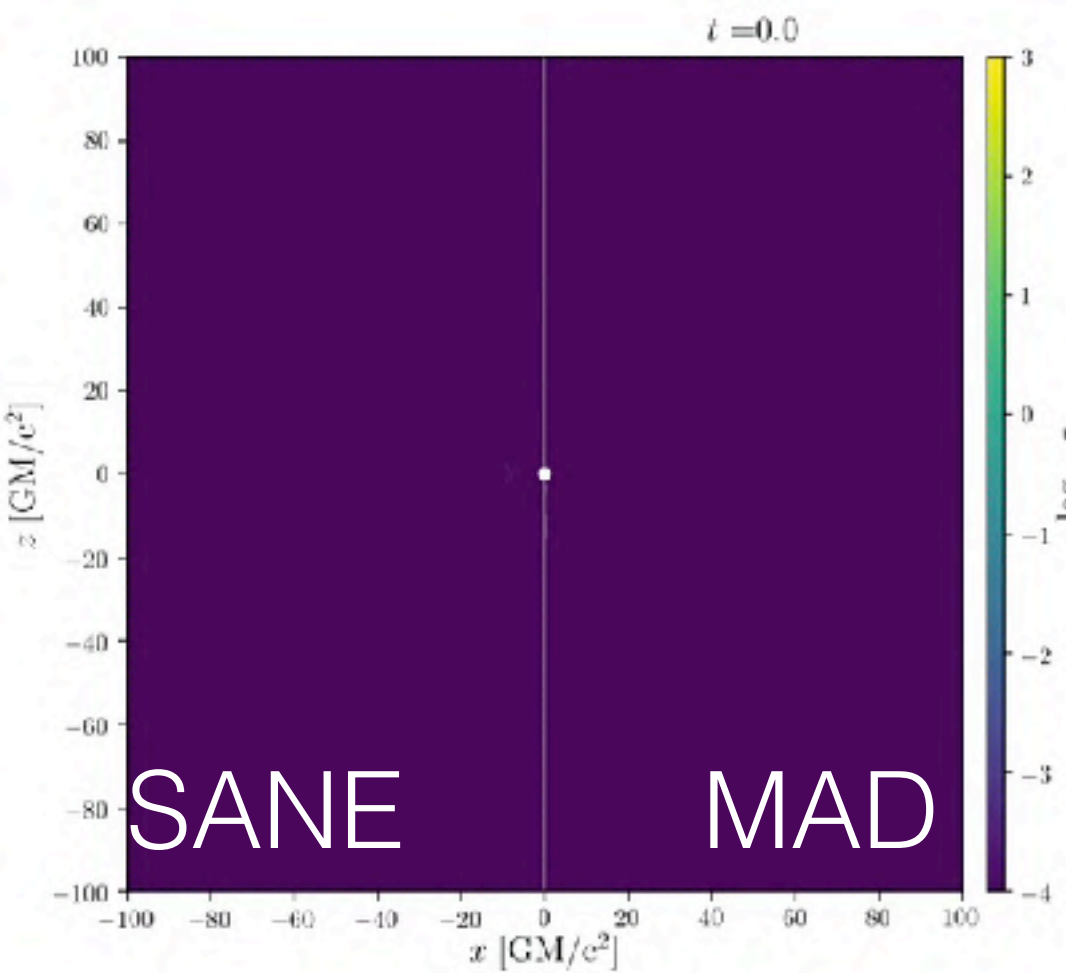
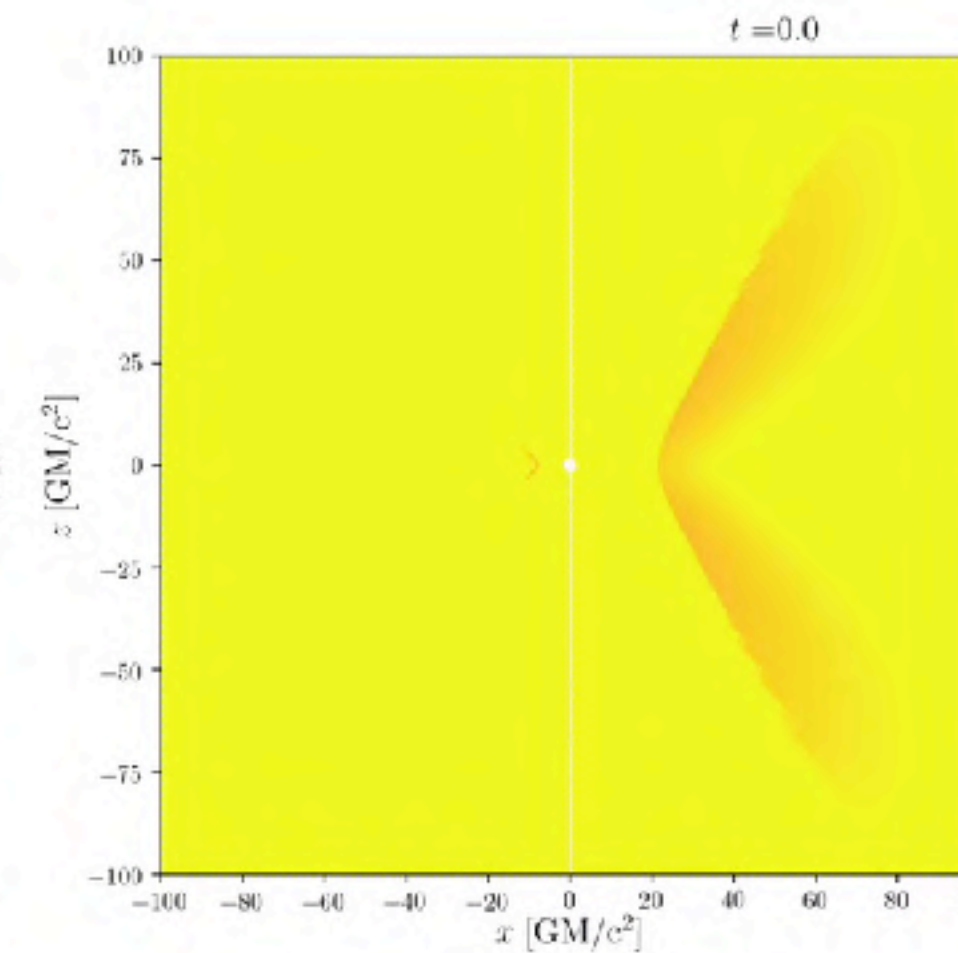
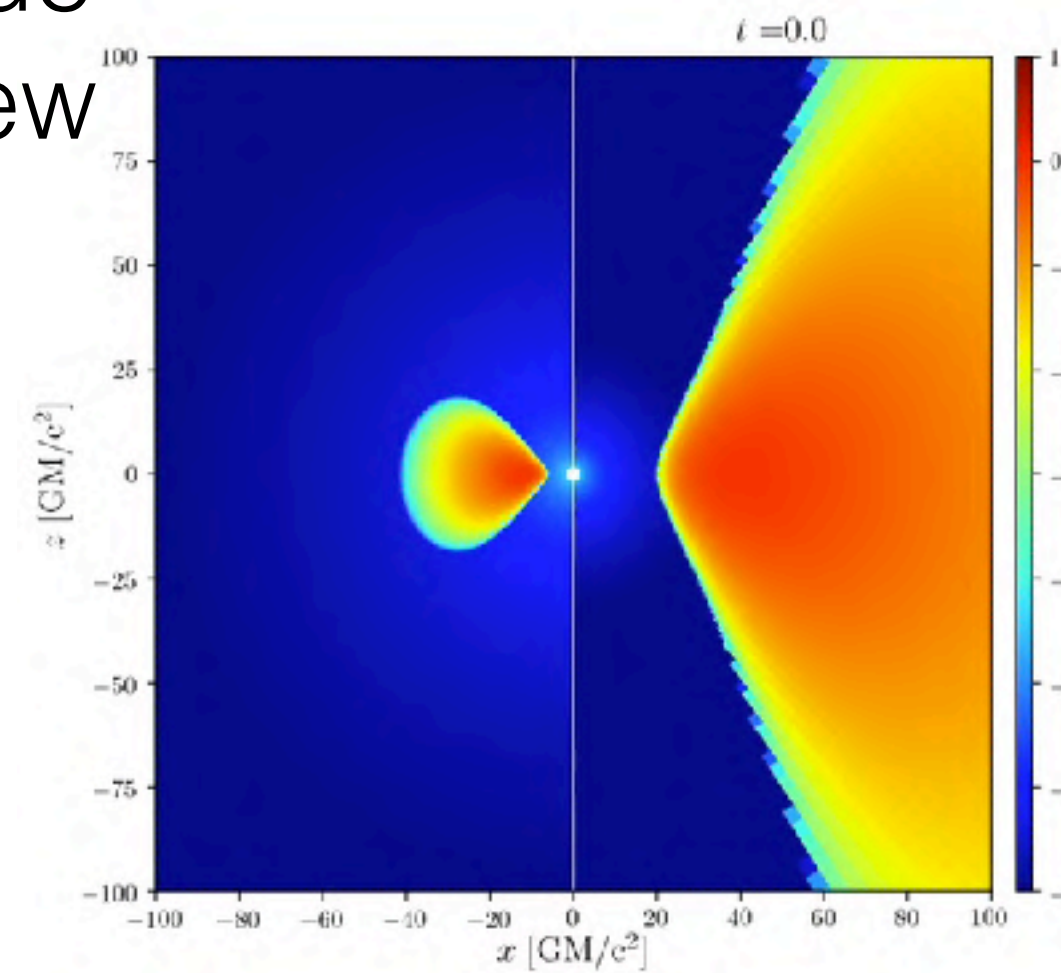


density

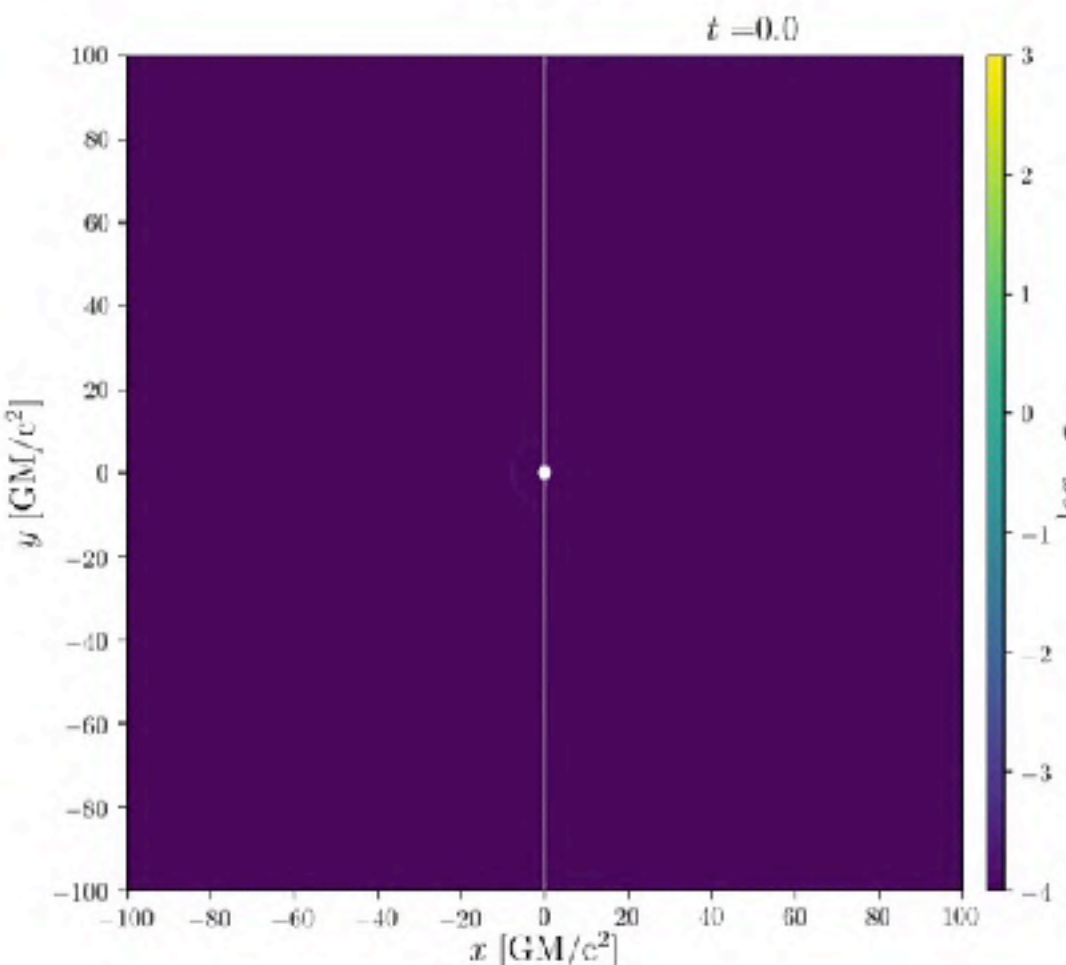
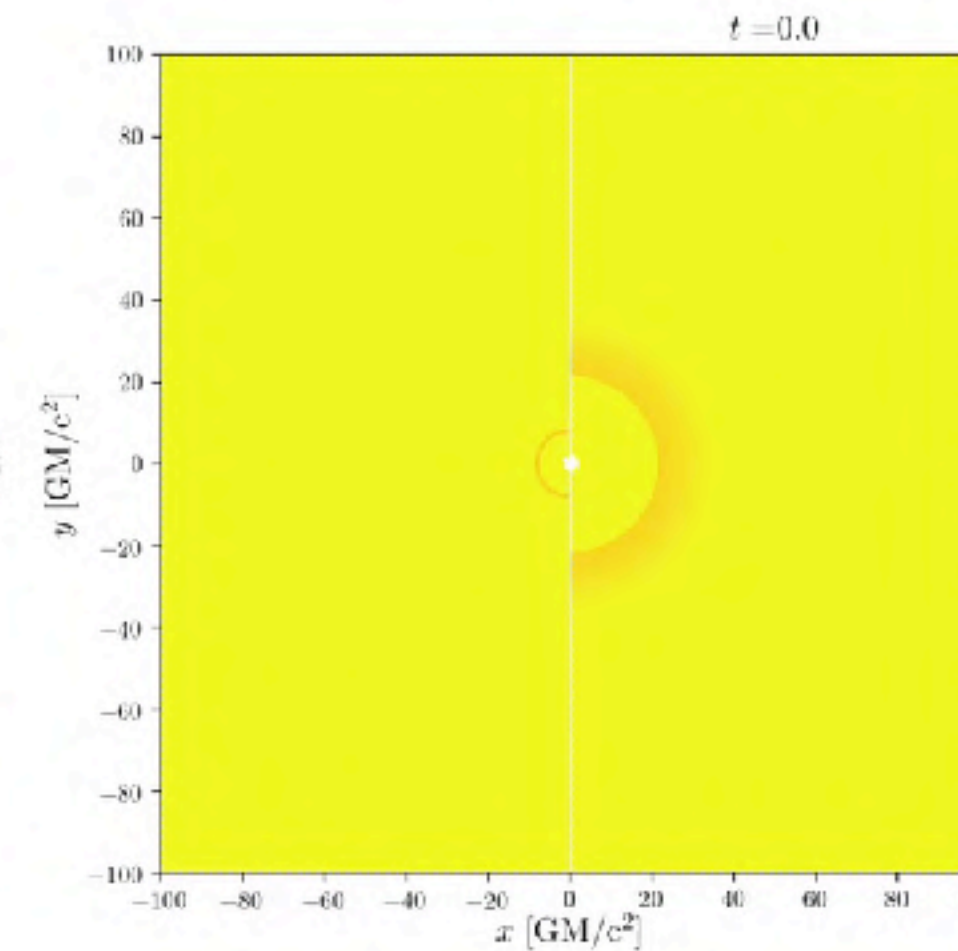
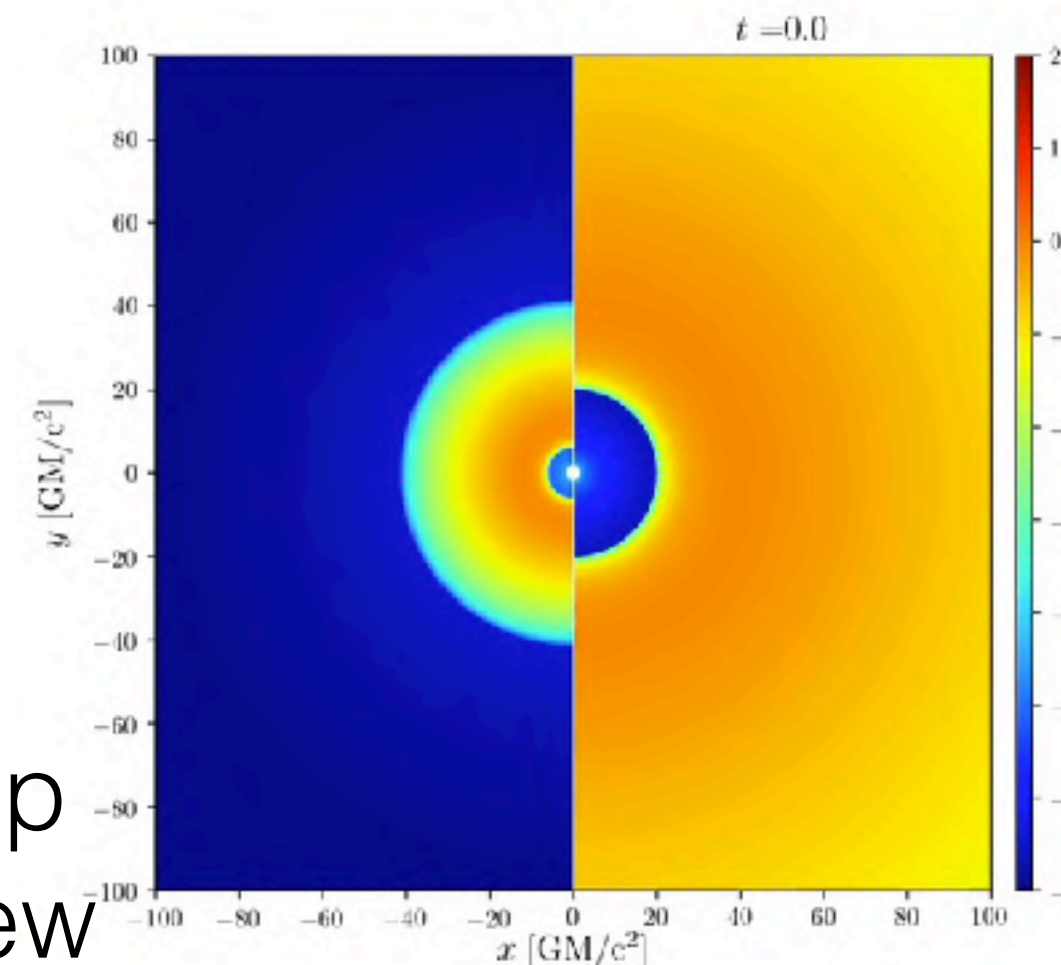
plasma beta

magnetisation

side  
view



top  
view



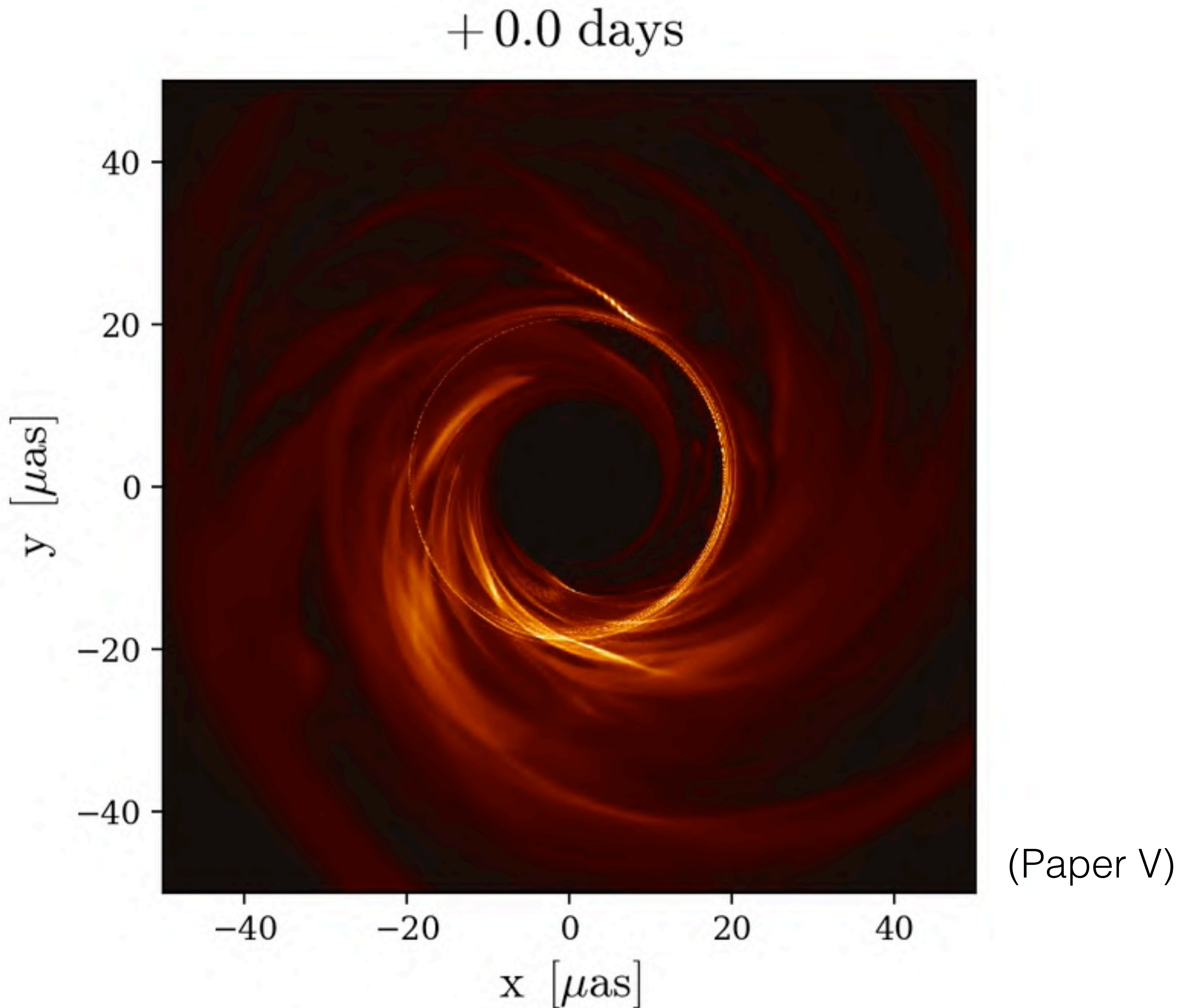
Event Horizon Telescope



---

# GRRT Image at 230 GHz

- MAD,  $a=+0.94$ ,  $R_{\text{high}}=160$
- $i=163$  deg
- each frame corresponds to 1M ( $\sim 0.35$  day)





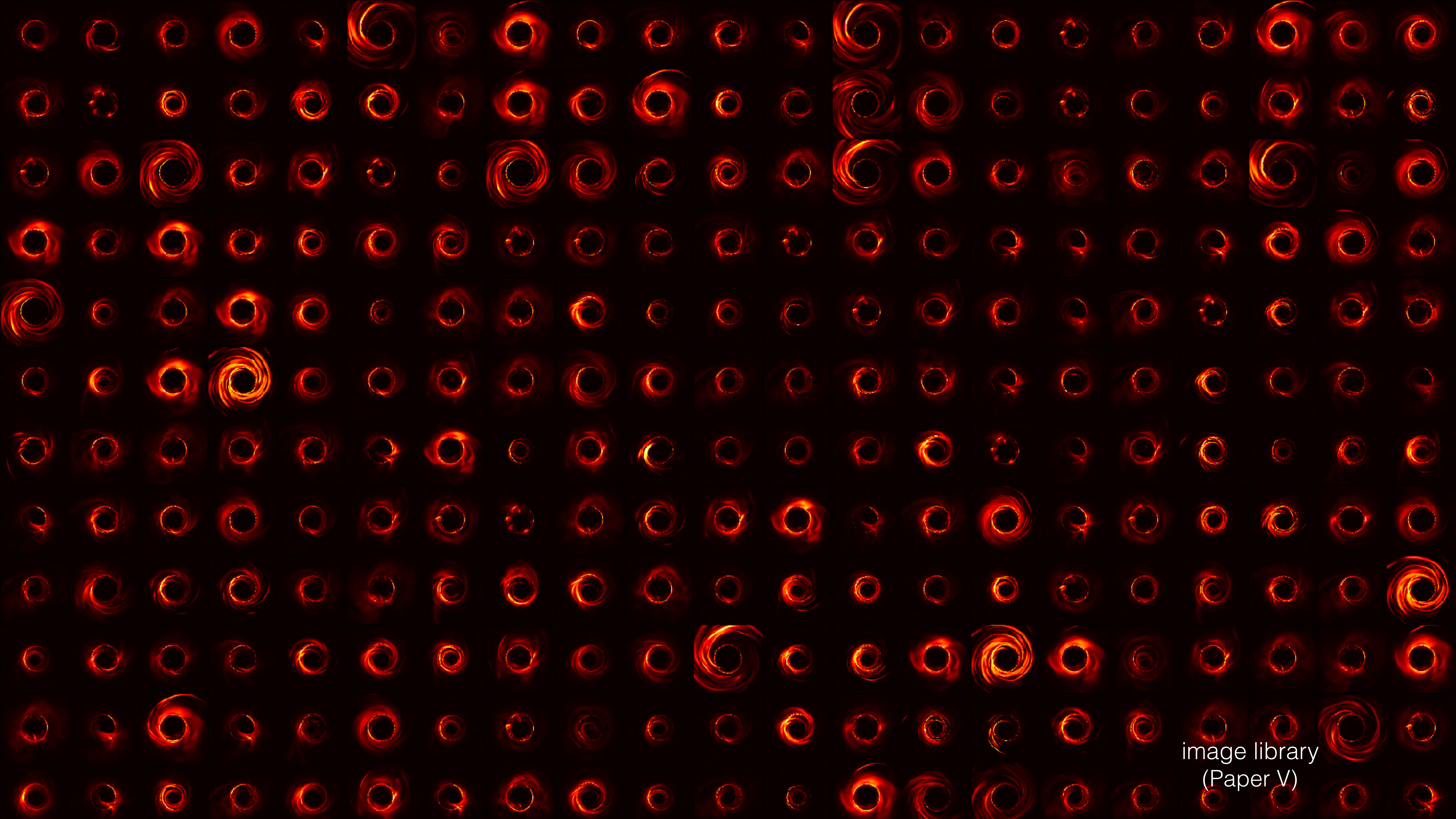
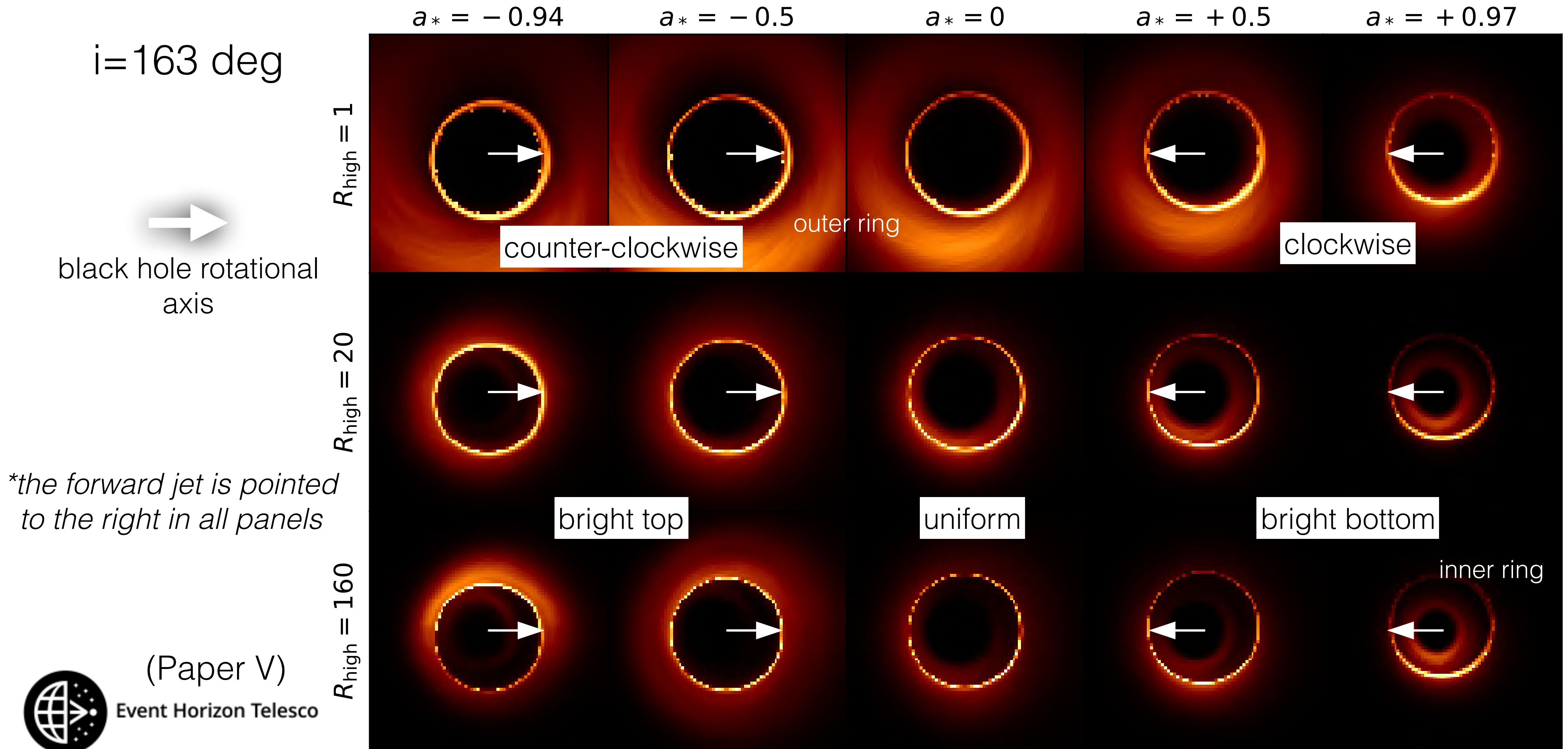


image library  
(Paper V)



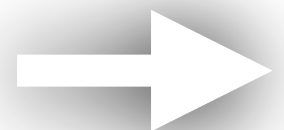
# SANE averaged GRRT images



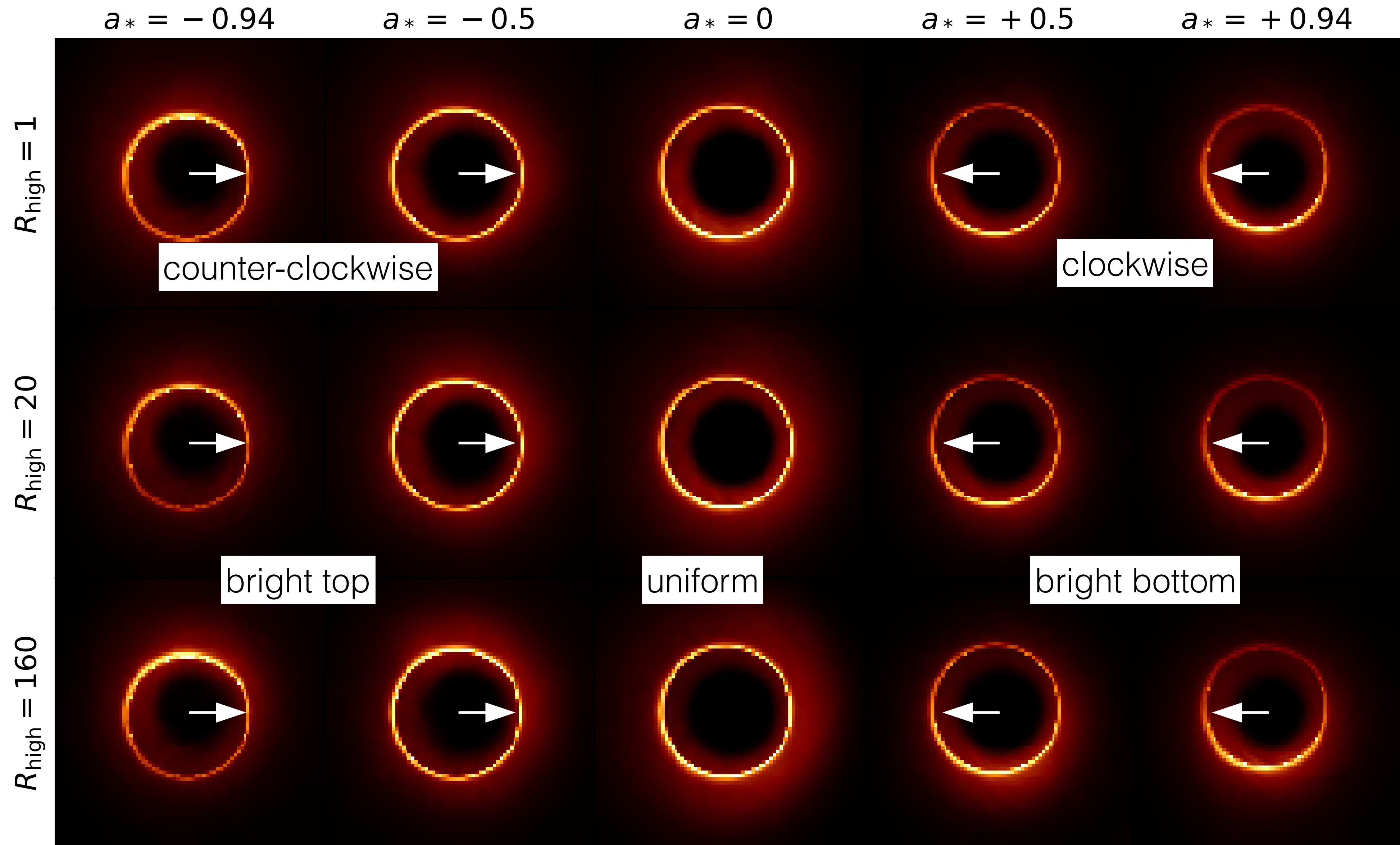


# MAD averaged GRRT images

$i=163$  deg

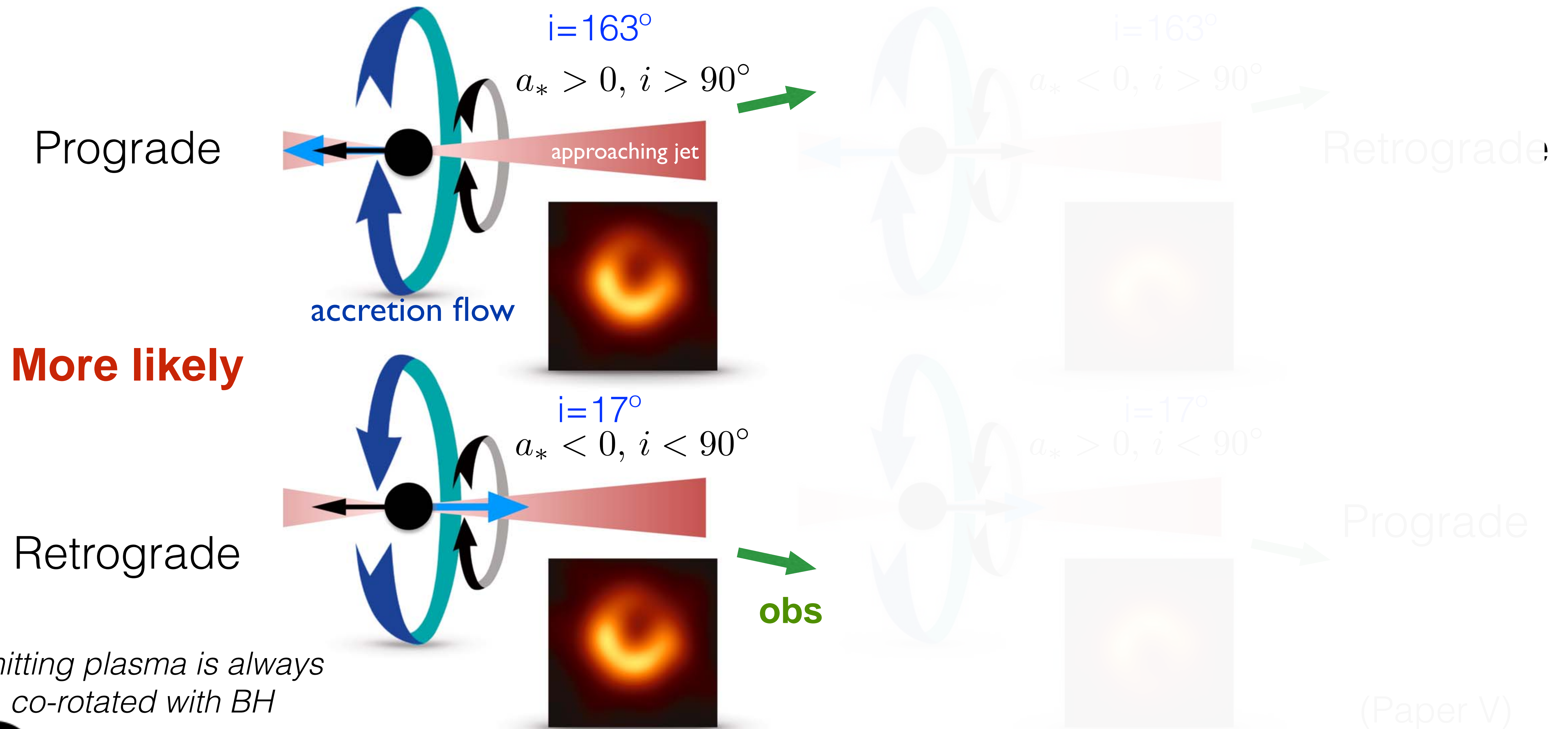
  
black hole rotational  
axis

*\*the forward jet is pointed  
to the right in all panels*





# Why is it asymmetric?



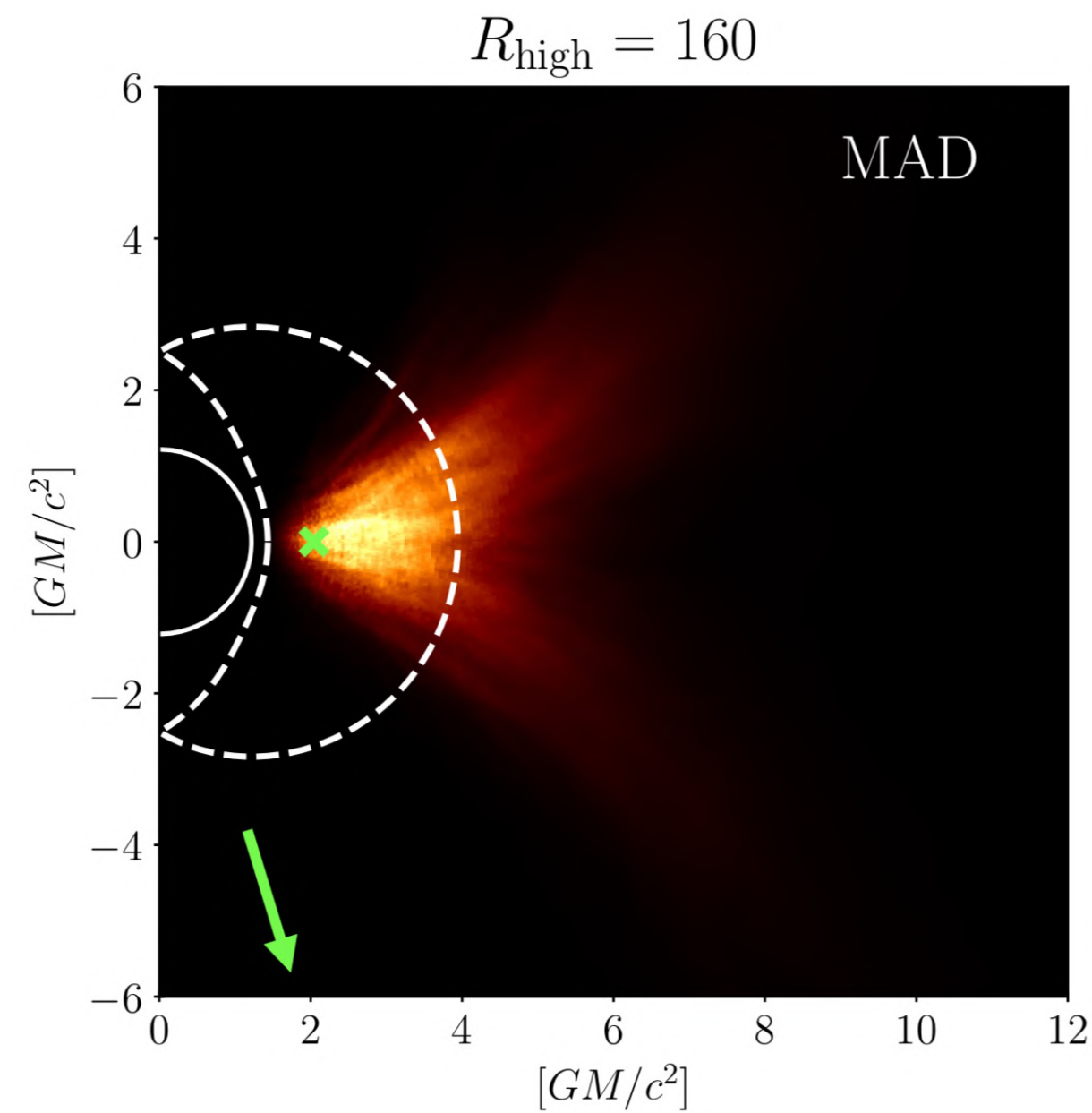
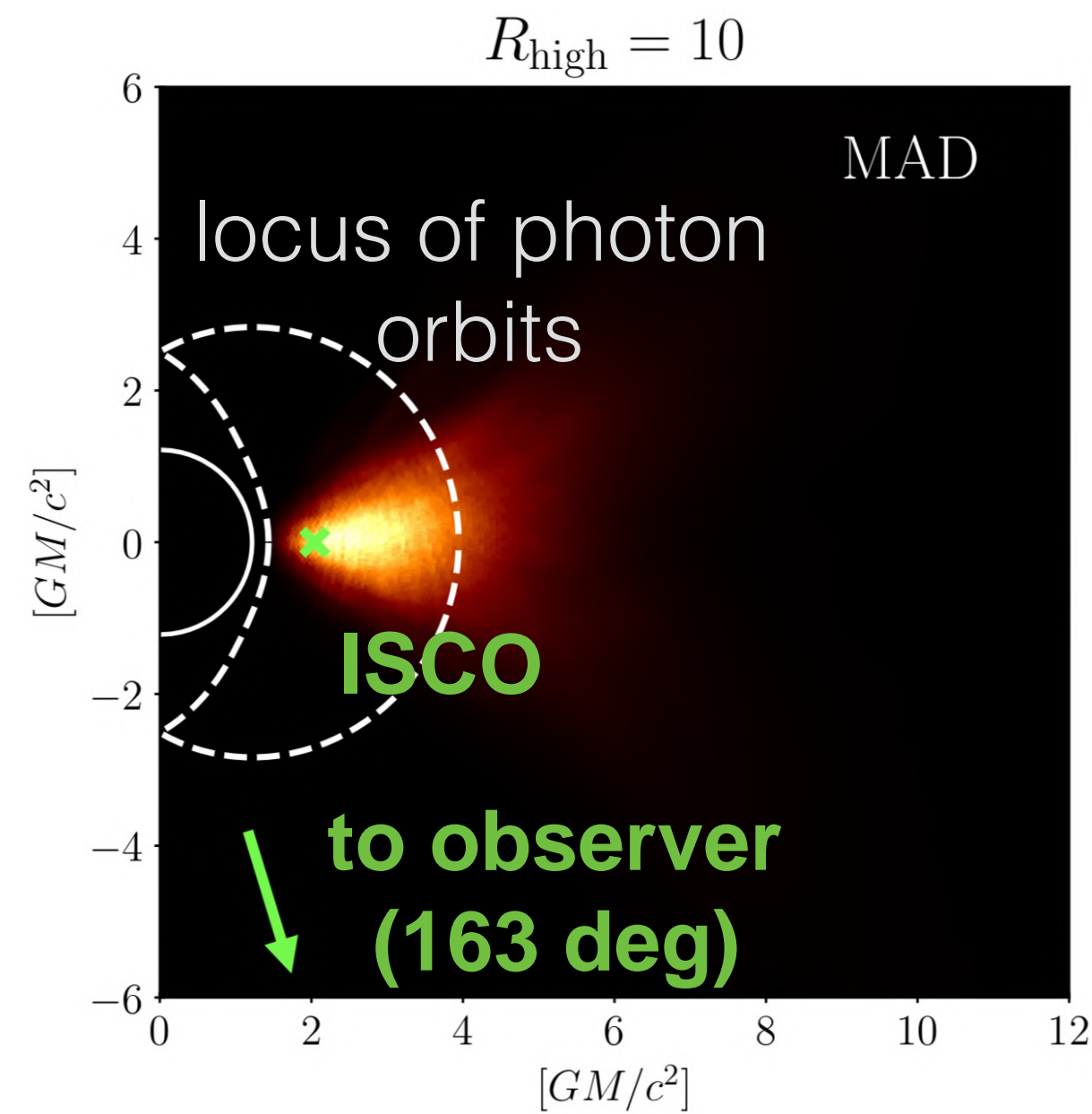
*Emitting plasma is always  
co-rotated with BH*



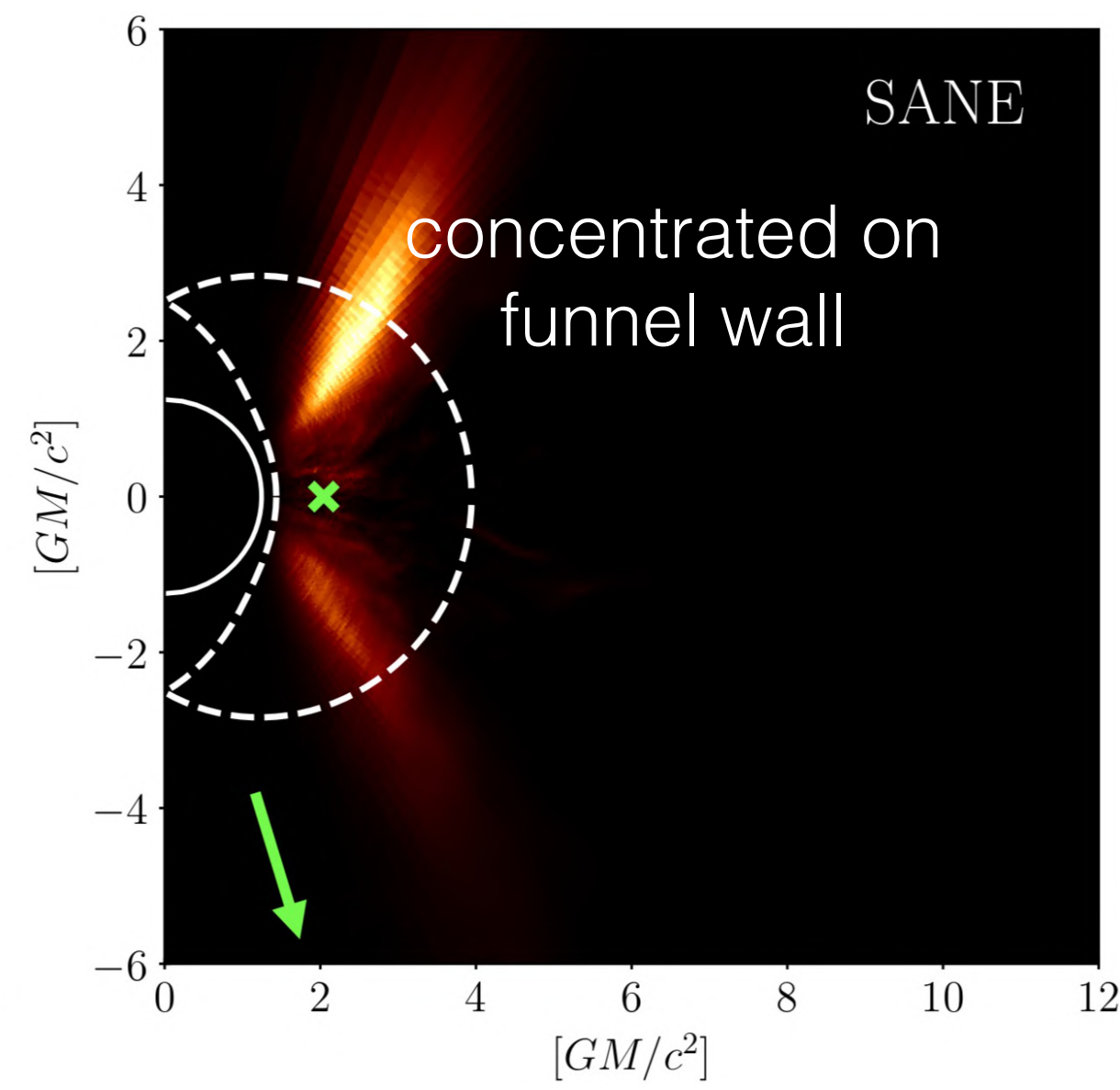
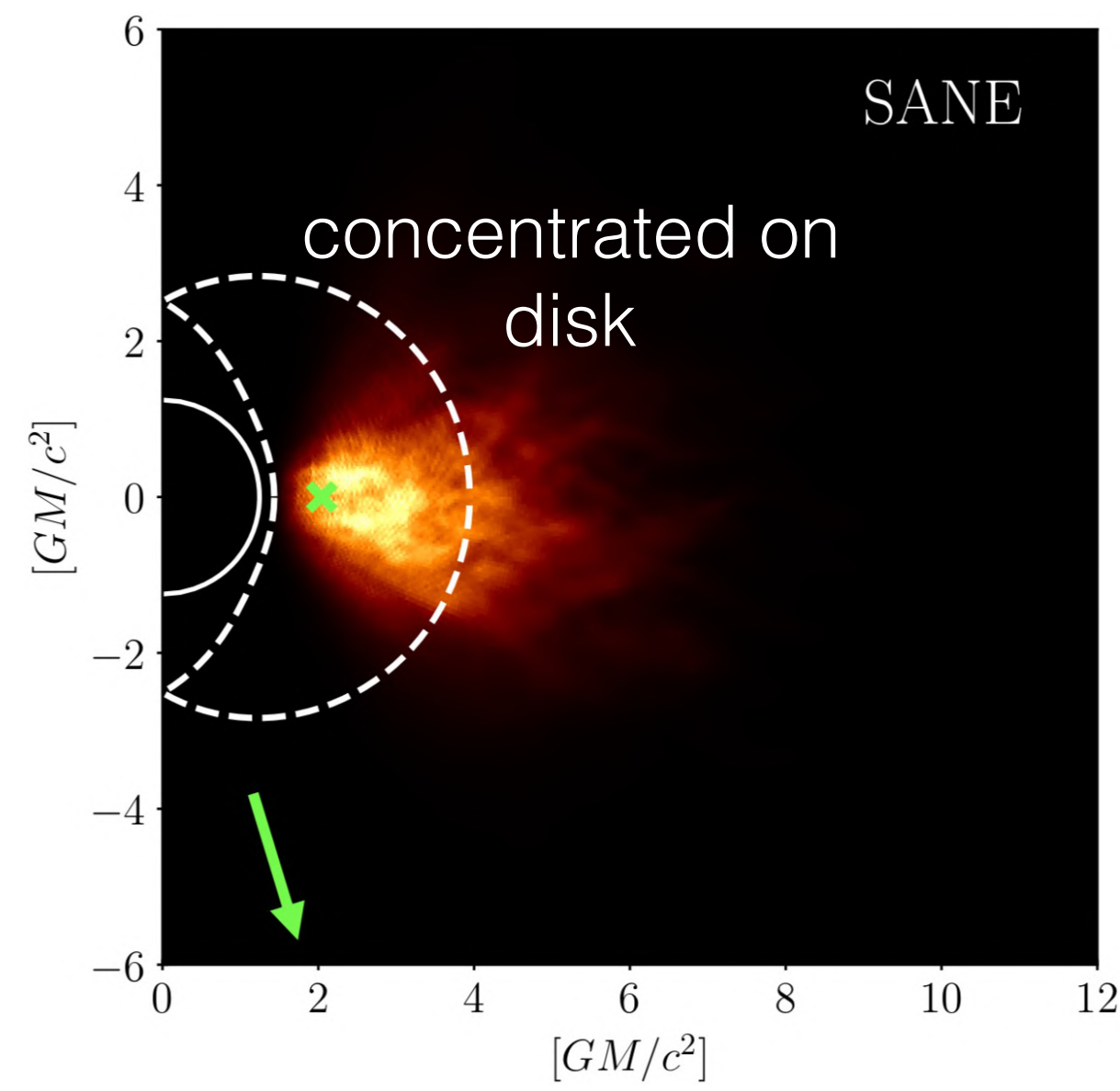
Event Horizon Telescope



# Where do mm photons originate?



MAD,  $a=0.94$

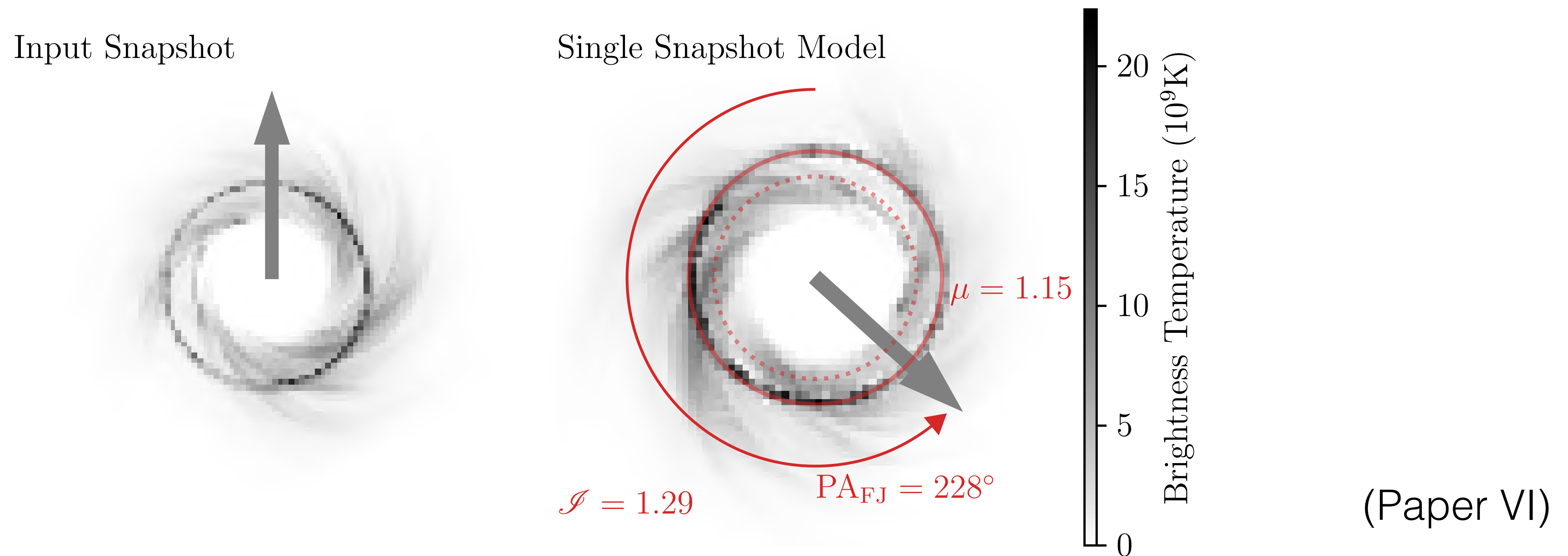


SANE,  $a=0.94$



# Fitting GRRT images to EHT data

- Fourier transformed synthetic images (visibility data) and fit to observed data
- Re-scale flux, stretch (M/D), and rotate image (P.A.) (allowed when optically thin)



Two independent codes: MCMC (Themis) & evolutionary algorithm (**GENA**)

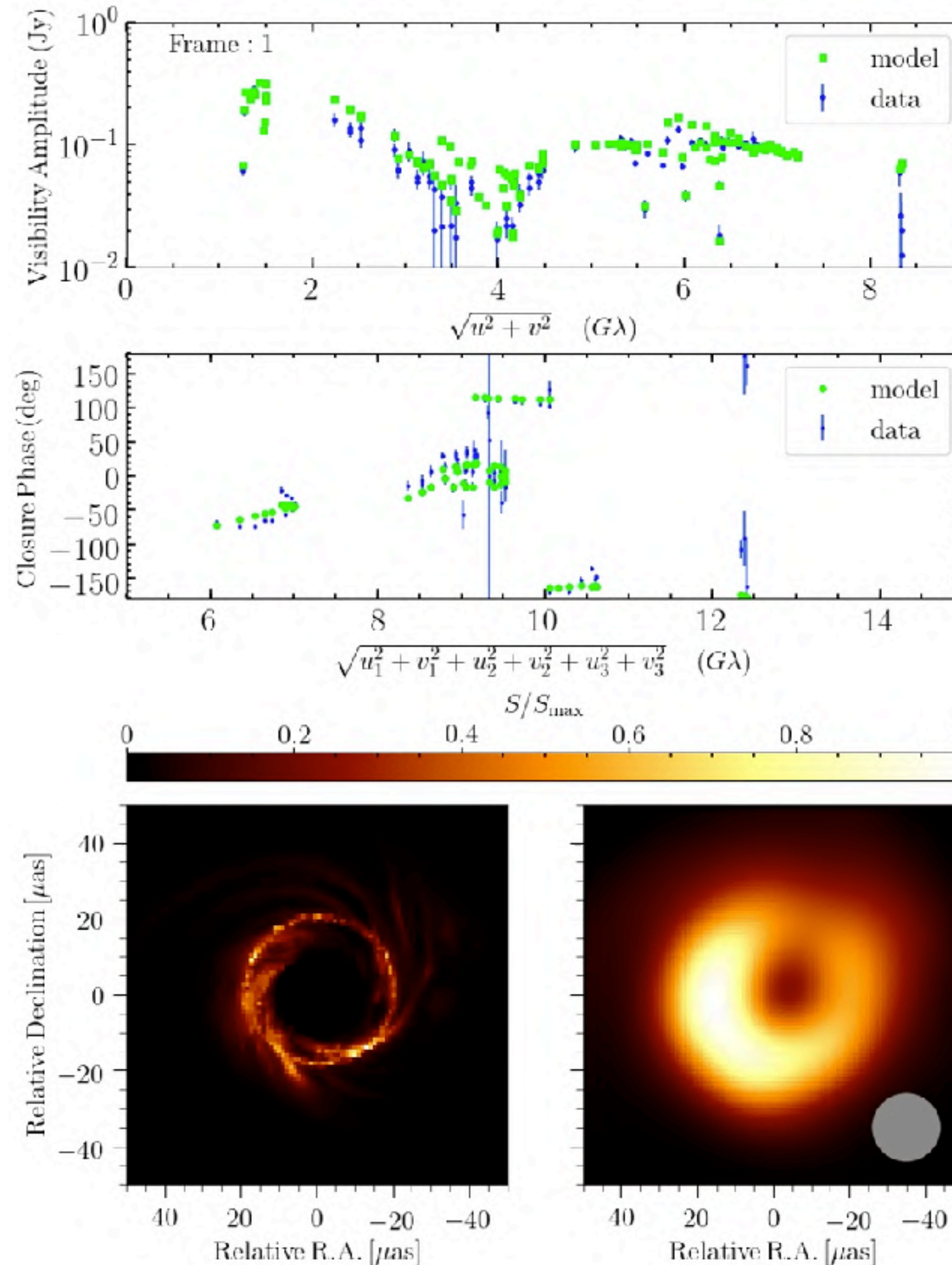


# Fitting GRRT images to EHT data

visibility  
amplitude  
(VA)

Closure  
phase (CP)

GRMHD image  
(left) &  
convolved  
image (right)



GENA fitting procedure  
(a single GRMHD simulation)

(Paper V)







OBSERVATIONS

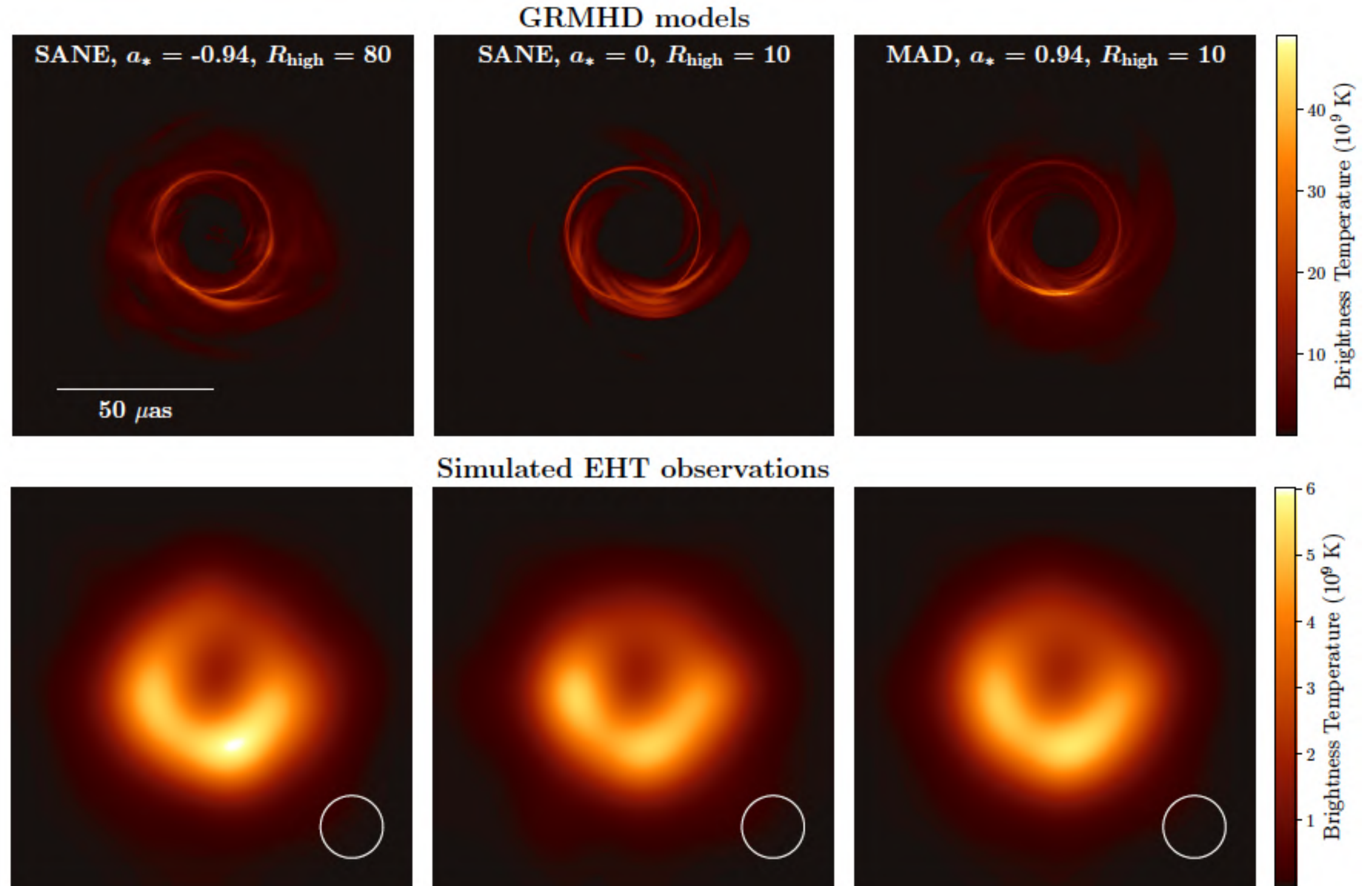


THEORETICAL MODEL



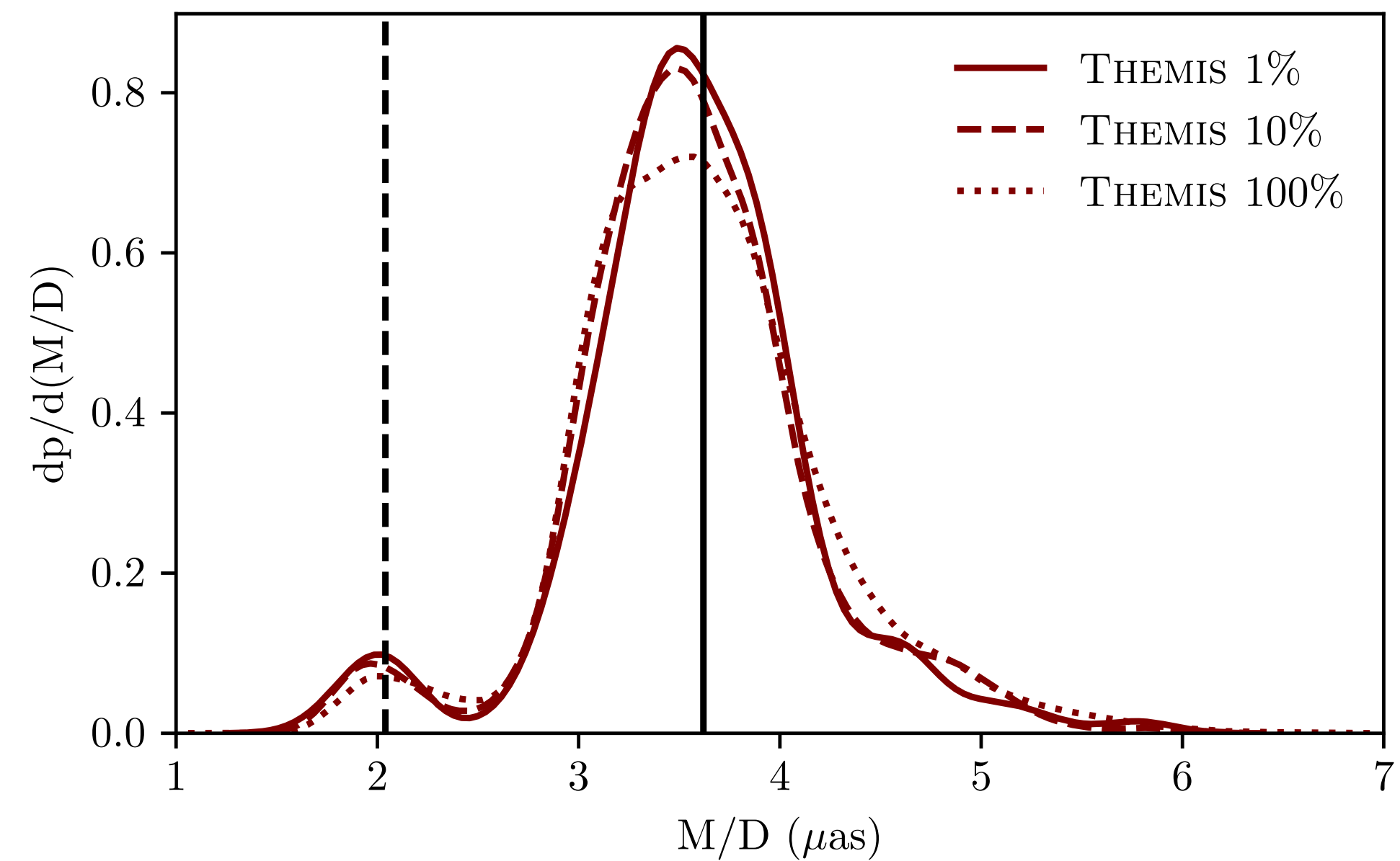
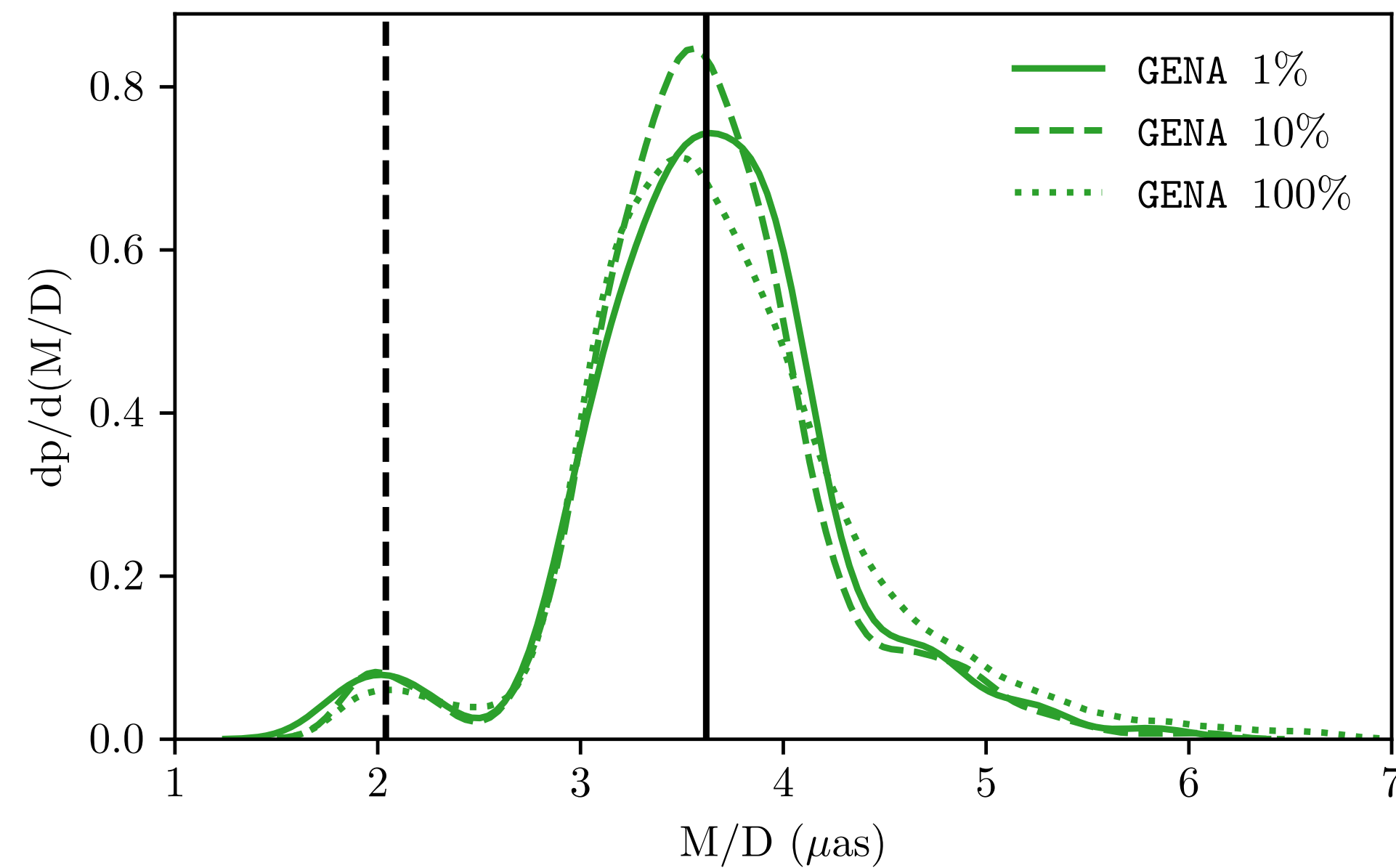
# Best Fitting Images

- Degeneracies are present in the physical conditions and scenarios.
- Good and bad: robustness conclusions (*EHT observed image is BH shadow*) and more accurate observations to determine black-hole spin.





# Distribution of Best-Fit Black Hole Angular Size



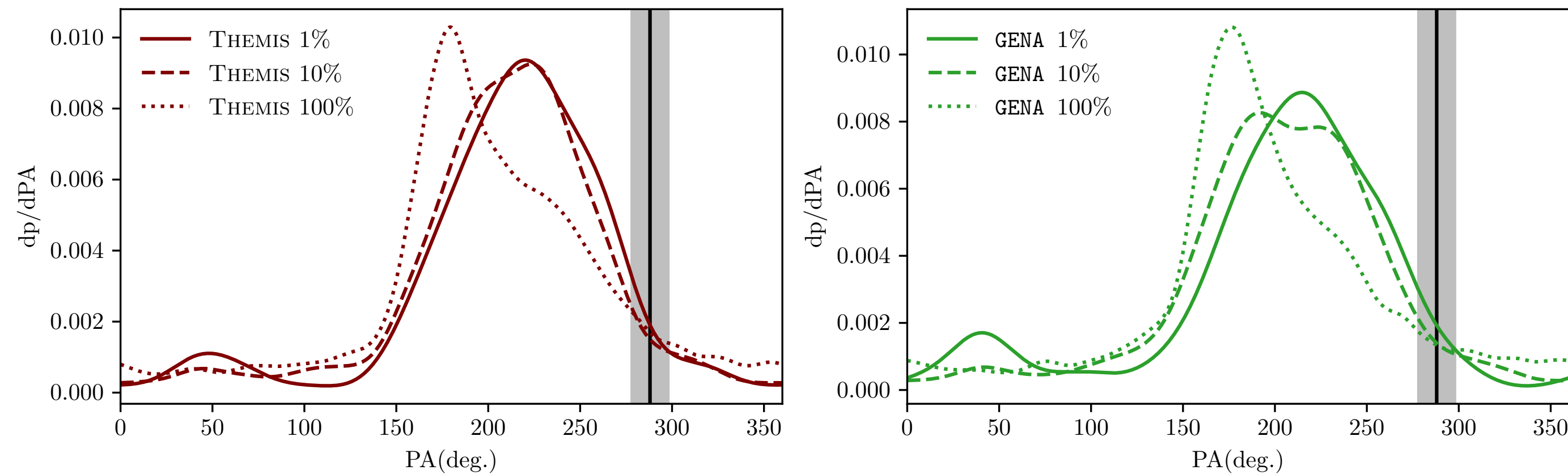
- Distribution of  $M/D$  from fitting Image Library snapshots to 2017 April 6th EHT data
- Results by Themis & GENA pipelines are qualitatively similar
- The distribution peaks close to  $M/D \sim 3.6 \mu\text{as}$  with a width of  $\sim 0.5 \mu\text{as}$
- The models are broadly consistent with stellar mass estimate
- $M = 6.5 \times 10^9 M_{\text{sun}}$  (using  $D = 16.8 \text{ Mpc}$ )



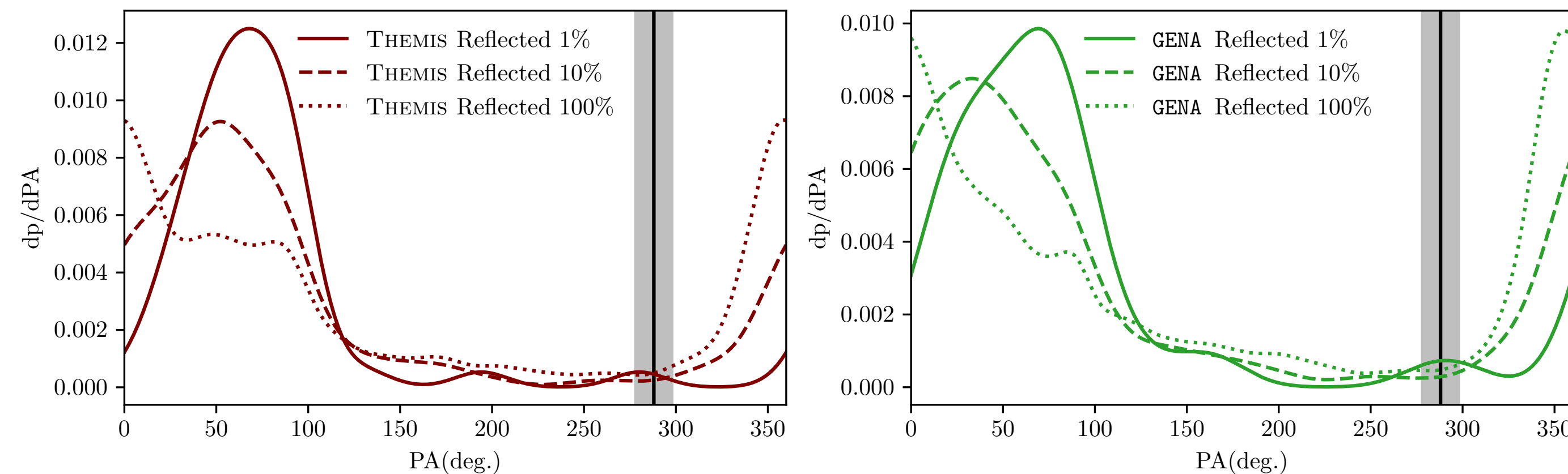


# Distribution of Model Best-Fit Position Angle

## BH spin vector pointing away from Earth



## BH spin vector pointing toward Earth



- Large scale jet orientation lies on the shoulder of the spin-away models ( $\langle PA \rangle \sim 200$  deg,  $\sigma_{PA} \sim 55$  deg)
- Large scale jet orientation lies off the shoulder of the spin-toward models
- BH spin-away models are strongly favored
- Width of distributions arises from brightness fluctuations in the ring





# Other Constraint

---

Apply **three** additional constraints:

1. Close to radiative equilibrium
  - Radiative efficiency  $<$  classical thin disk model radiative efficiency
2. Must not overproduce X-rays (in SED)
  - 2-10 keV luminosity:  $L_x = 4.4 \pm 0.1 \times 10^{40}$  erg/s (NuSTAR & Chandra obs.)
3. Must produce jet power  $>$  minimal jet power =  $10^{42}$  erg/sec





# Results: SANE model

Constraint: data fitting, radiative efficiency, X-ray, jet power

| $a/R_{\text{high}}$ | 1       | 10      | 20      | 40      | 80      | 160     |
|---------------------|---------|---------|---------|---------|---------|---------|
| -0.94               | - + + + | + + + + | + + + + | + + + + | + + + + | - + + + |
| -0.5                | + + —   | + + —   | + + + - | + + + - | - + + - | + + - + |
| 0                   | + + + - | + + + - | + + —   | + + + - | + + —   | + + —   |
| 0.5                 | + + + - | + + + - | + + + - | + + + - | + + + - | + + + - |
| 0.94                | + - + - | + - + - | + + + - | + + + - | + + + + | + + + + |



# Results: MAD model

Constraint: data fitting, radiative efficiency, X-ray, jet power

| $a/R_{\text{high}}$ | 1       | 10      | 20      | 40      | 80      | 160     |
|---------------------|---------|---------|---------|---------|---------|---------|
| -0.94               | — + +   | - + + + | - + + + | - + + + | - + + + | - + + + |
| -0.5                | + - + - | + + + - | + + + + | + + + + | + + + + | + + + + |
| 0                   | + - + - | + + + - | + + + - | + + + - | + + + - | + + + - |
| 0.5                 | + - + - | + + + + | + + + + | + + + + | + + + + | + + + + |
| 0.94                | + — +   | + - + + | + + + + | + + + + | + + + + | + + + + |





# Which Gravitational Theory?

---

- VLBI observation of EHT has provided the first images of the BH shadow in M87\* and will be soon provide it in our galactic centre, Sgr A\*.
- If the observations are sufficiently accurate, it will provide
  1. the evidence for the existence of an event horizon
  2. Testing the no-hair theorem in GR
  3. Testing of GR itself against a number of alternative theories of gravity.

We investigate alternatives of Kerr black hole through realistic theoretical modeling of shadow image



# BH Alternatives

---

1. black holes within GR that include additional fields
  - e.g., electromagnetic charge, NUT charge, cosmological constant, dark matter halo, hair etc.
2. black hole solutions from alternative theories of gravity or incorporating quantum effects
  - classical modification to GR as well as the effect of quantum gravity.
3. black hole “mimickers,” i.e., exotic compact objects (with or without surface), both within GR or in alternative theories
  - w.o. event horizon: e.g., naked singularity, supersupinar, wormhole
  - w.o. event horizon & w.o. surface: e.g., boson star
  - w.o. event horizon & w. surface: Gravastar

Most of alternatives represent **a shadow similar to a Kerr black hole**

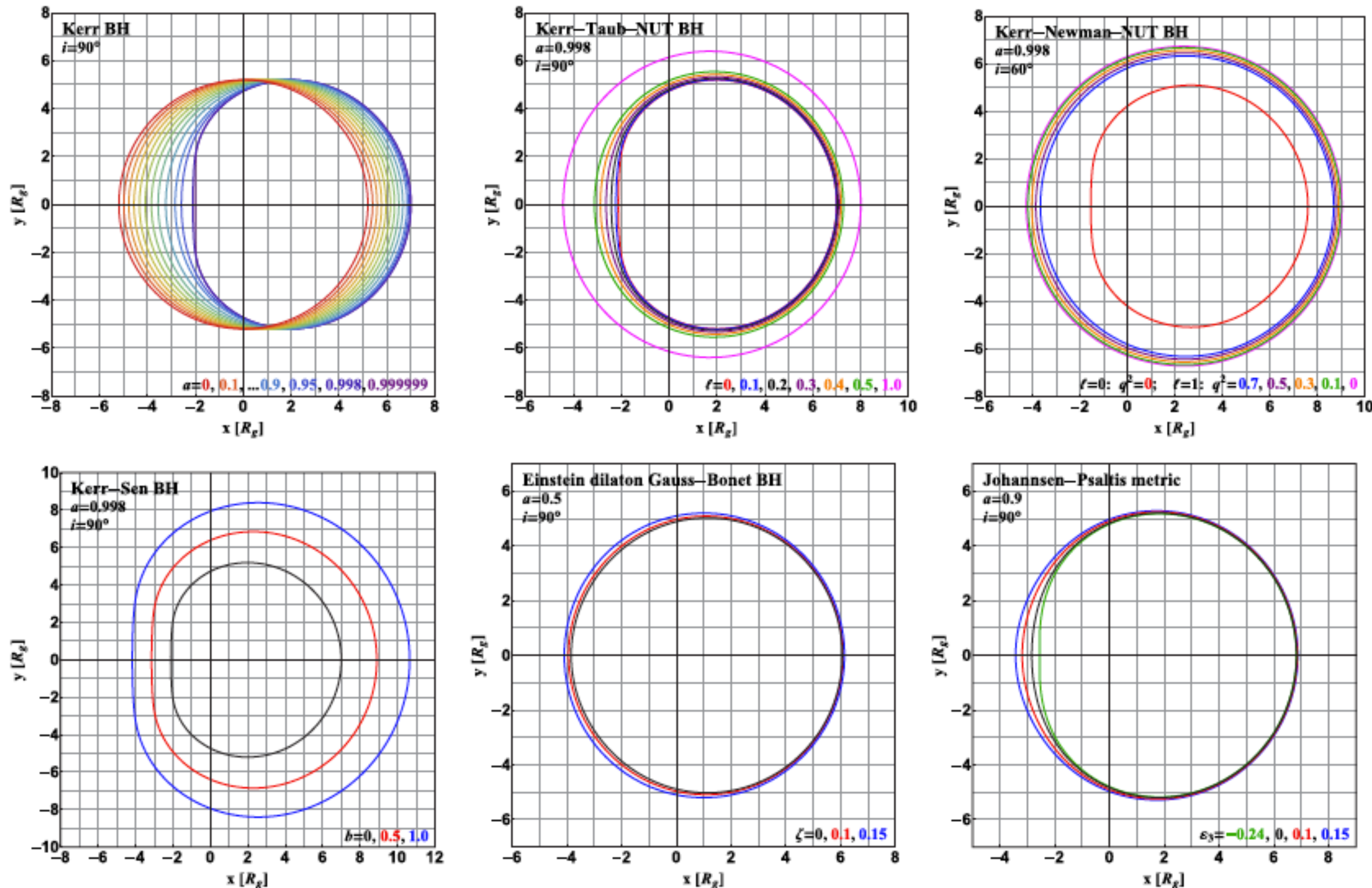




# Shadow Industry: Different Spacetime

Variety of BH shadow boundary curve in different theory of gravity

Younsi et al. (2016)



From BHCam review by Goddi et al. (2017)



Event Horizon Telescope

✓ Stellar Mass:  $6.2 \times 10^9 M_{\text{sun}}$   
(Gebhardt et al. 2011)

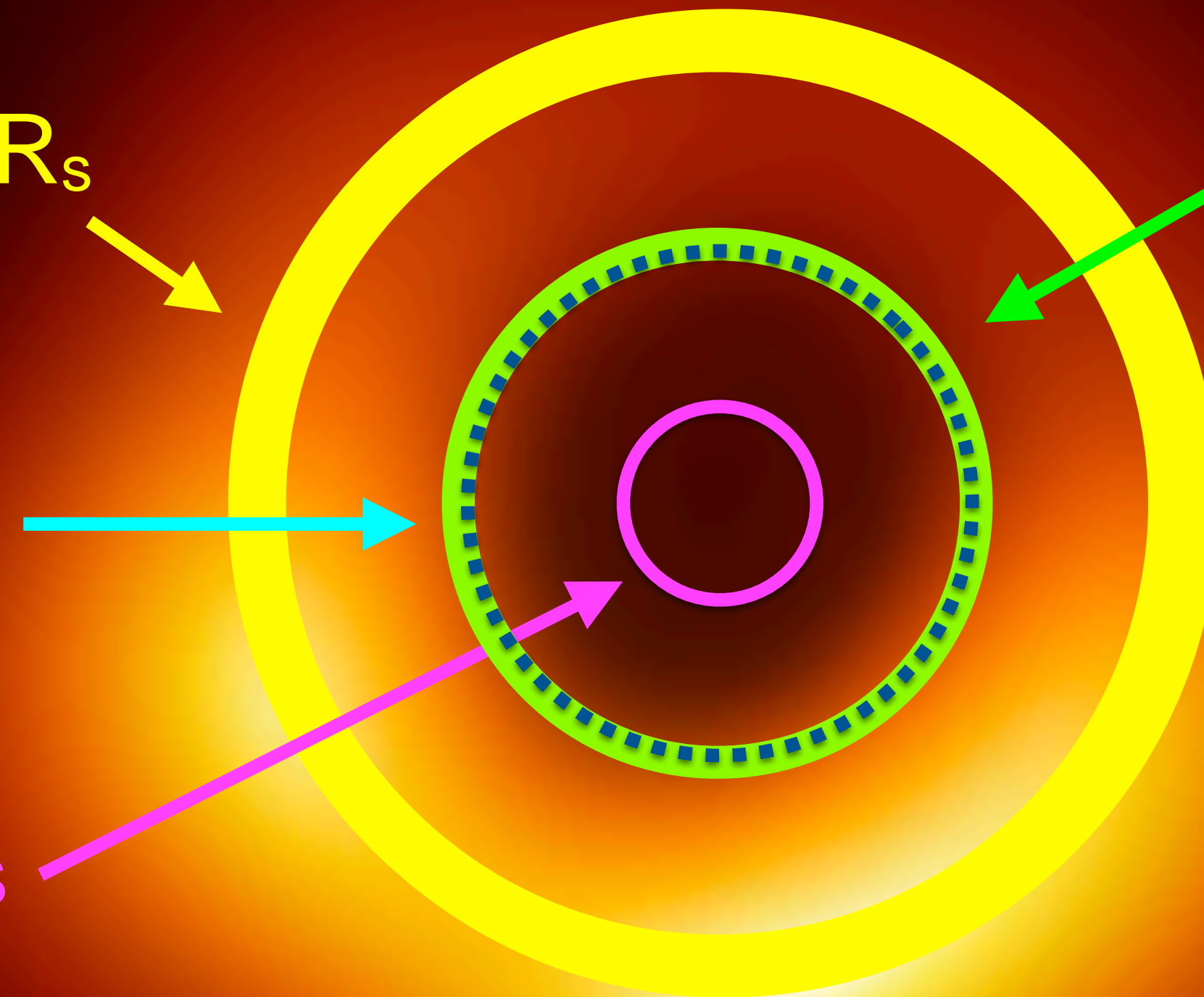
Gas Mass:  $3.5 \times 10^9 M_{\text{sun}}$  ✗  
(Walsh et al. 2013)

✓ Black Hole:  $4.84\text{--}5.2 R_s$

Black Hole:  $4.84\text{--}5.2 R_s$  ✗

✗ Worm Hole:  $\sim 2.7 R_s$   
(e.g., Bambi 2013)

✗ Naked Singularity:  $1 R_s$   
(superspinar)  
(e.g., Bambi & Freese 2009)



6 Billion Solar Mass Black Hole



# What we have learned from data and images?

---

- Einstein's GR has passed another test at a strong gravitational field
- The strongest evidence for the presence of black holes
- AGN and jets are powered by super massive black hole
- The M87 Black hole is likely spinning (from GRMHD fits + constraints)
- The stellar dynamical mass is correct (6.5 billion masses)
- Testing BH alternatives are important topic for next EHT



# Testing BH Alternatives

**Realistic shadow imaging** (GRMHD simulation of accretion flows onto central object+GRRT imaging) for BH alternatives

- Dilaton BH** (alternative theories of gravity), Mizuno et al. (2018)
- Boson Star** (w.o. event horizon & surface), Olivares et al. (2019)
- Gravastar** (w.o. event horizon, w. surface), Olivares et al. (2019 in prep)

*Considered Future EHT array  
(including 345GHz & space-VLBI)*  
(Fromm et al. 2019 in prep.)



Event Horizon Telescope

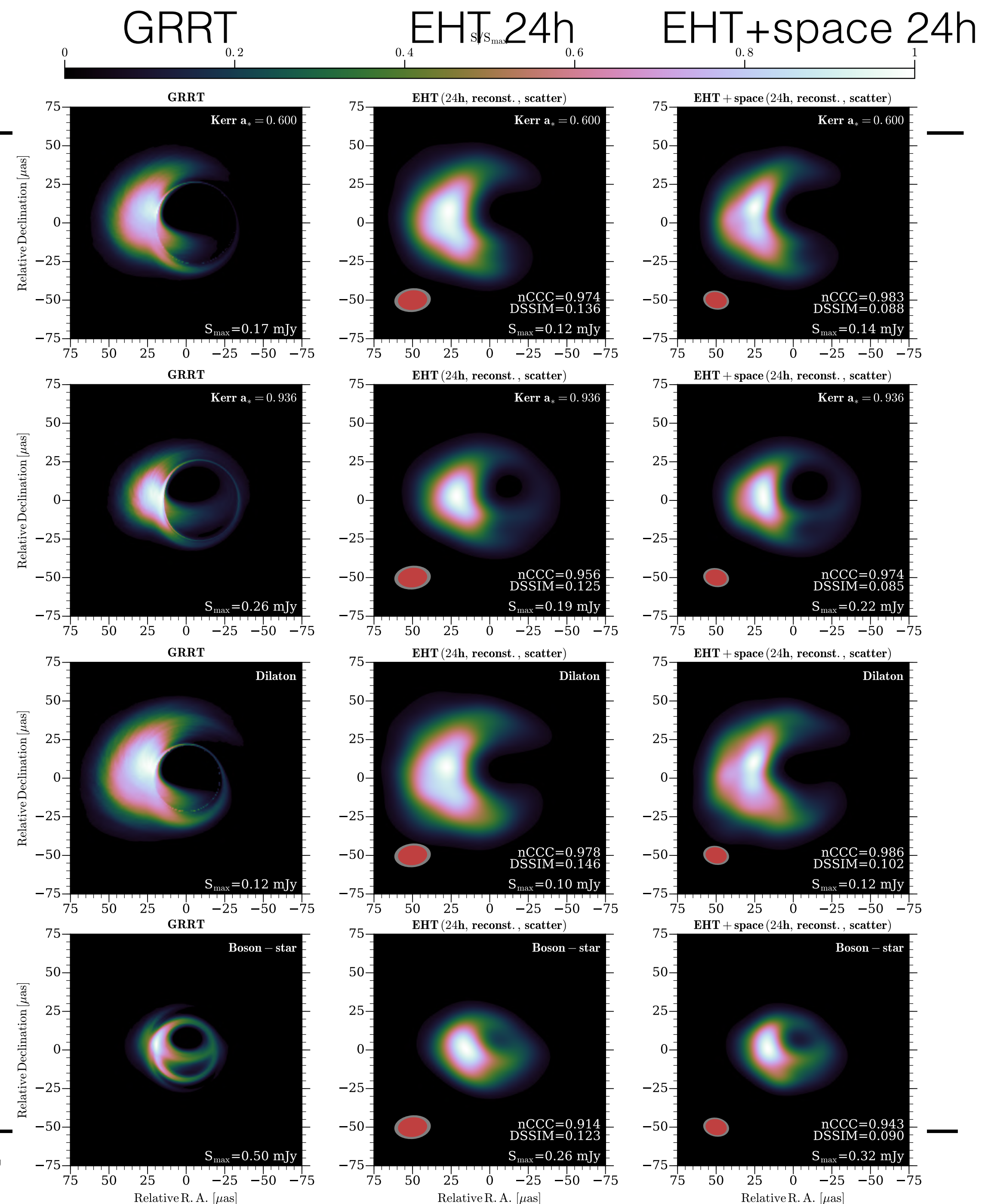
@230GHz,  $i=60^\circ$  deg,  
for Sgr A\*

Kerr BH  
( $a=0.6$ )

Kerr BH  
( $a=0.9375$ )

Dilation BH  
( $b=0.5$ )

Boson star





# Testing BH Alternatives

**Realistic shadow imaging** (GRMHD simulation of accretion flows onto central object+GRRT imaging) for BH alternatives

- **Dilaton BH** (alternative theories of gravity),  
**Mizuno et al. (2018)**

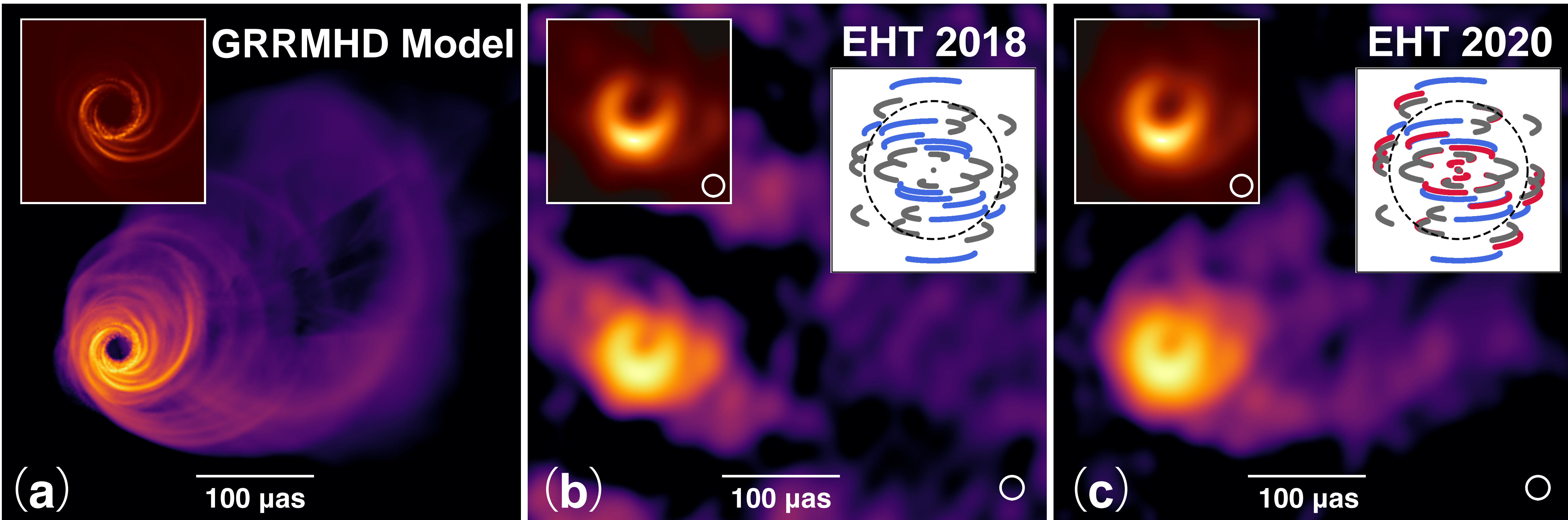
nature  
**astronomy**



The shadow of a black hole



# Weather forecast



(Chael et al. 2019)

(RML Reconstruction with SMILI)

EHT Collaboration, ALMA Cycle 7 M87 Proposal



Event Horizon Telescope



# Concluding Remarks



**Dr. Elisabeth Mills**

@astronomills

Following

I still love you, Sgr A\* [#EHTBlackHole](#)



Event Ho

**NO, NO, Sgr A\*, WE STILL LOVE YOU, TOO**



# Thank you for listening



2018 EHT collaboration meeting



---

# Back Up Slide



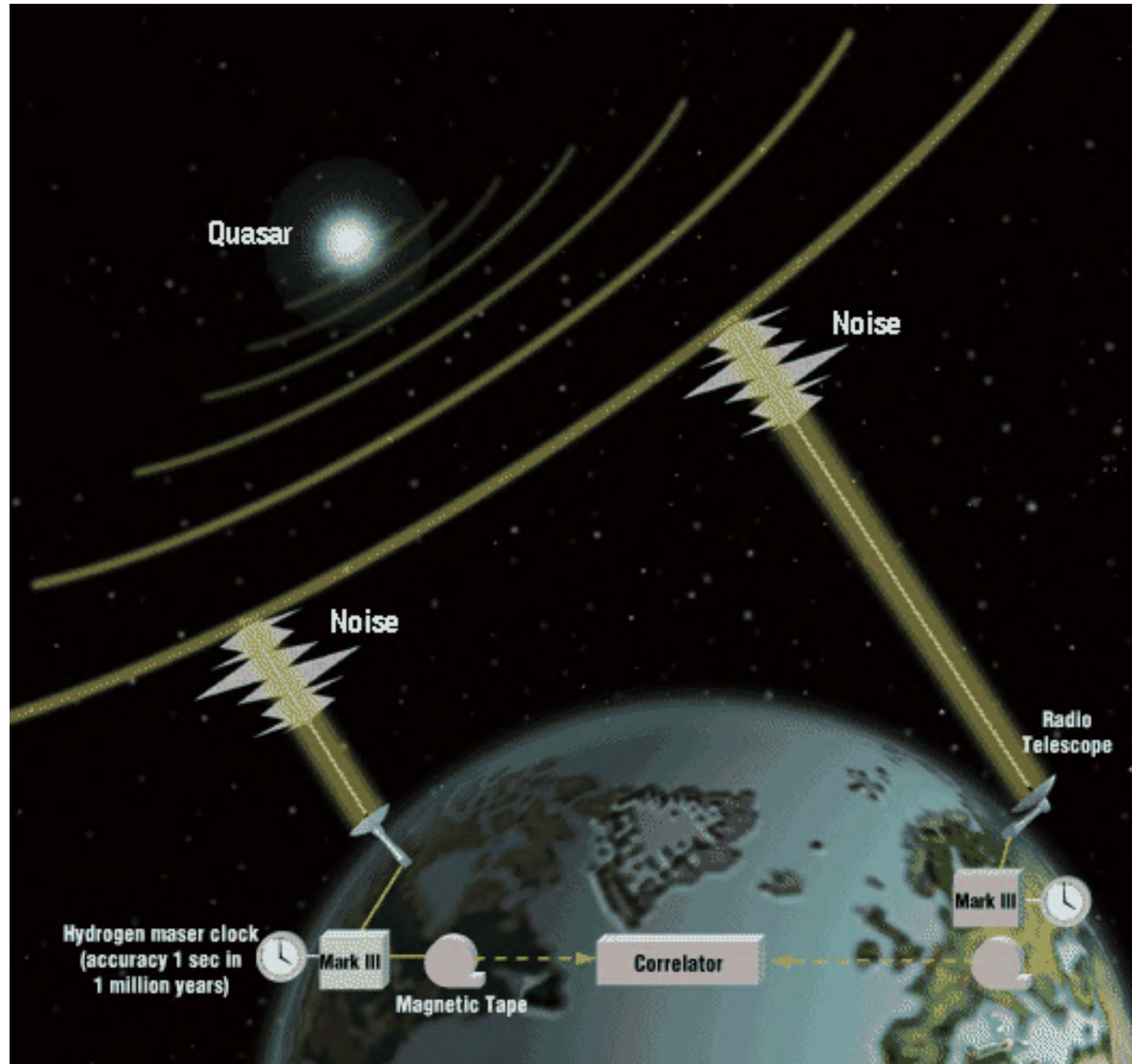


---

EHT related slide



# Short wavelength VLBI



Angular Resolution:

$$\lambda/D \text{ (cm)} \sim 0.5 \text{ mas}$$

$$\lambda/D \text{ (1.3mm)} \sim 30 \text{ } \mu\text{as}$$

$$\lambda/D \text{ (0.8mm)} \sim 20 \text{ } \mu\text{as}$$

ISM scatter (Sgr A\*):

$$\Theta_{\text{scat}} \sim \lambda^2$$

BH Shadow size:

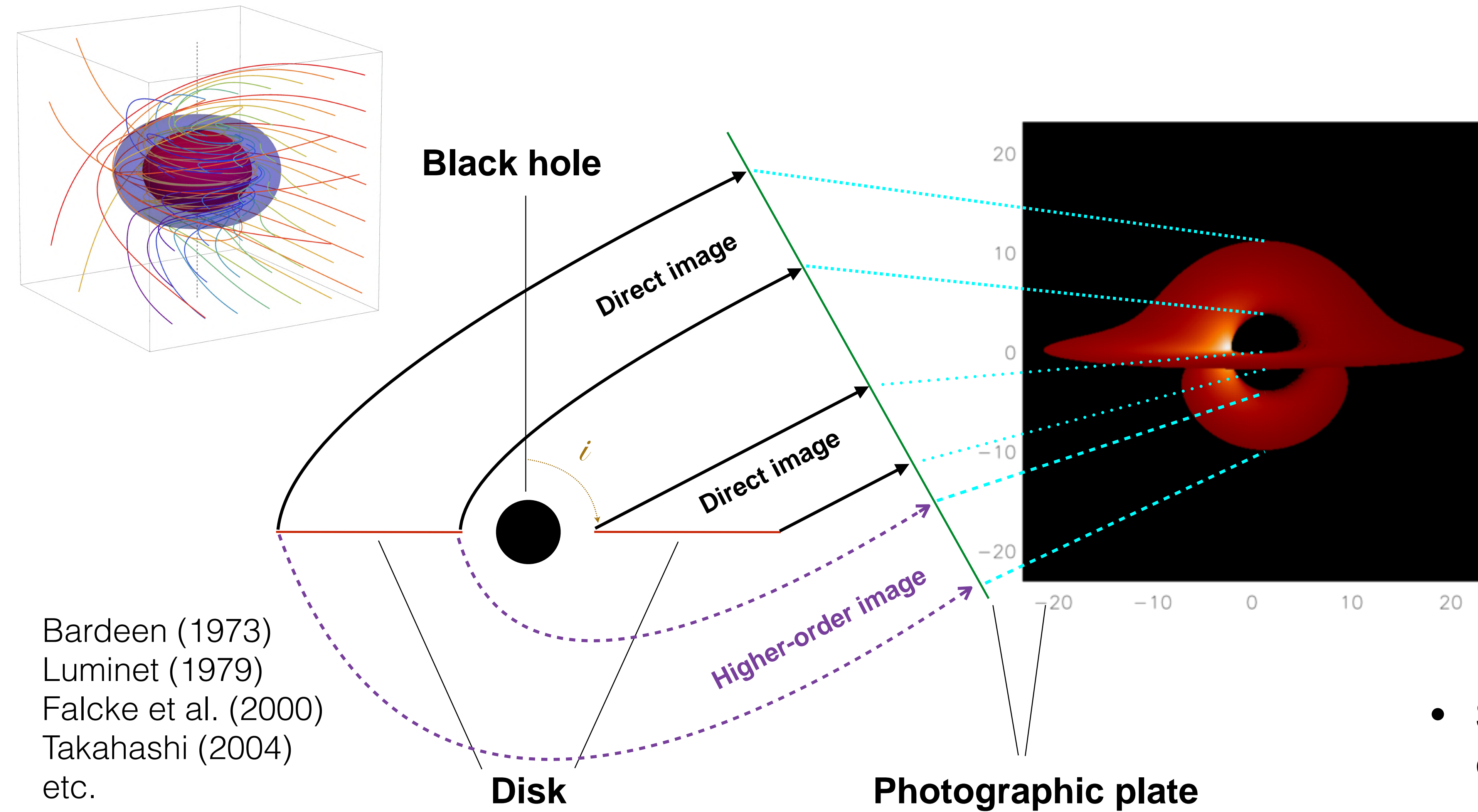
$$\text{Sgr A*}: 50 \text{ } \mu\text{as}$$

$$\text{M87}: 40 \text{ } \mu\text{as}$$





# Strong GR: Black Hole Shadow



Shadow diameter:

### Non-spinning ( $a=0$ )

$$D_{\text{sh}} \sim 5.2 * R_{\text{sch}}$$

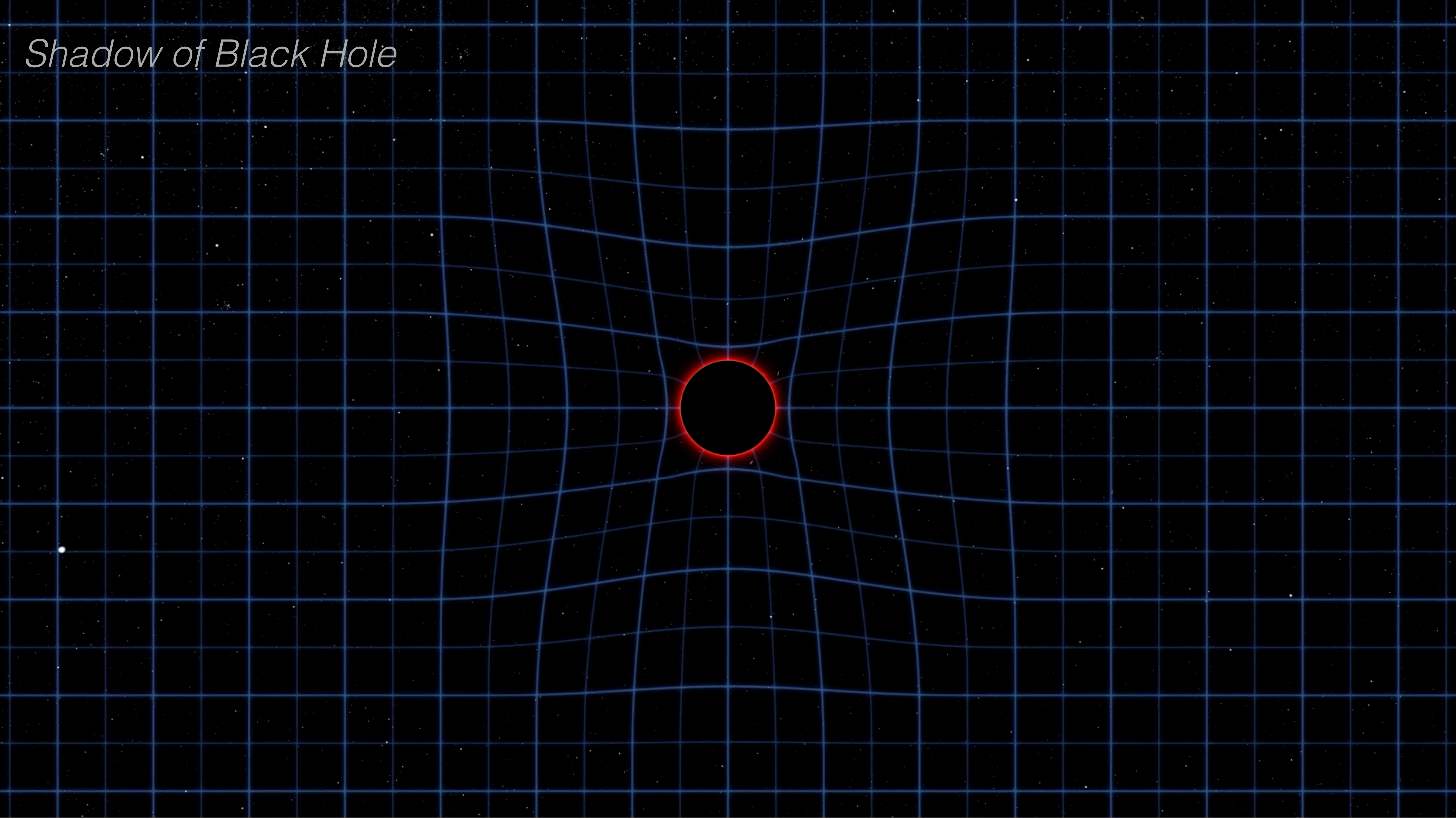
## Spinning ( $a=1$ )

$$D_{\text{sh}} \sim 4.8 * R_{\text{sch}}$$

- Shadow size and shape encodes GR (e.g., Johannsen & Psaltis 2010)



# *Shadow of Black Hole*





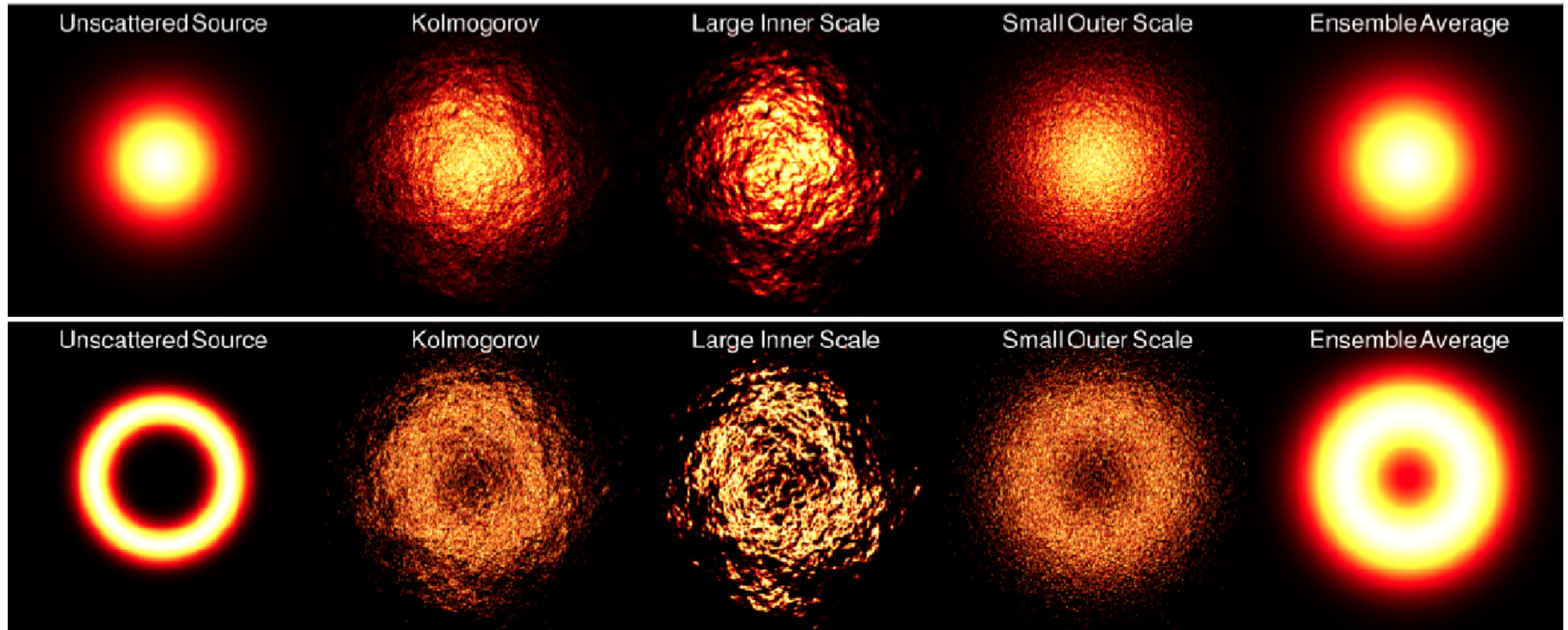
# Sgr A\* vs M87

|                           | M87                            | Sgr A*            |
|---------------------------|--------------------------------|-------------------|
| Mass ( $M_{\text{sun}}$ ) | $3\text{-}6 \times 10^9$ (?)   | $4 \times 10^6$   |
| Distance                  | 16 Mpc                         | 8.5 kpc           |
| Luminosity                | $10^{44}$ erg/s                | $10^{36}$ erg/s   |
| Mdot ( $M_{\text{edd}}$ ) | $10^{-4}$                      | $10^{-8}$         |
| BH Spin Axis              | Gal disk?                      | 10-25 deg los     |
| @ the BH?                 | Maybe                          | Yes               |
| B field @ BH              | 60-130 G                       | 10-100 G          |
| Scattered?                | No                             | yes               |
| Shadow Size               | 640 AU                         | 0.5 AU            |
| Shadow Angle              | 20-40 $\mu\text{as}$           | 52 $\mu\text{as}$ |
| GM/c <sup>3</sup>         | 8 hrs                          | 20 sec            |
| ISCO Period               | 4-54 days                      | 4-54 min          |
| Jet Power                 | $10^{42}\text{-}10^{43}$ erg/s | ?                 |





# Better Modeling of ISM Scatter



Johnson & Gwinn (2015)



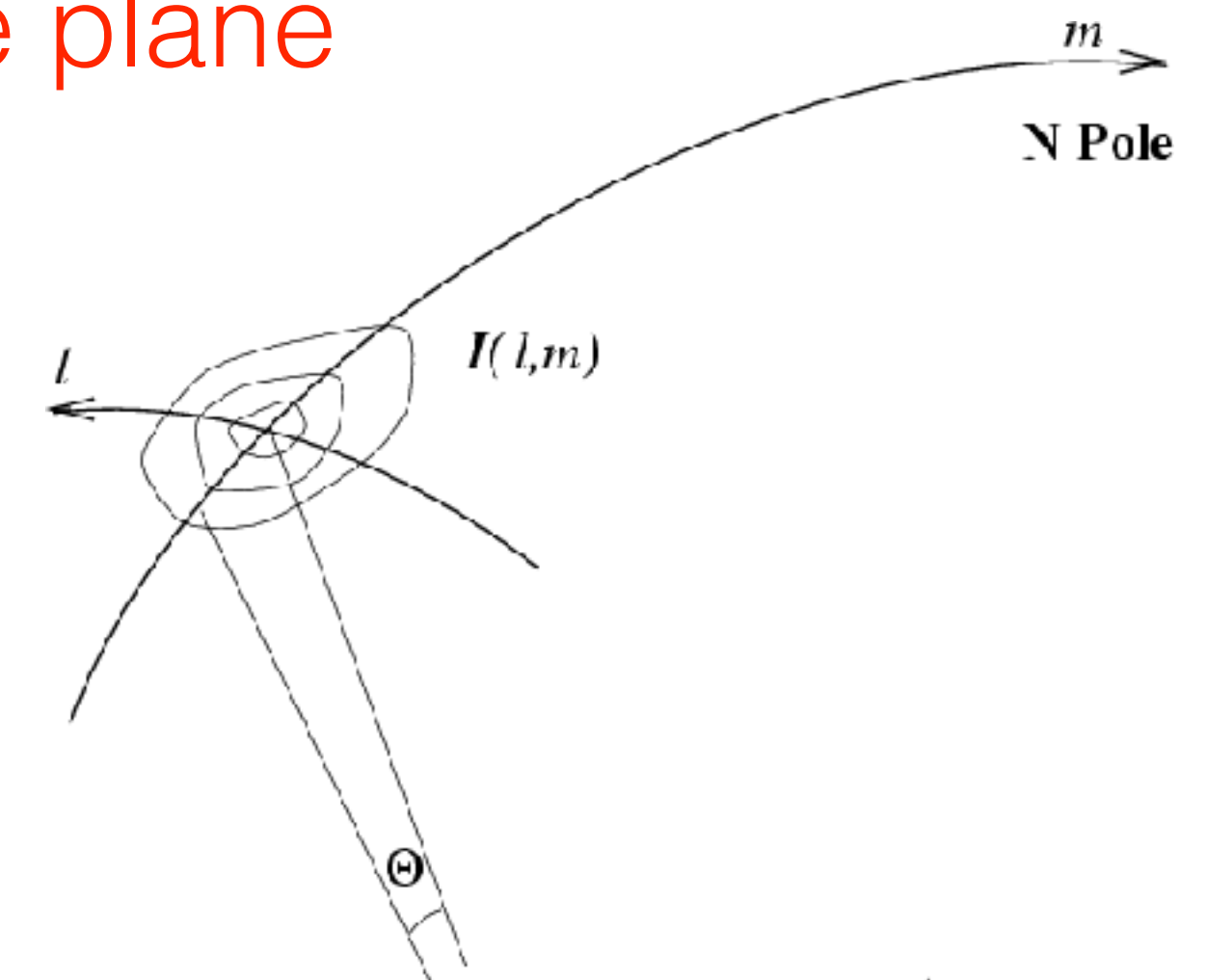


# From Sky Brightness to Visibility

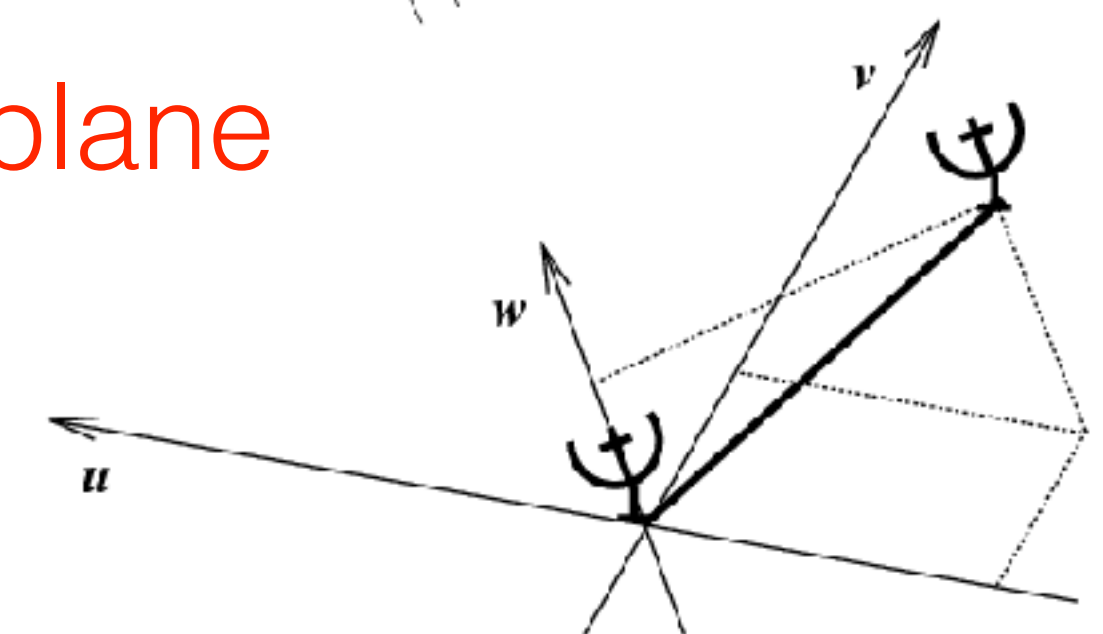
1. An Interferometer measures the interference pattern produced by two apertures.
2. The interference pattern is directly related to the source brightness. In particular, for small fields of view the complex visibility,  $V(u,v)$ , is the 2D Fourier transform of the brightness on the sky,  $T(x,y)$

(van Cittert-Zernike theorem)

Image plane



UV plane



Fourier space/domain

$$V(u, v) = \iint T(x, y) e^{2\pi i(ux + vy)} dx dy$$

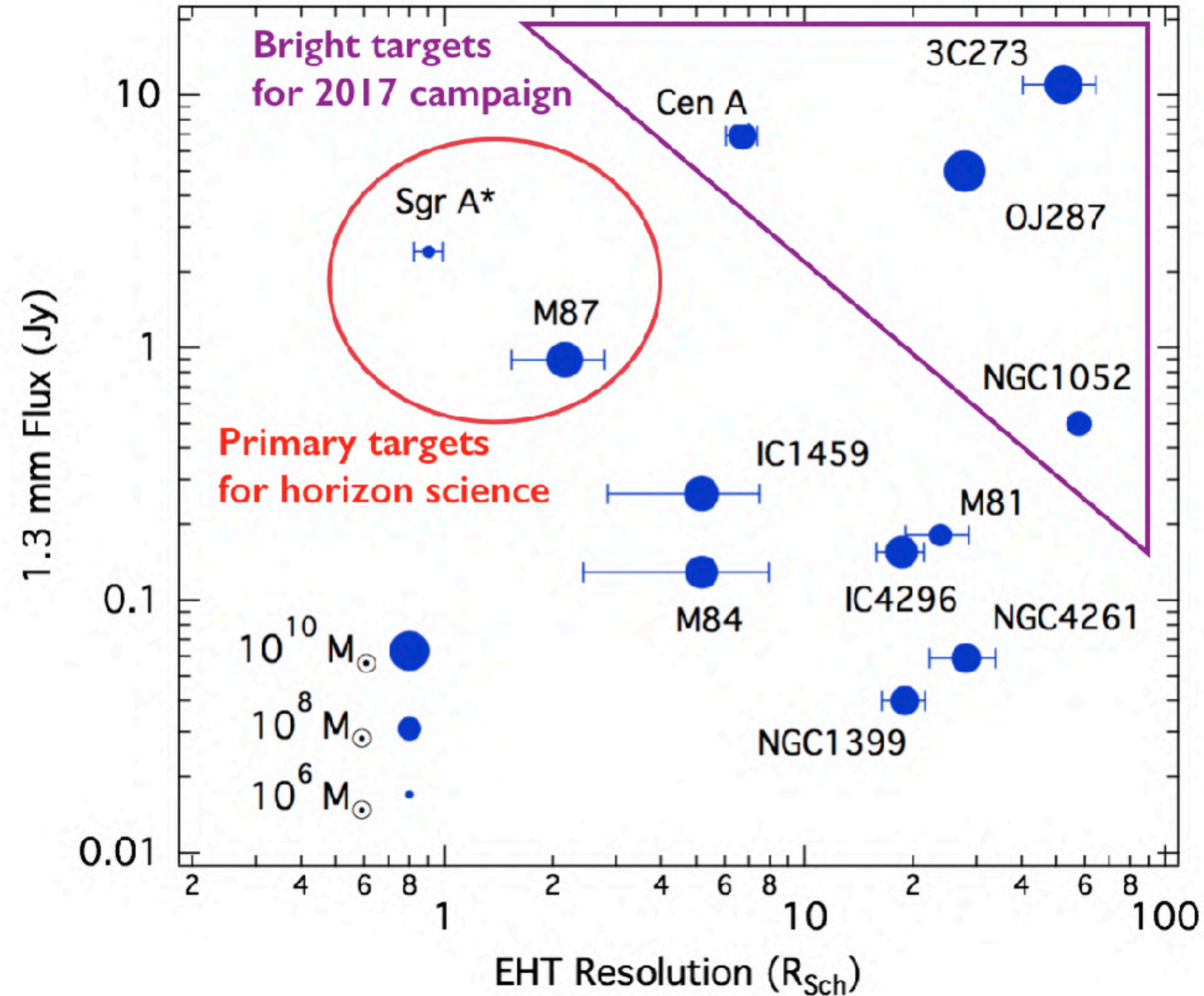
$$T(x, y) = \iint V(u, v) e^{-2\pi i(ux + vy)} du dv$$

Image space/domain





# Primary Target for EHT

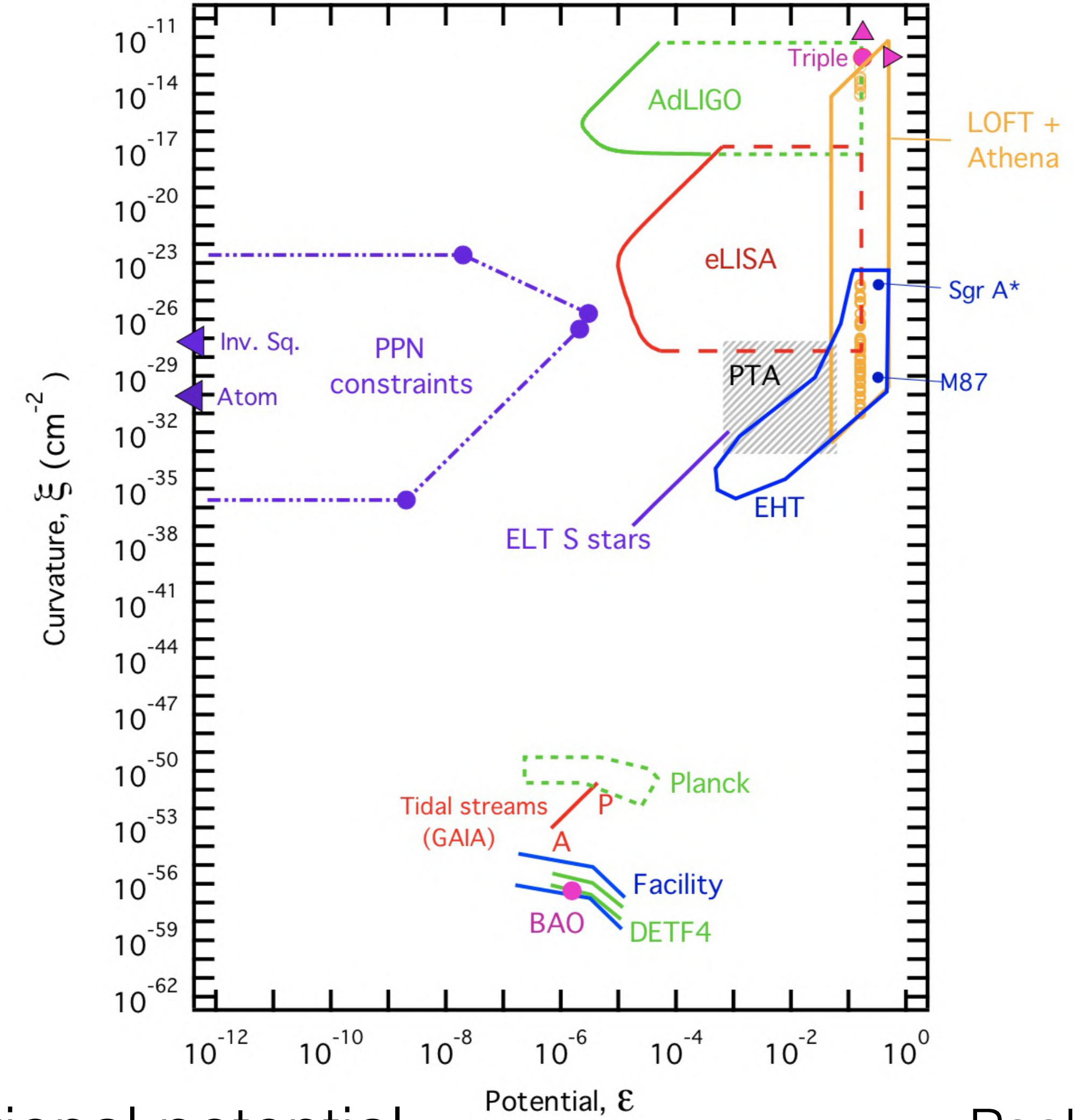
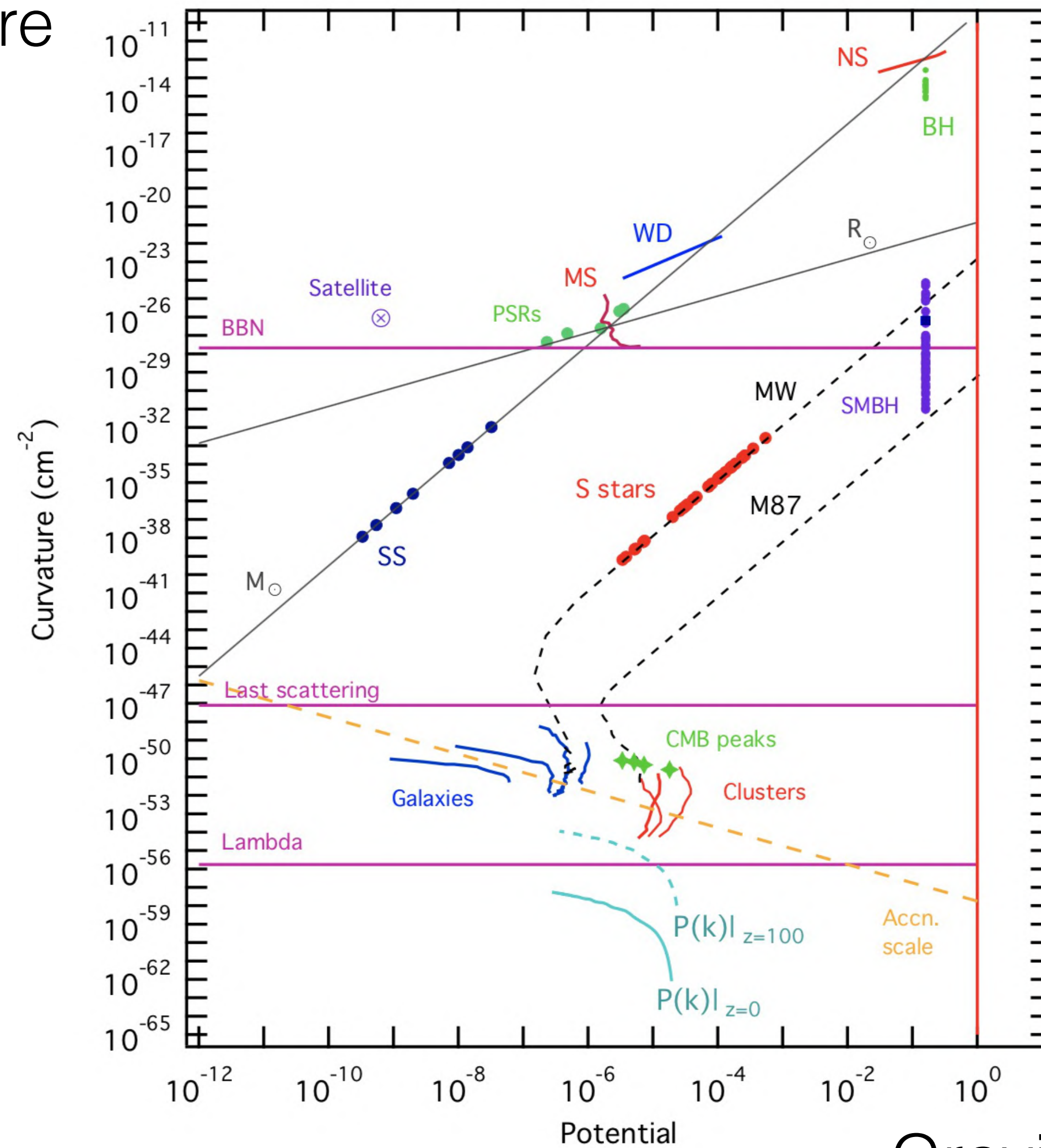


Psaltis (2018)



# Testing Theory of Gravity (experiments)

Curvature



Gravitational potential



Event Horizon Telescope

Psaltis (2018)



---

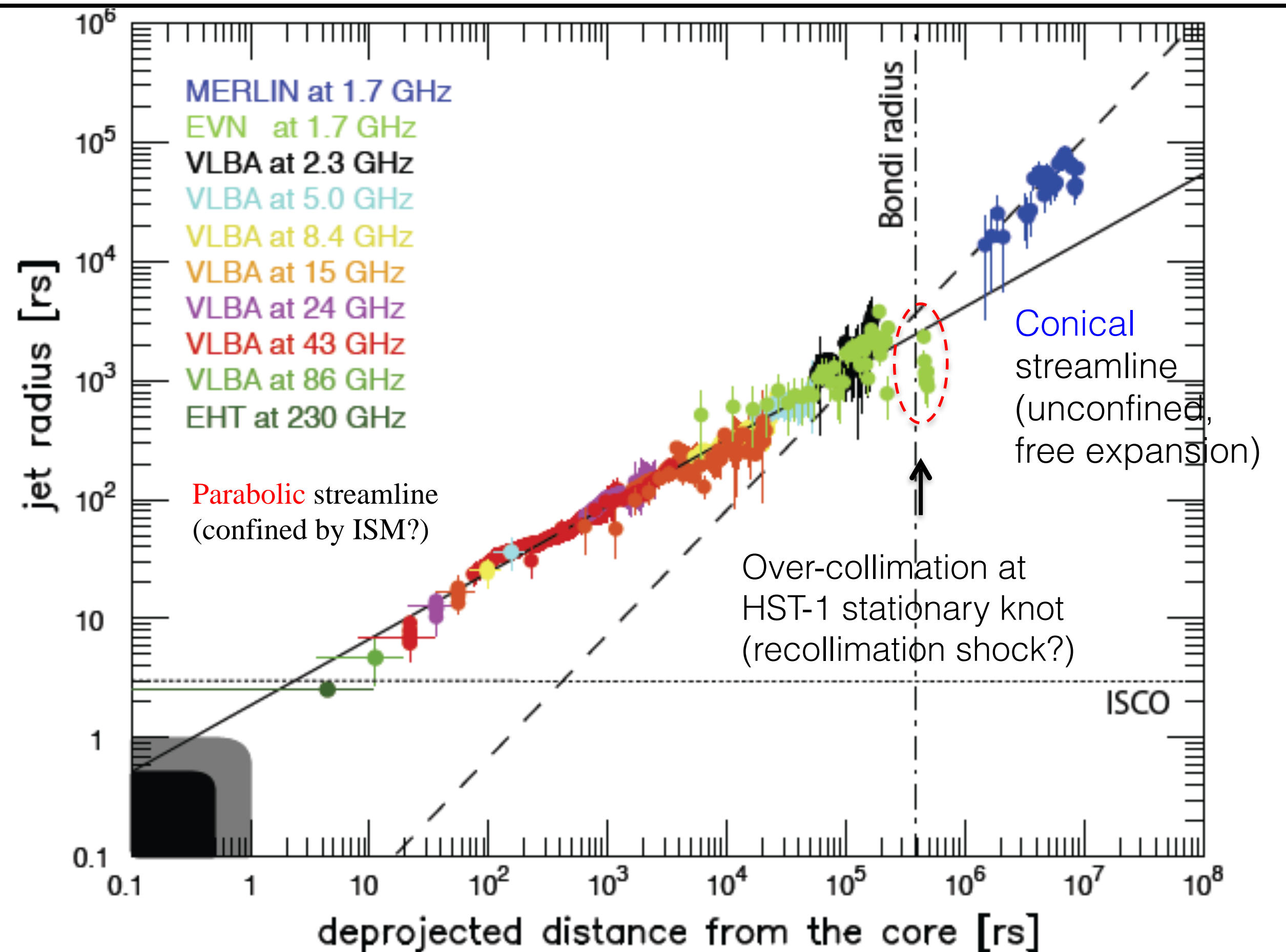
M87





# Global Structure of M87

- The parabolic structure ( $z \propto r^{1.7}$ ) maintains over  $10^5 r_s$ , external confinement is worked.
- The transition of streamlines presumably occurs beyond the gravitational influence of the SMBH (= Bondi radius)
- In far region, jet stream line is conical ( $z \propto r$ )
- Stationary feature HST-1 is a consequence of the jet recollimation due to the pressure imbalance at the transition



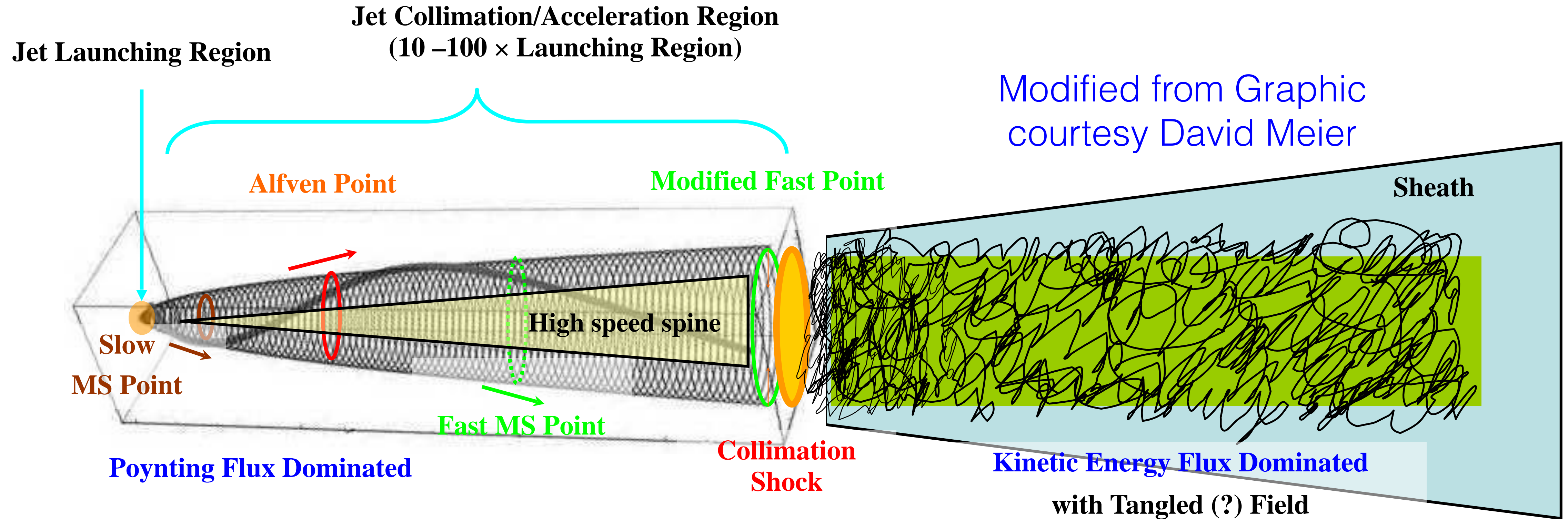
HST-1 region

Asada & Nakamura (2012),  
Hada et al. (2013)





# Regions of AGN Jet Propagation



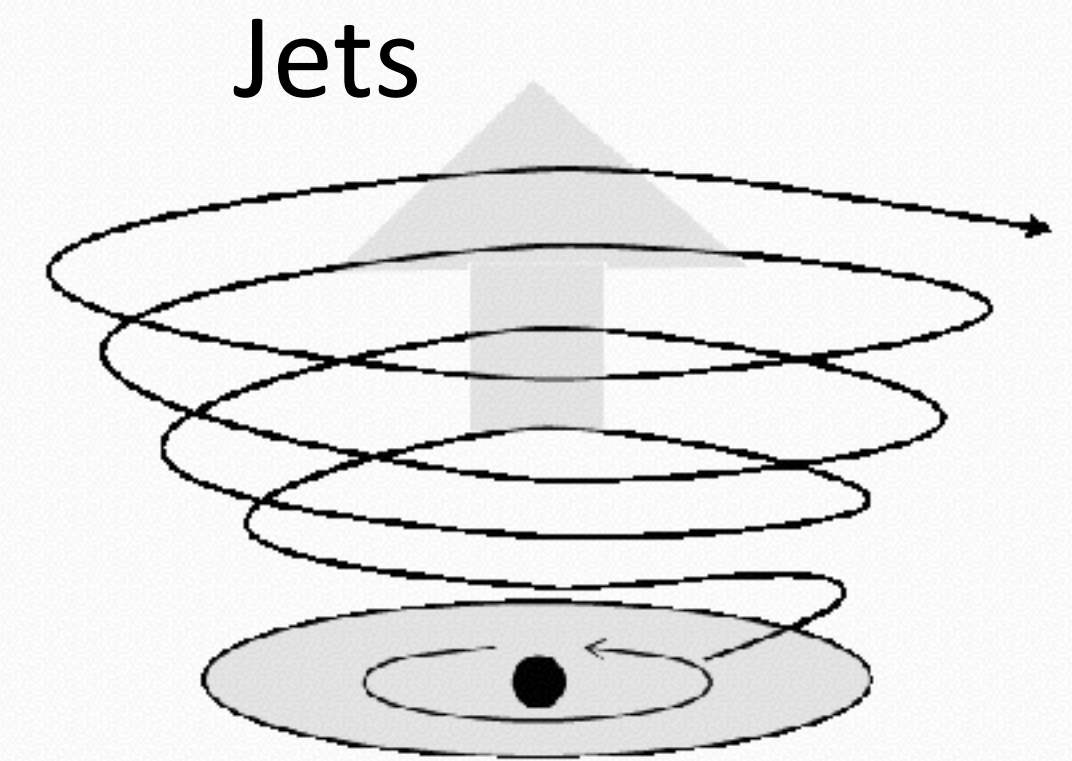
- Jet launching by MHD process  $\Rightarrow$  Poynting flux dominated jet with twisted magnetic field
- Need rapid magnetic energy dissipation to make a kinetic energy dominated jet



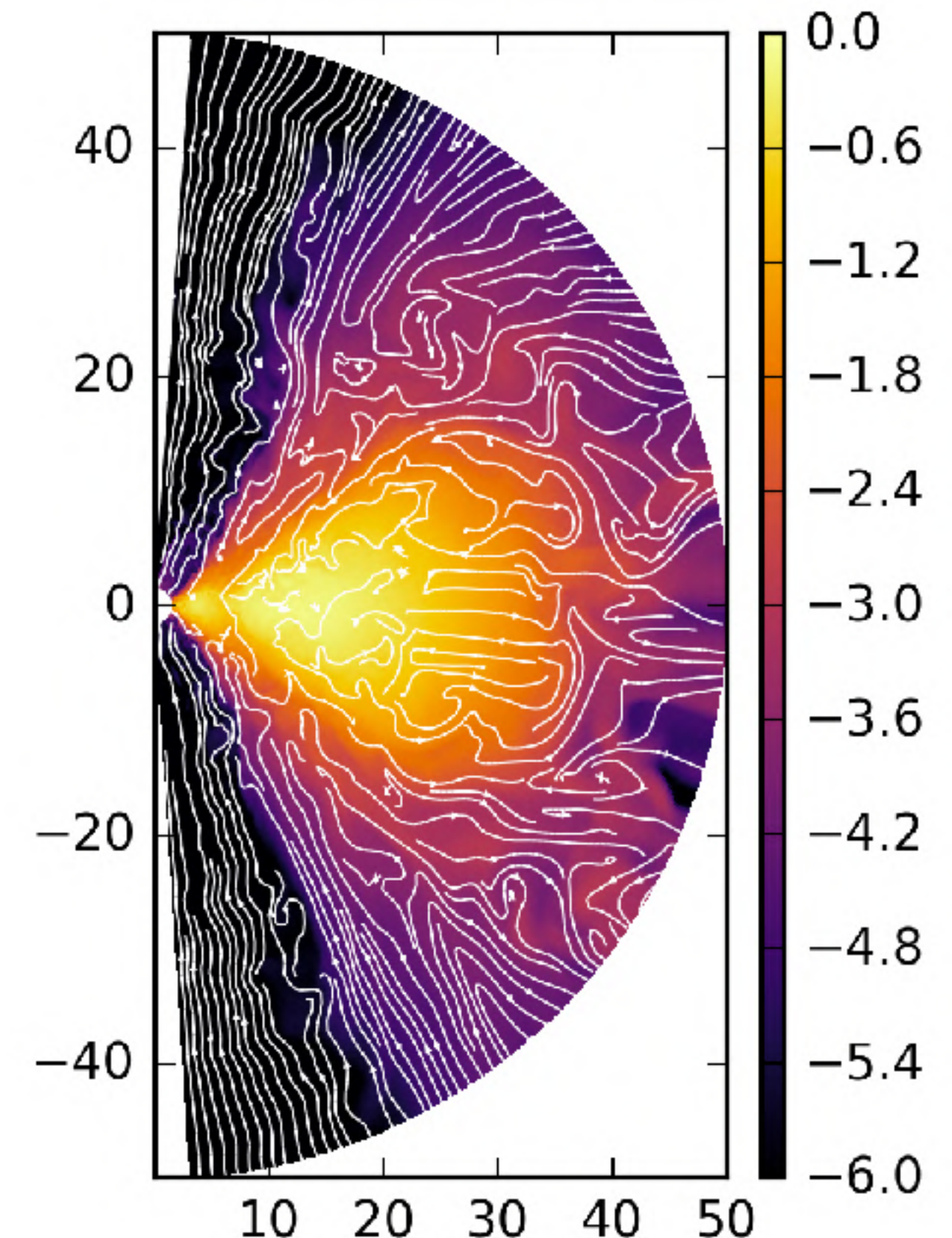


# Theory of Jet Formation & Acceleration

- Relativistic jet is formed and accelerated by macroscopic plasma (**MHD**) process with helically twisted magnetic field
  - Collimated jet is formed near the central BH and accelerates  $\gamma \gg 1$
  - **But**, it has problems
    - Most of energy remains in **Poynting energy** (**magnetic energy**)
    - Acceleration need take longer time (**slow** acceleration efficiency)
- ⇒ Rapid energy conversion (**dissipation**) should be considered



MHD process  
(schematic picture)



GRMHD simulations  
By BHAC code (Porth et al. 17)

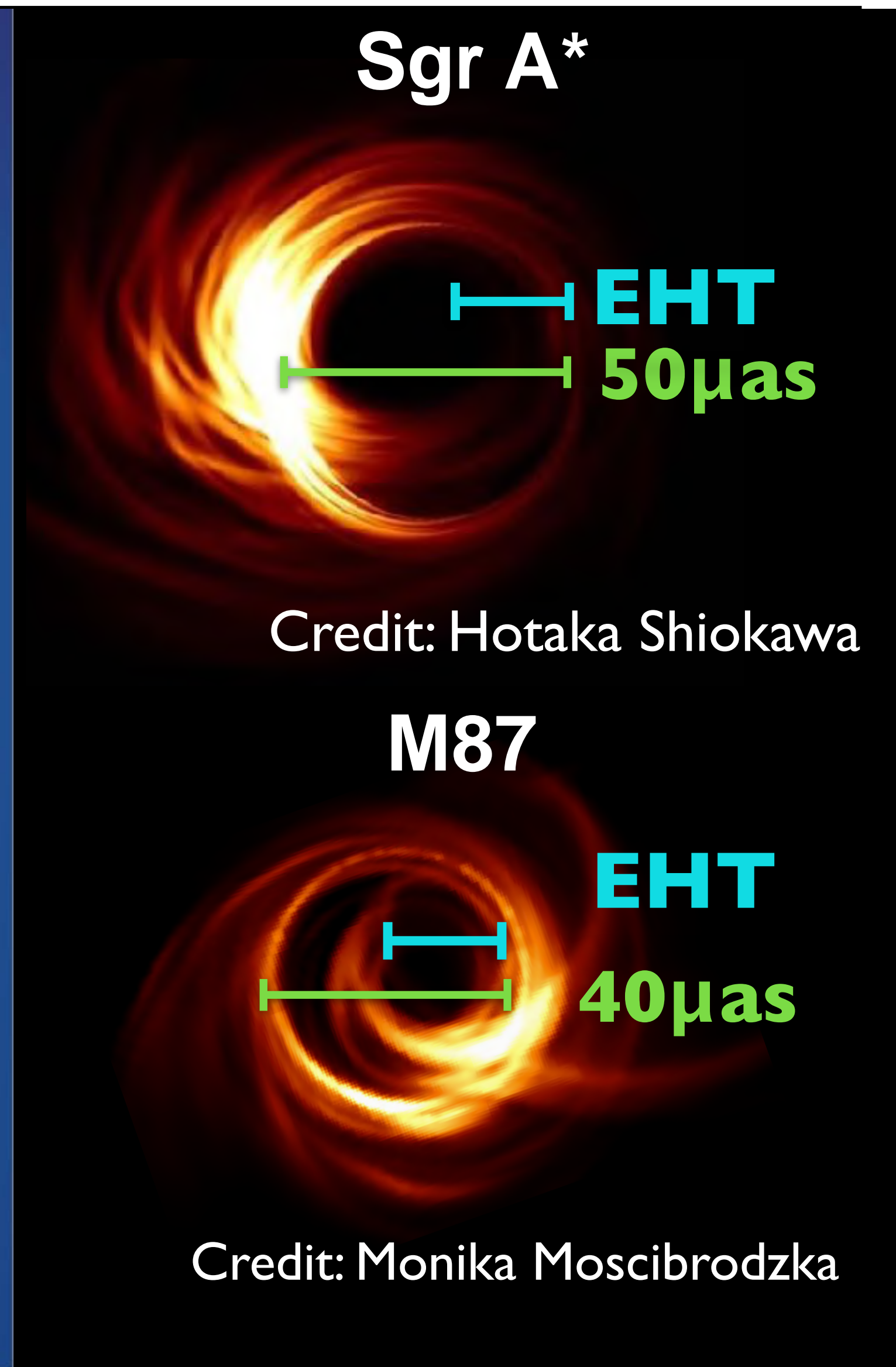


---

# Pre EHT results

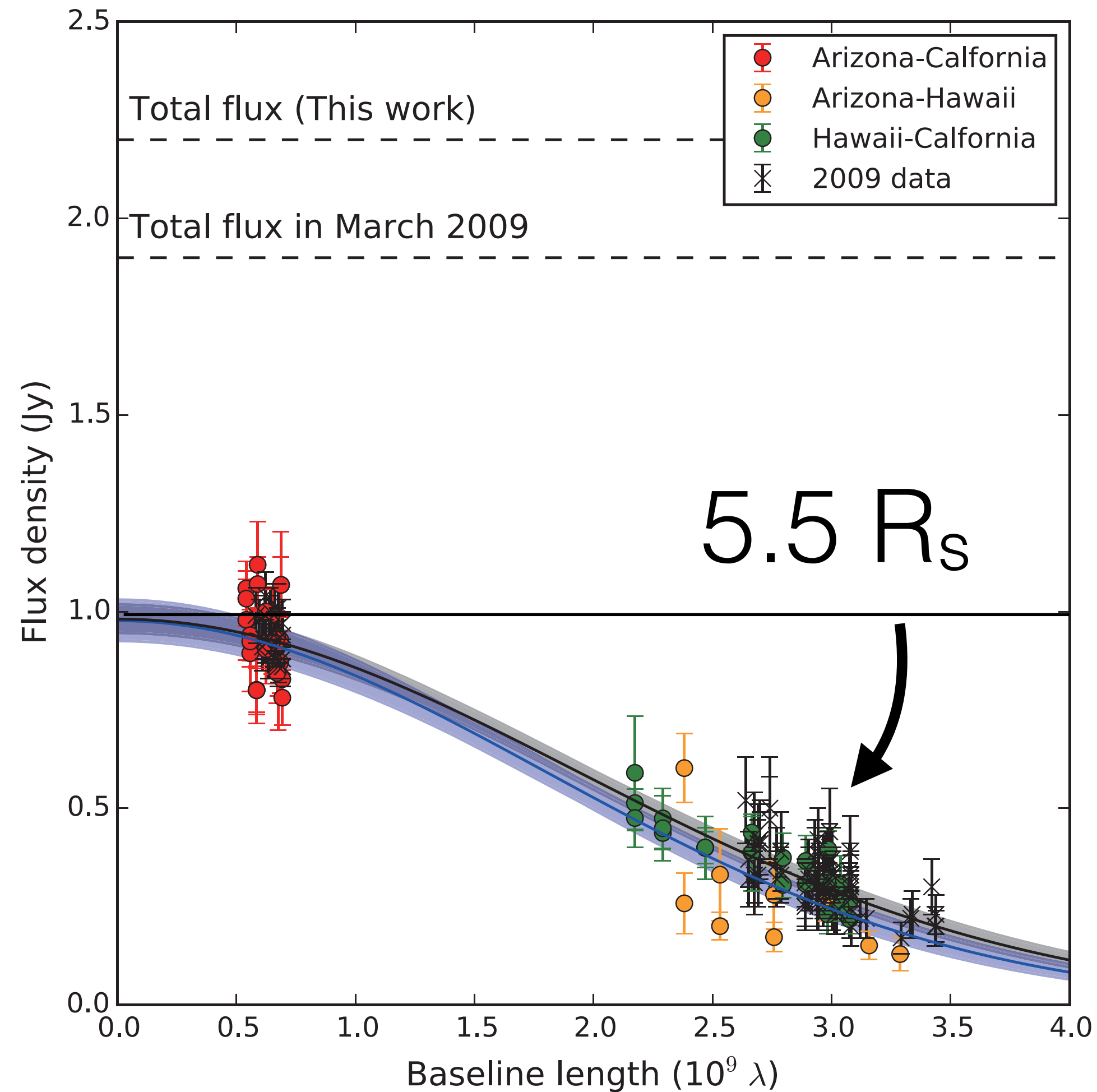


# Event Horizon Telescope

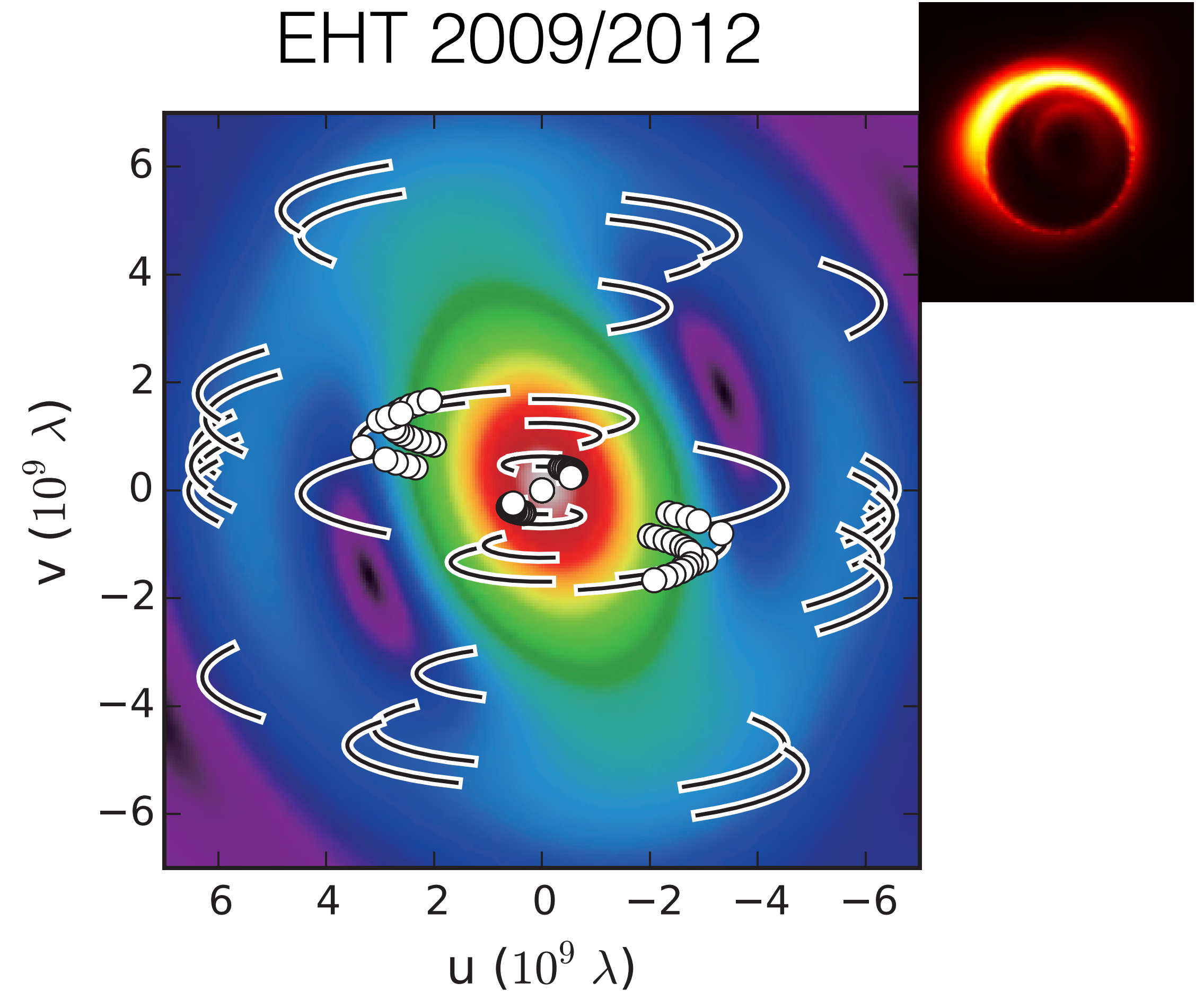




# Early EHT M87 Results: 2009 and 2012 observations



(Doeleman et al. 2012; Akiyama et al. 2015)



(Akiyama et al. 2015)





---

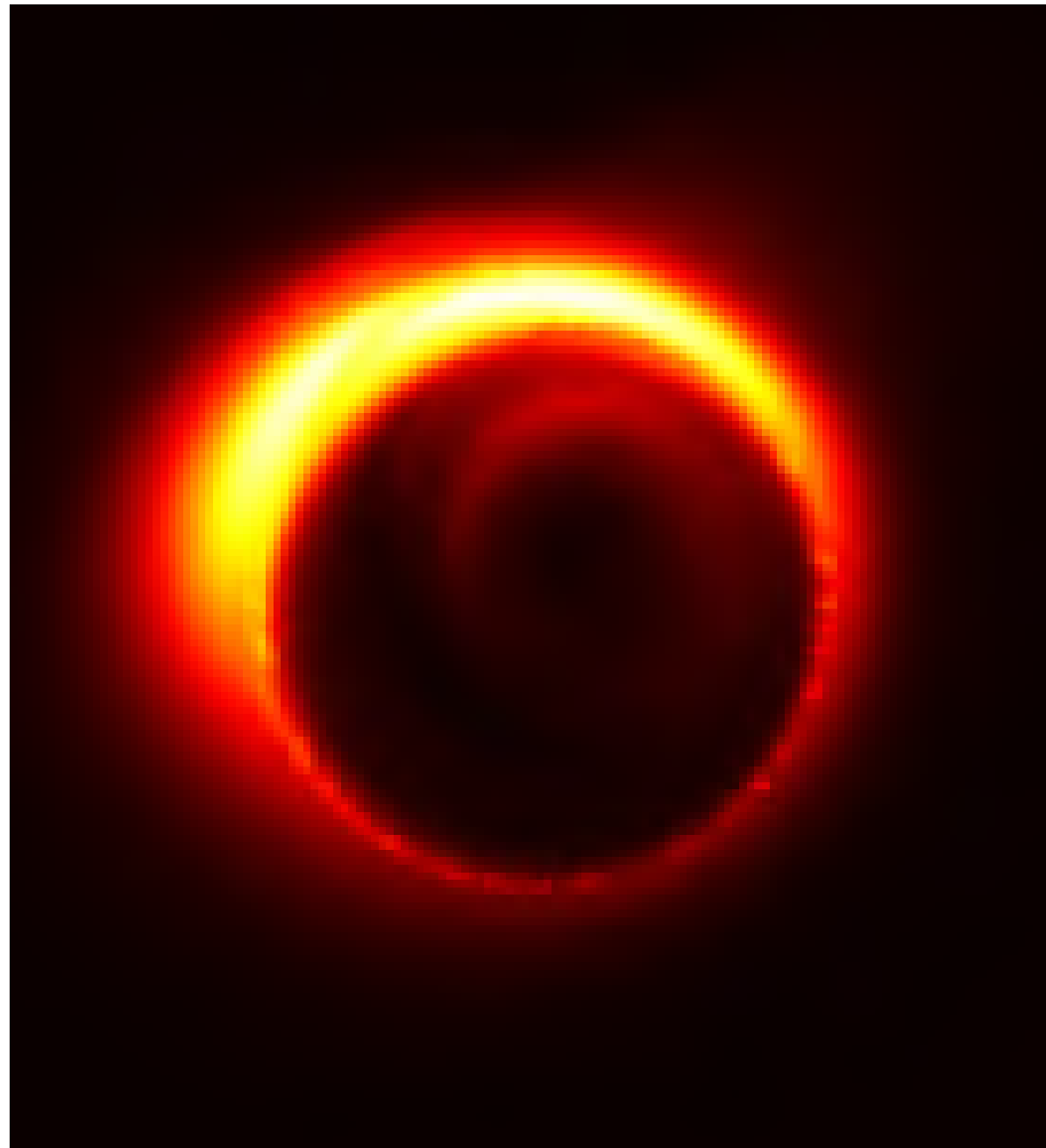
# EHT Imaging



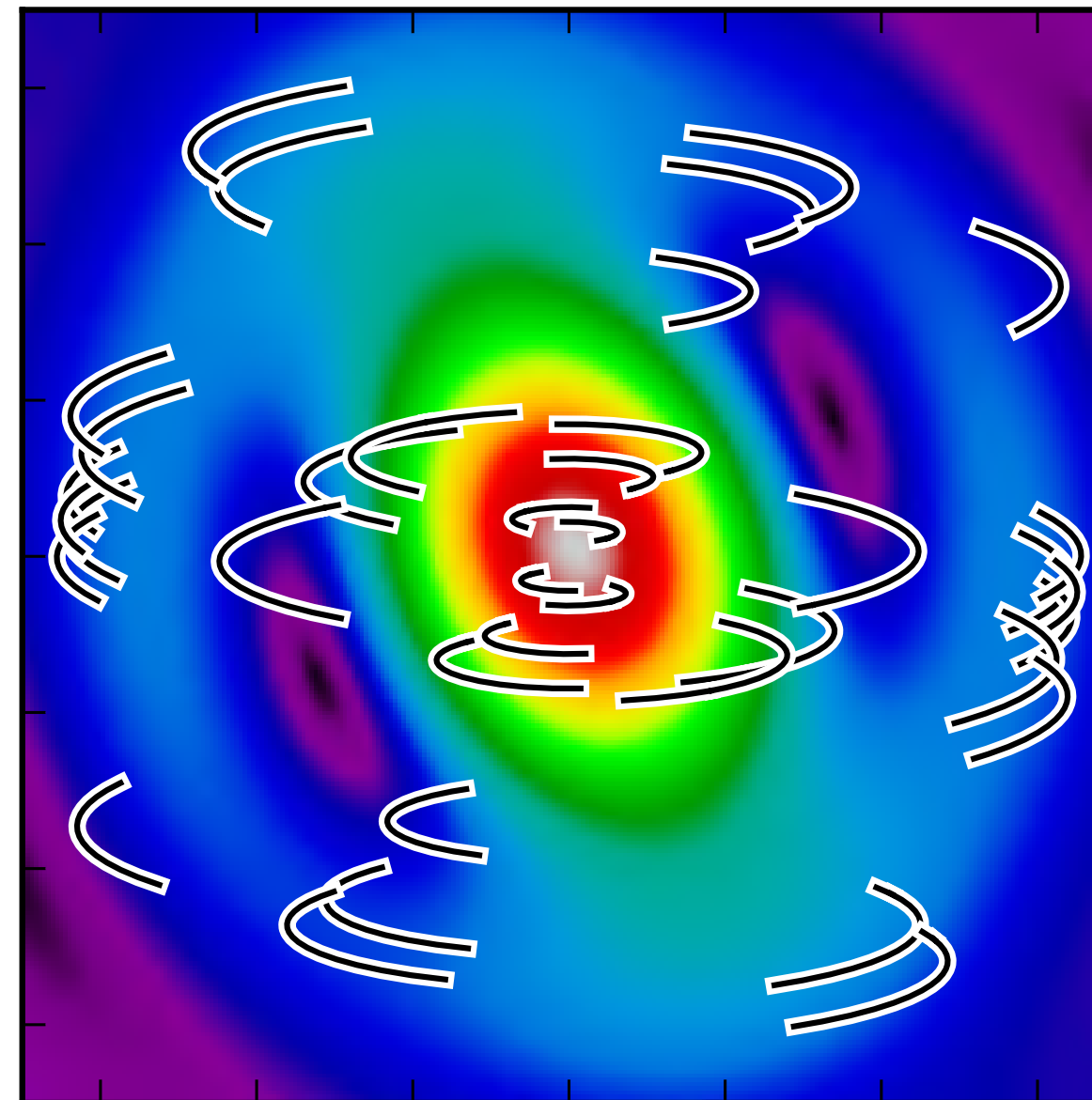


# How the EHT works?

Image

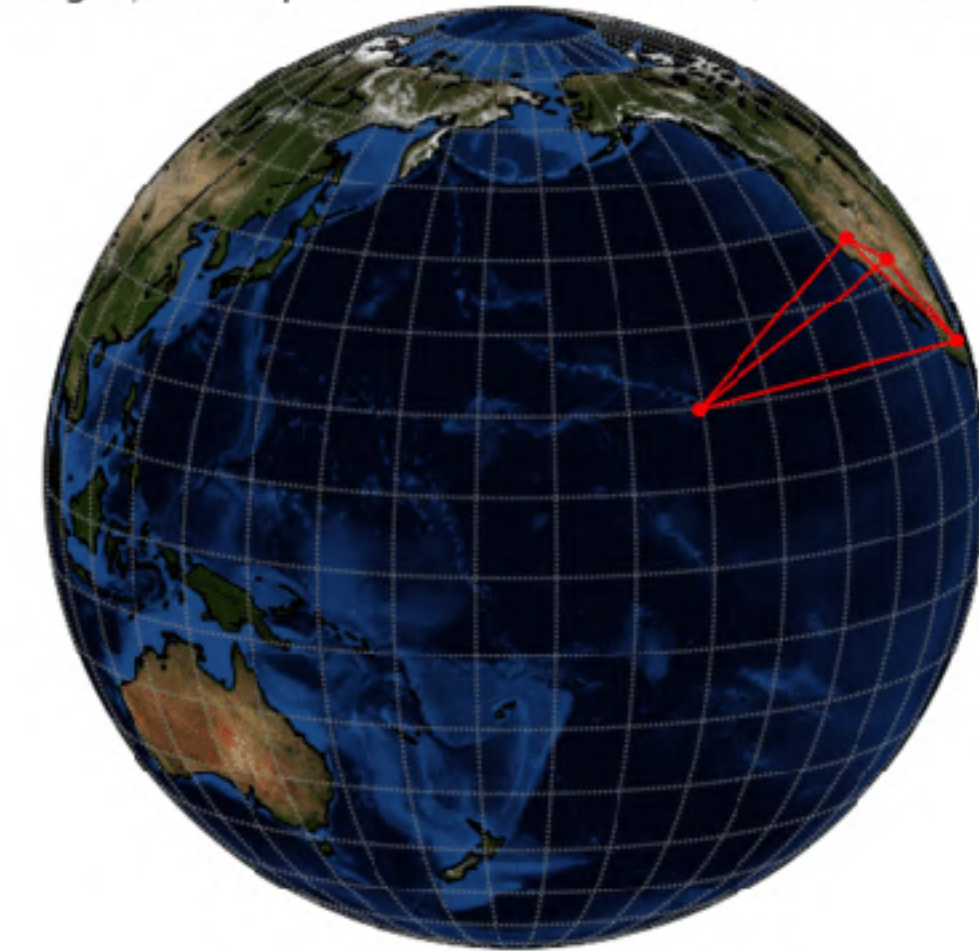


Fourier Domain  
(*Visibility*)



Sampling Process  
(Projected Baseline = Spatial Frequency)

Orthographic Map Centered on Lon=180, Lat=12.391123



(Images: Akiyama et al. 2015; Movie: L. Vertatschitsch)

Spatial Frequency = Baseline Length

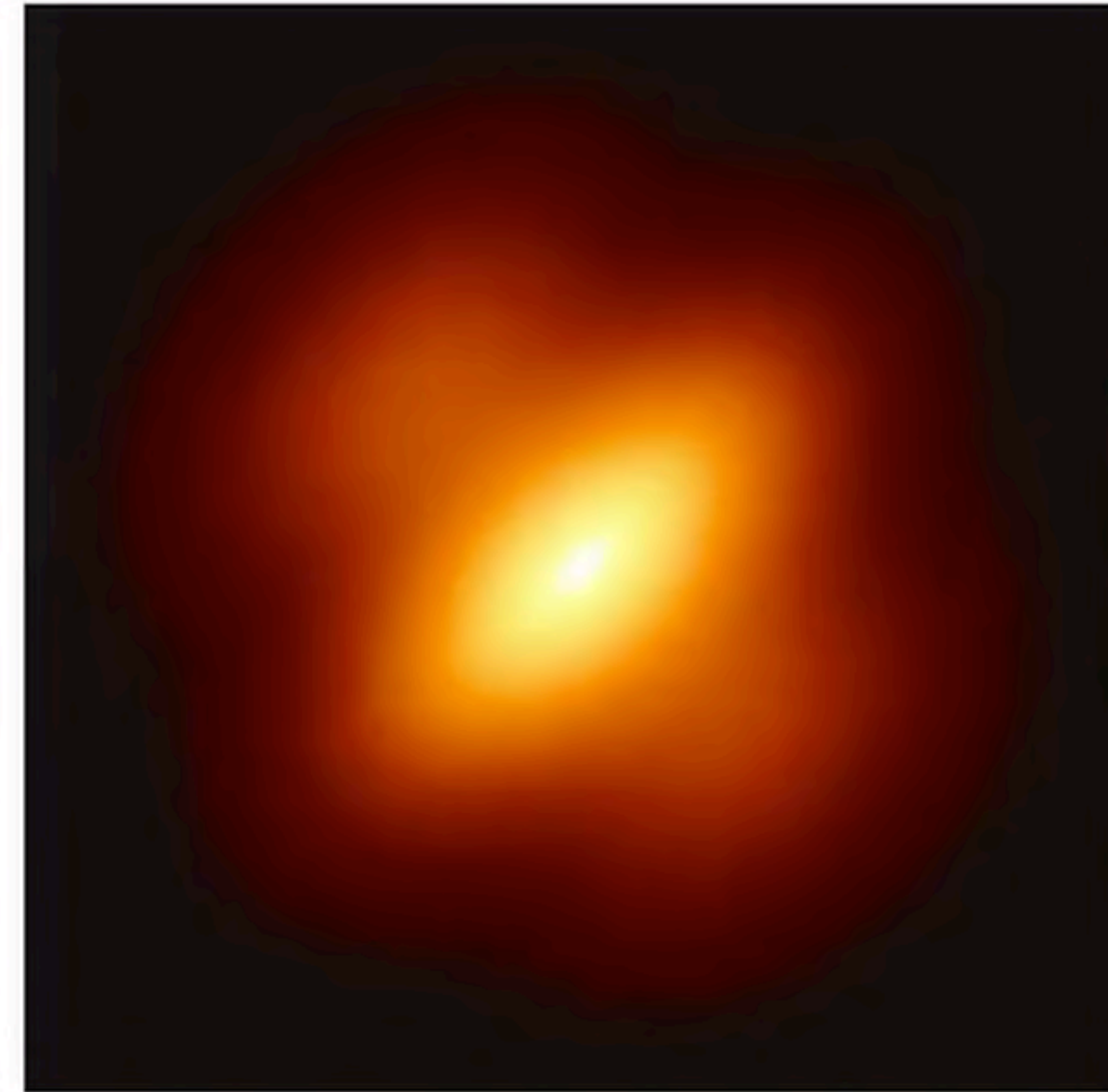
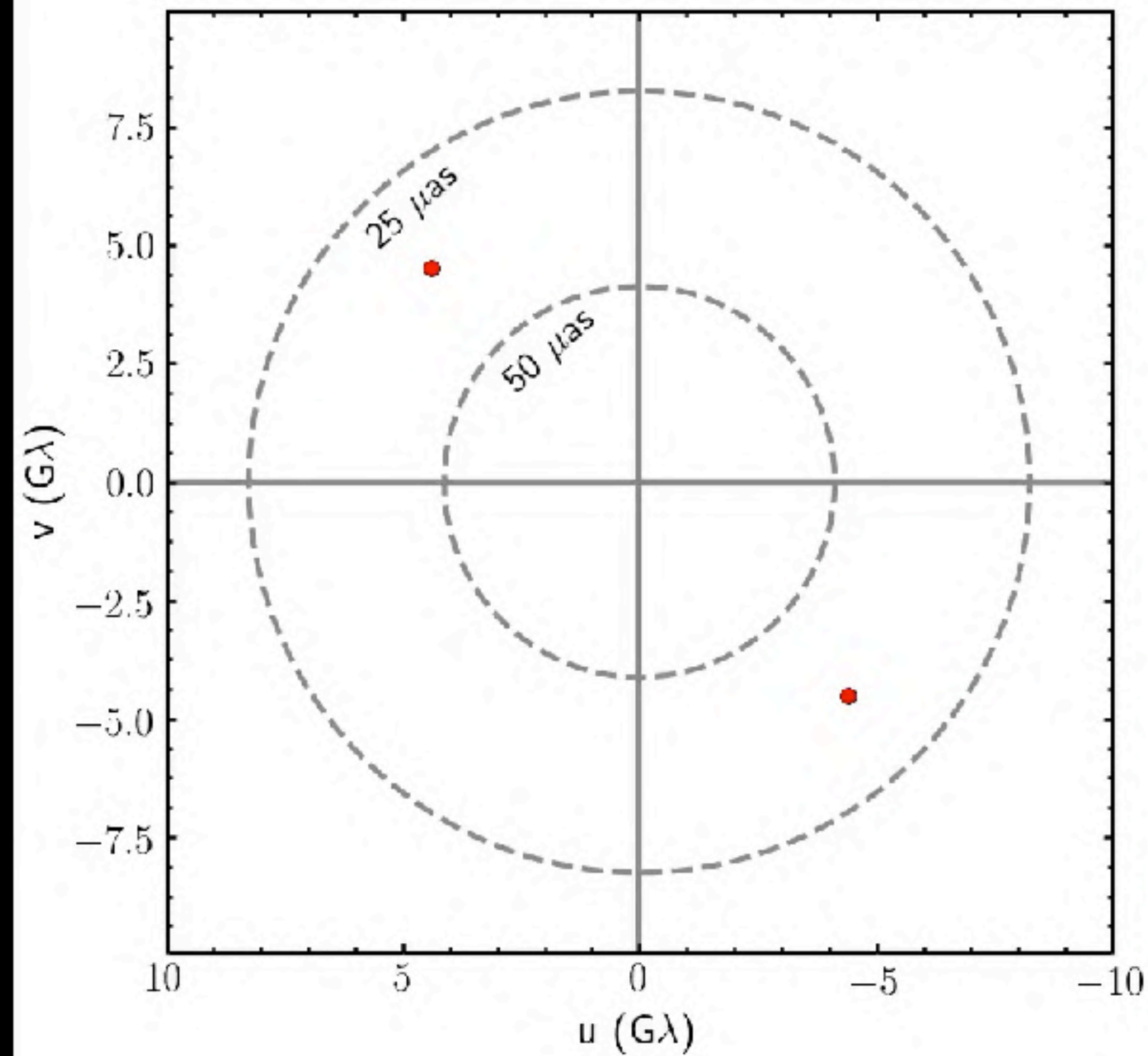
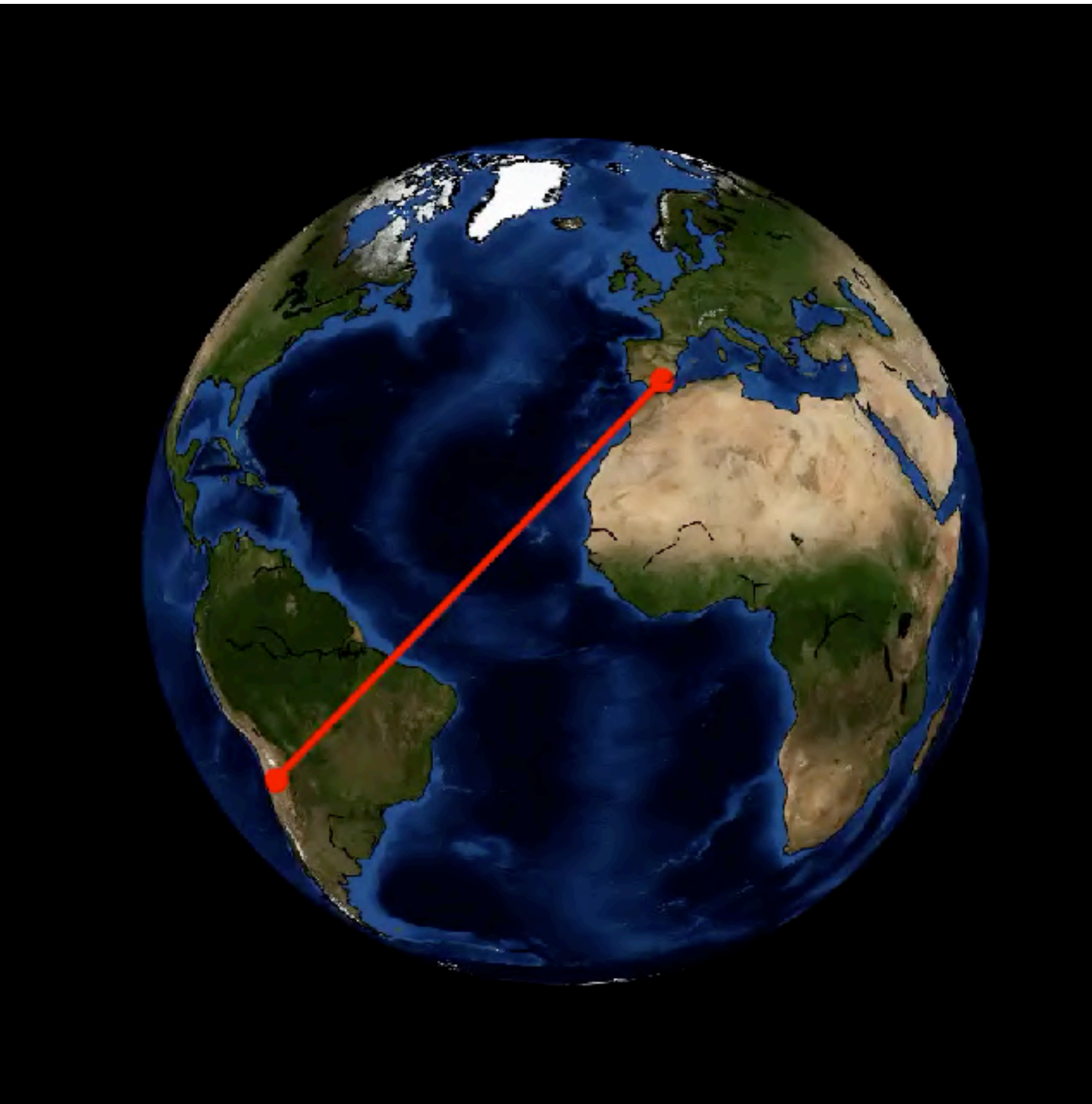
Longer Baselines trace more compact structure





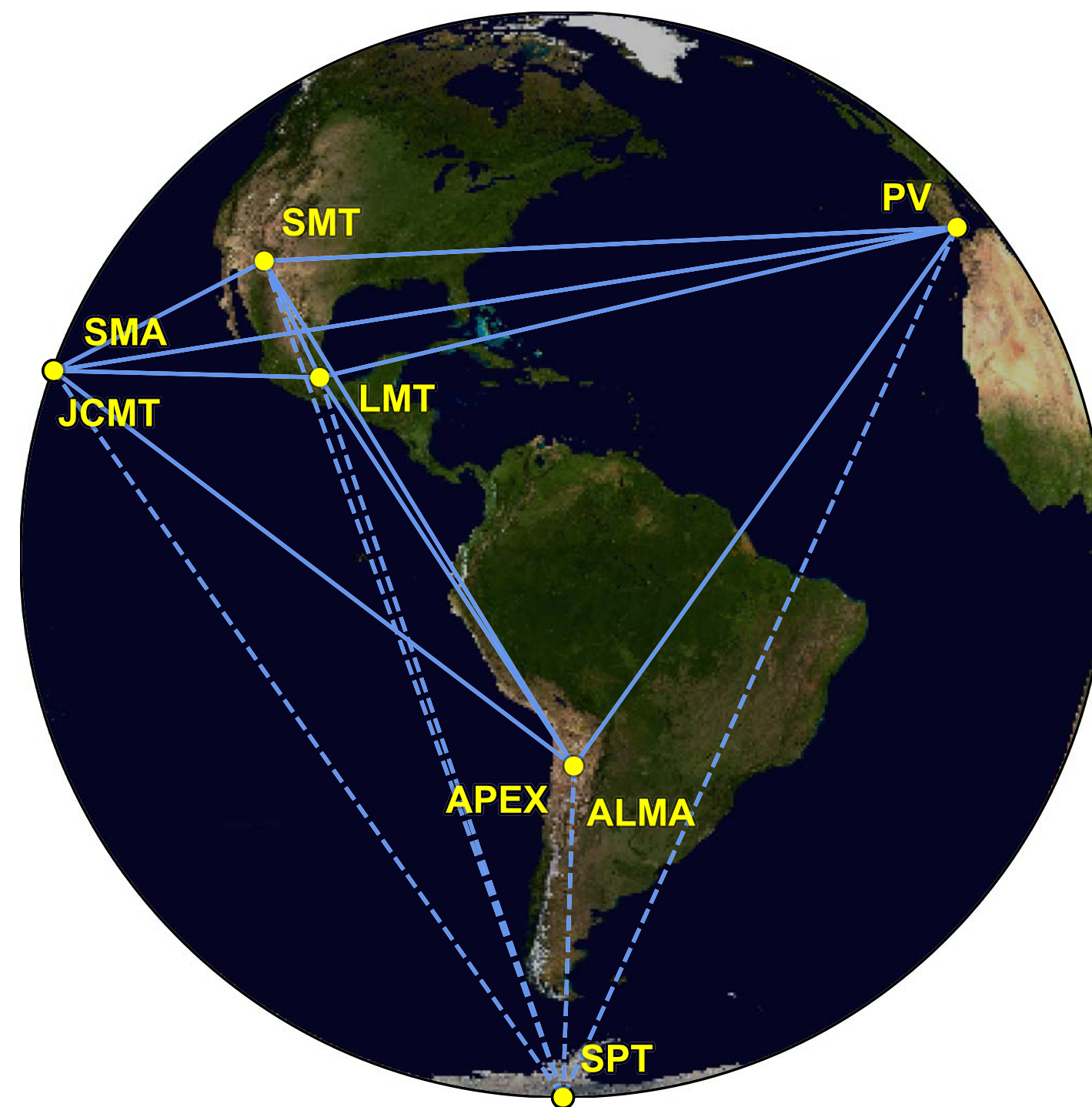
# Earth Rotation Synthesis

EHT 2017 observation of M87

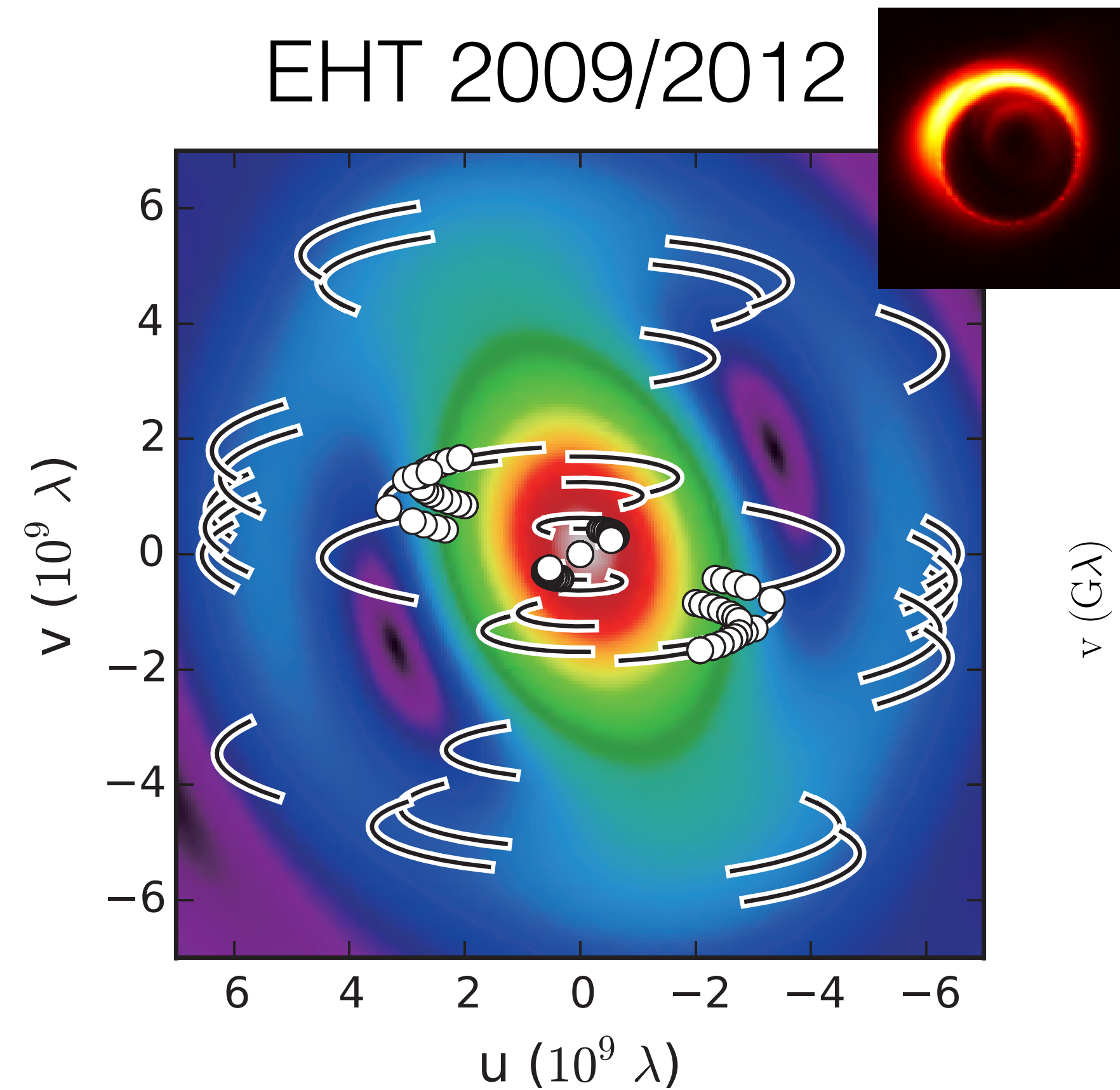




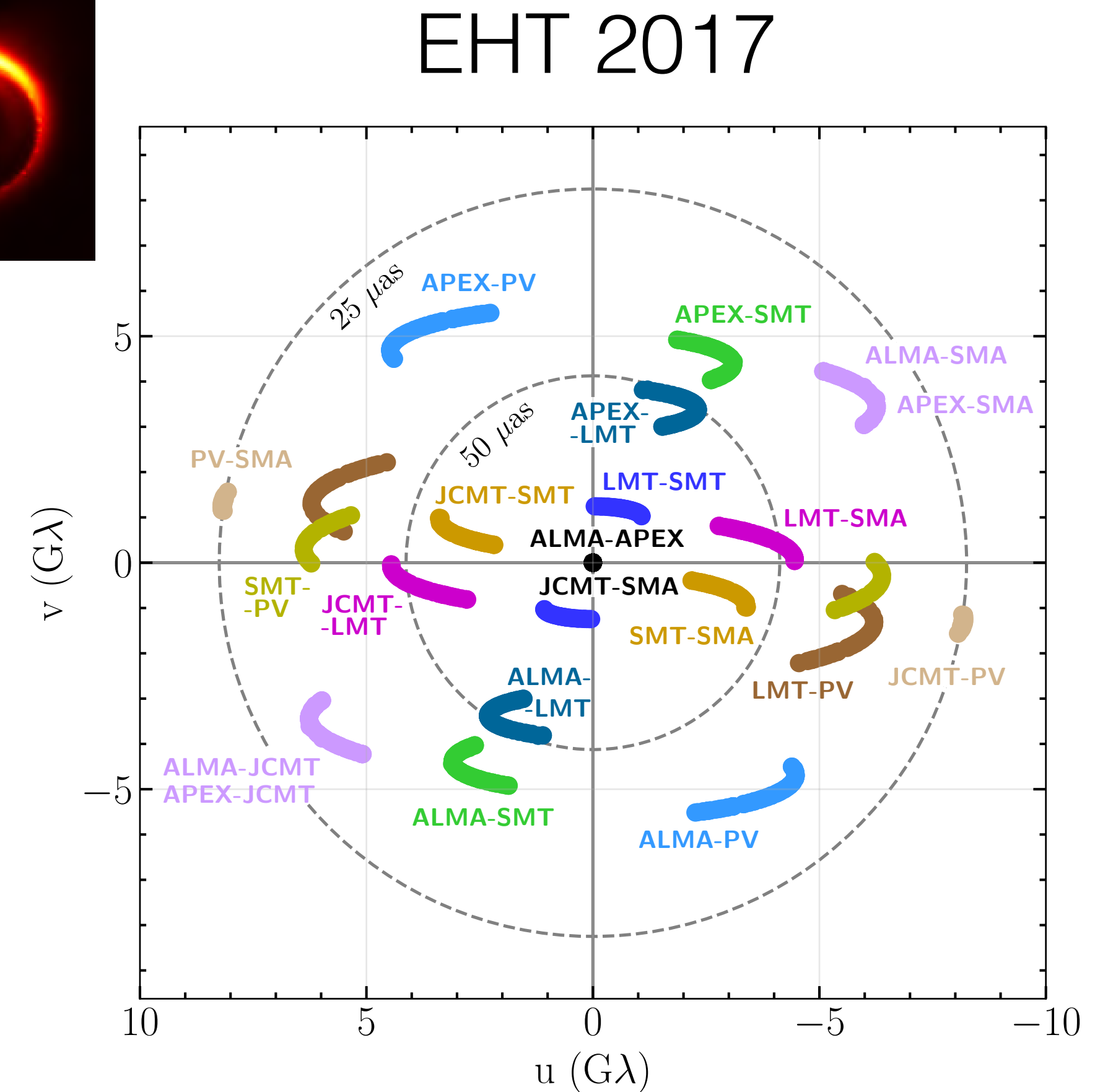
# Event Horizon Telescope 2017 Observations



(Paper III)



(Akiyama et al. 2015)



(Paper III)

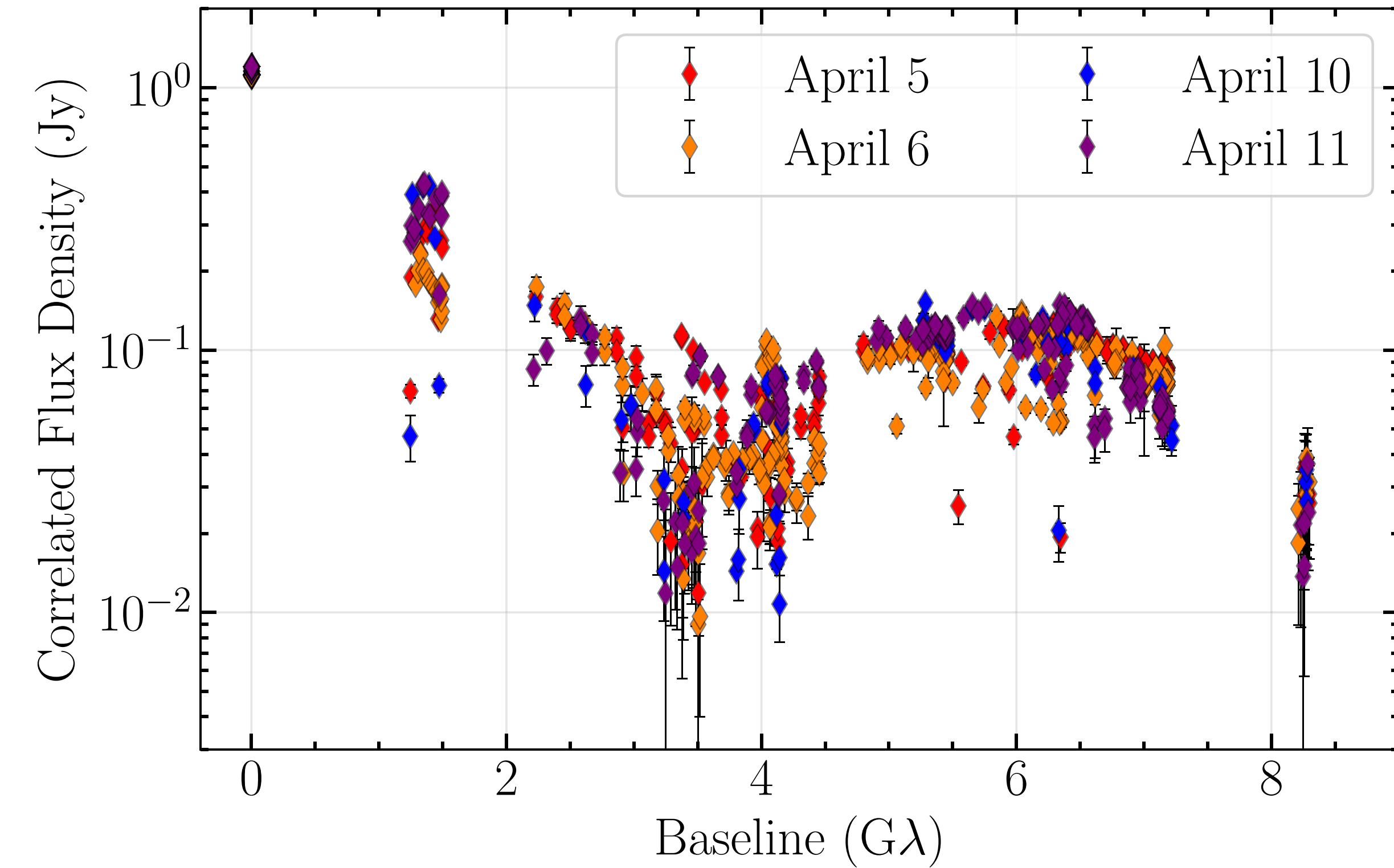
Three Data Processing Pipelines: HOPS (Blackburn+19), CASA (Janssen+19), AIPS



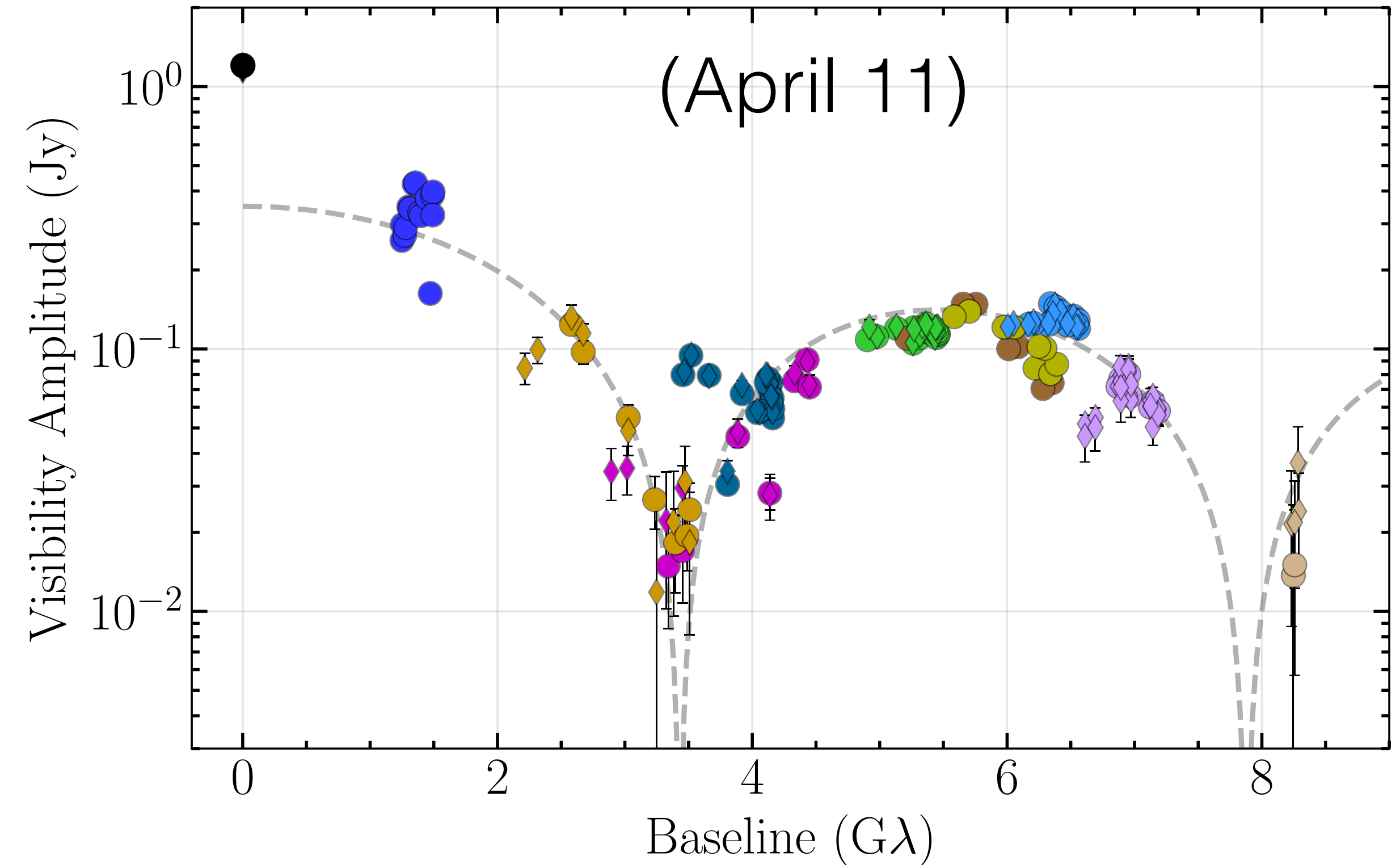
Event Horizon Telescope



# Calibrated data sets (before imaging)



(Paper III)



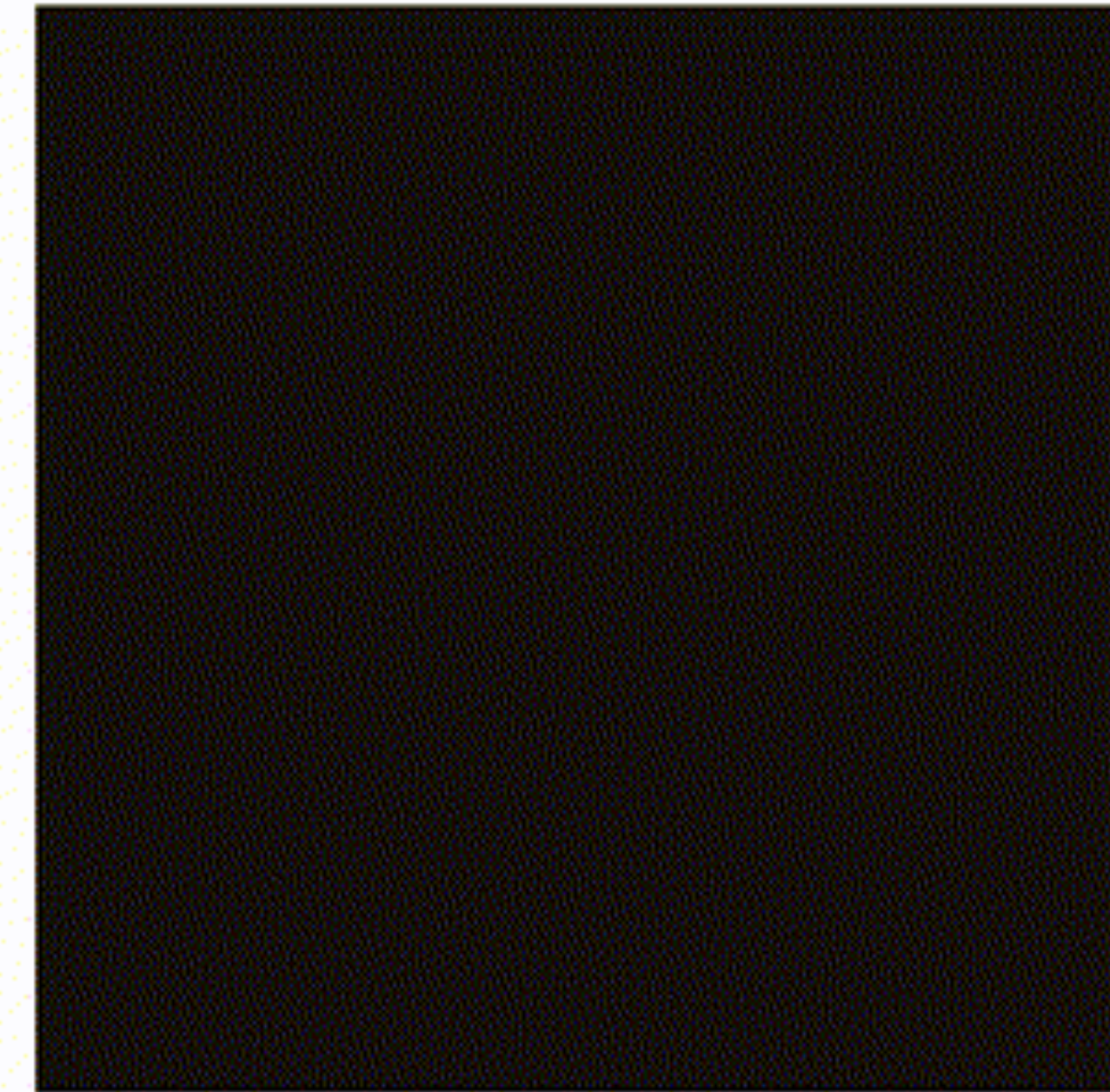
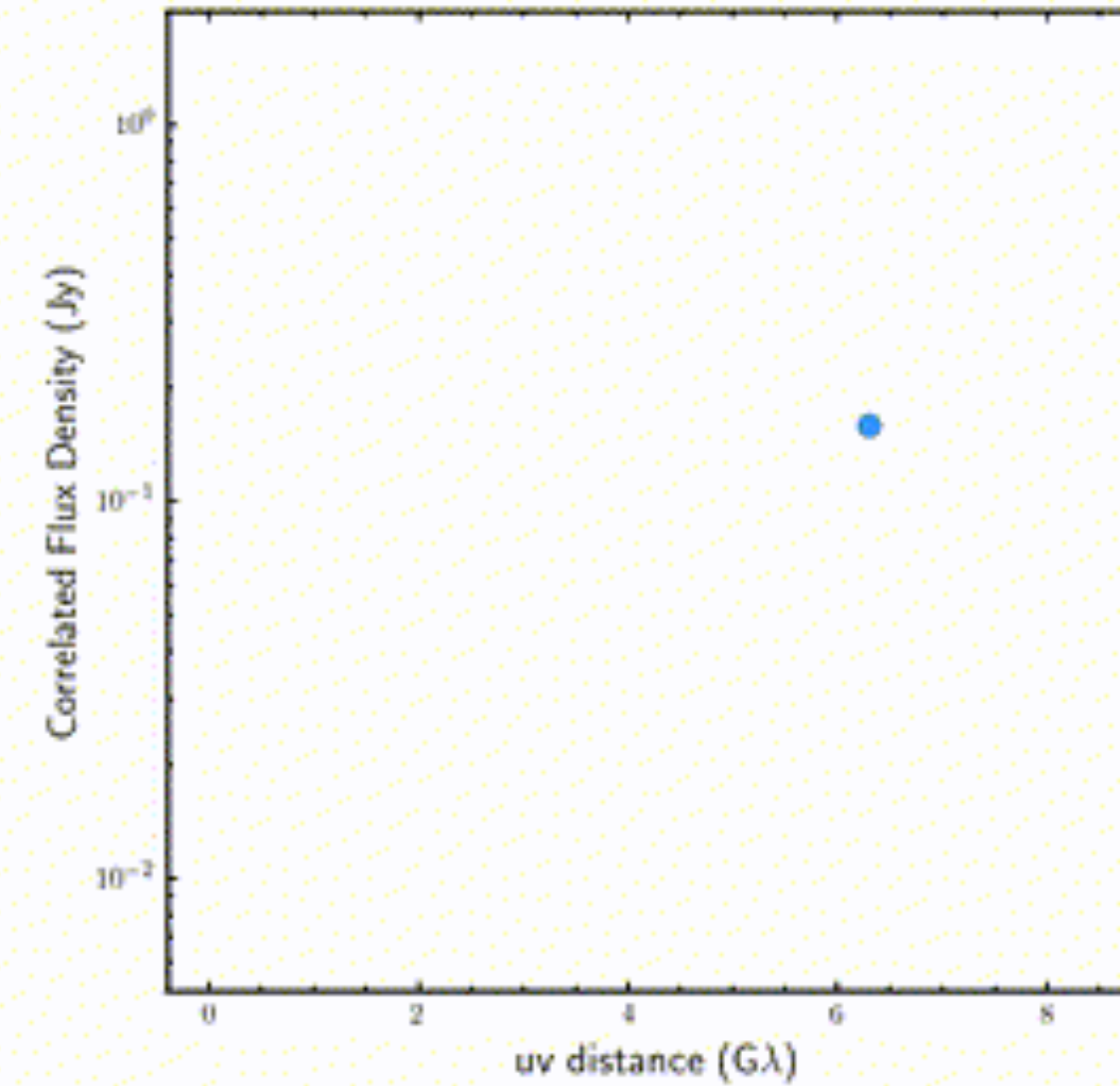
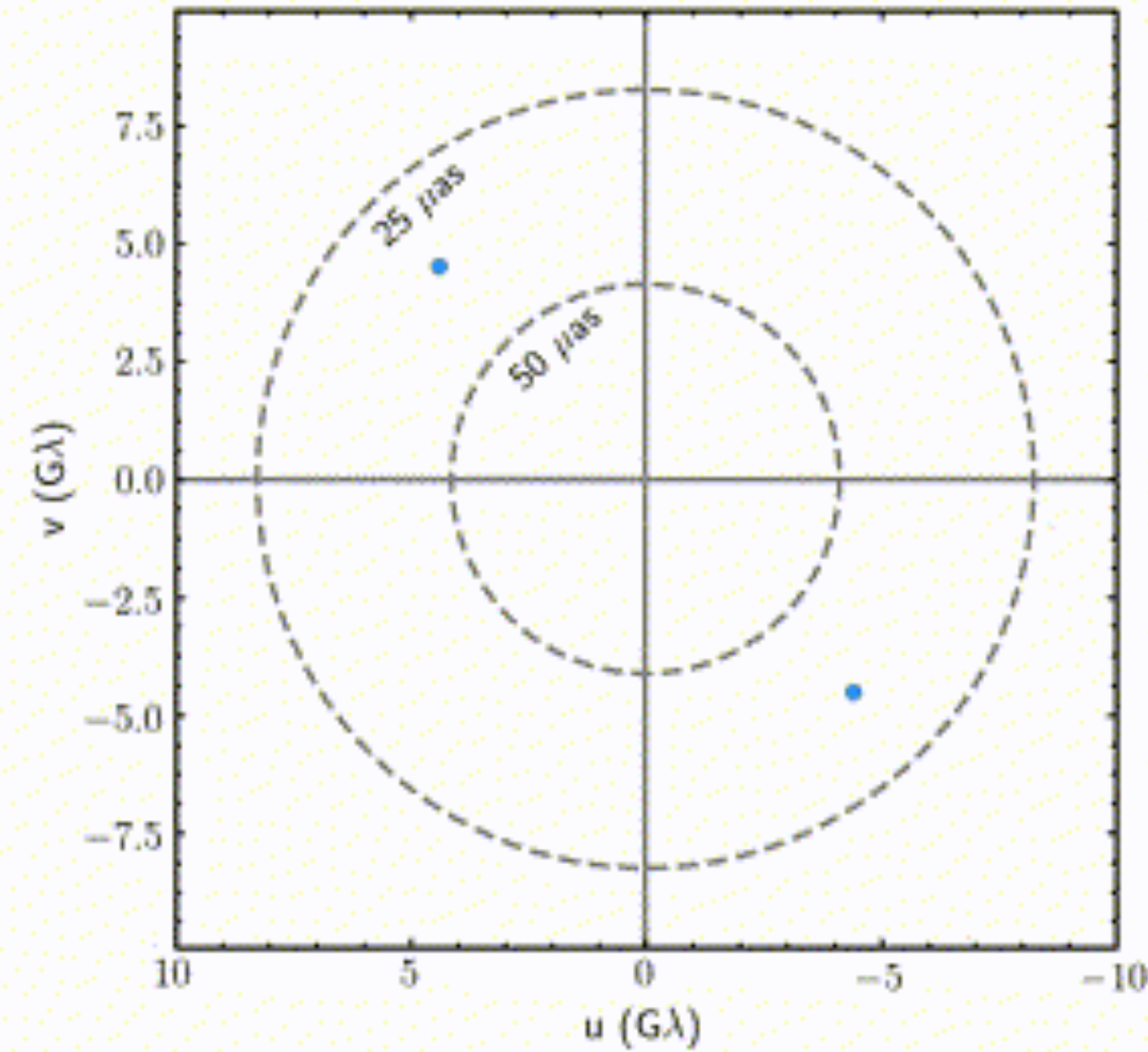
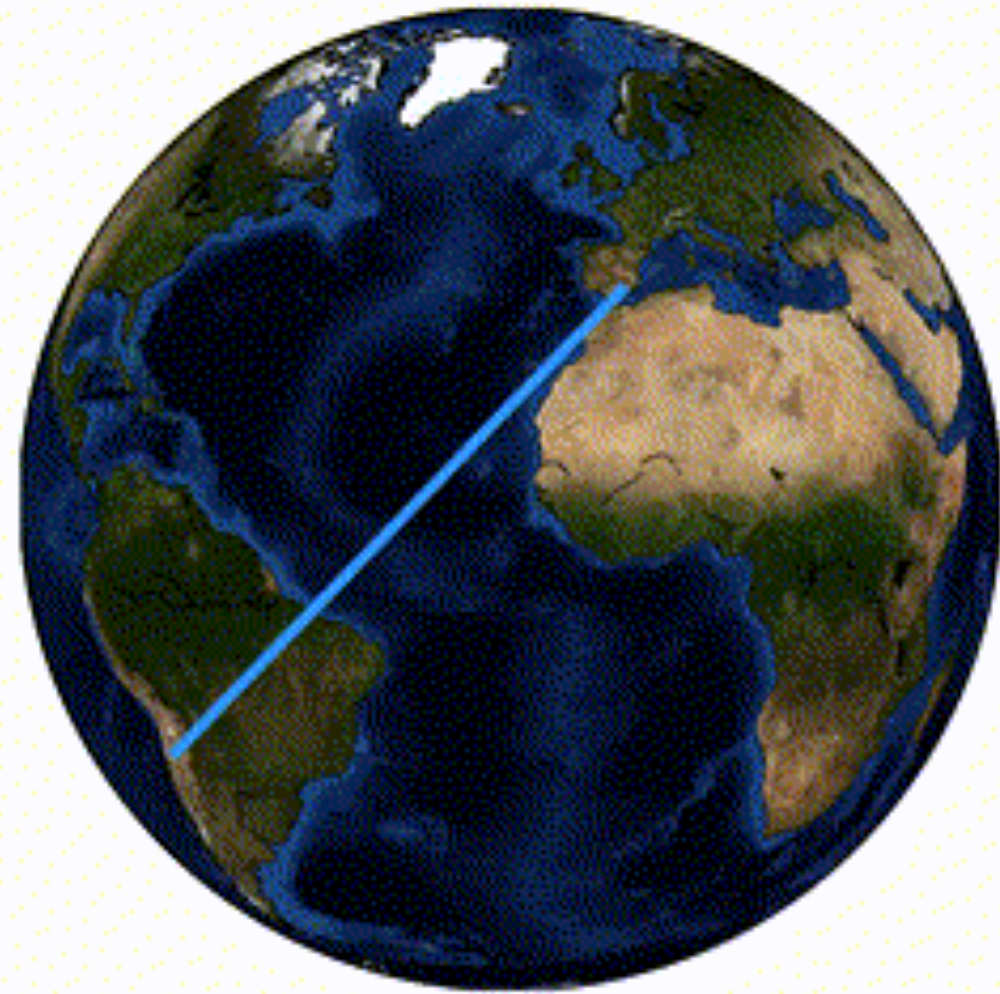
(Paper I)





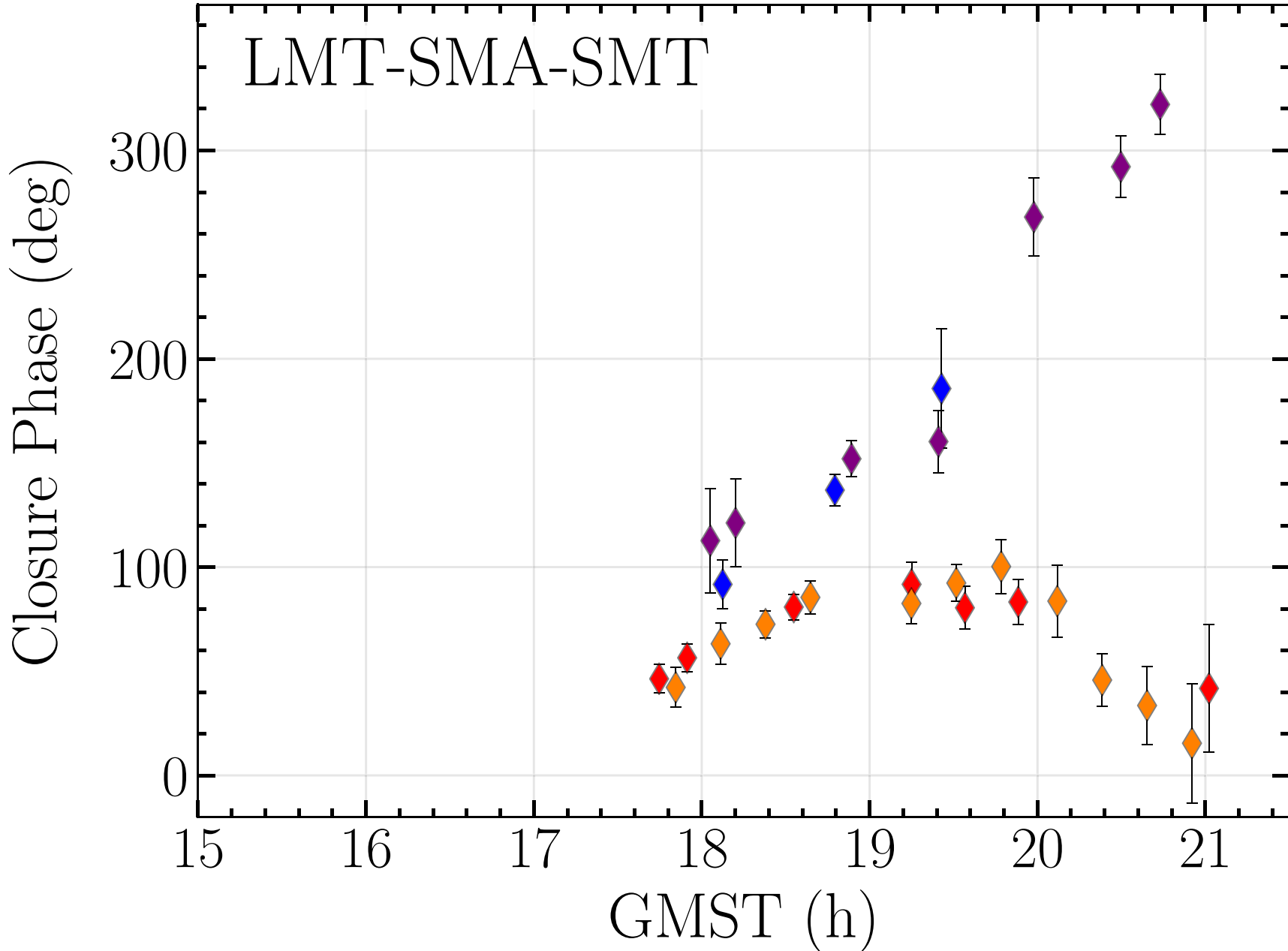
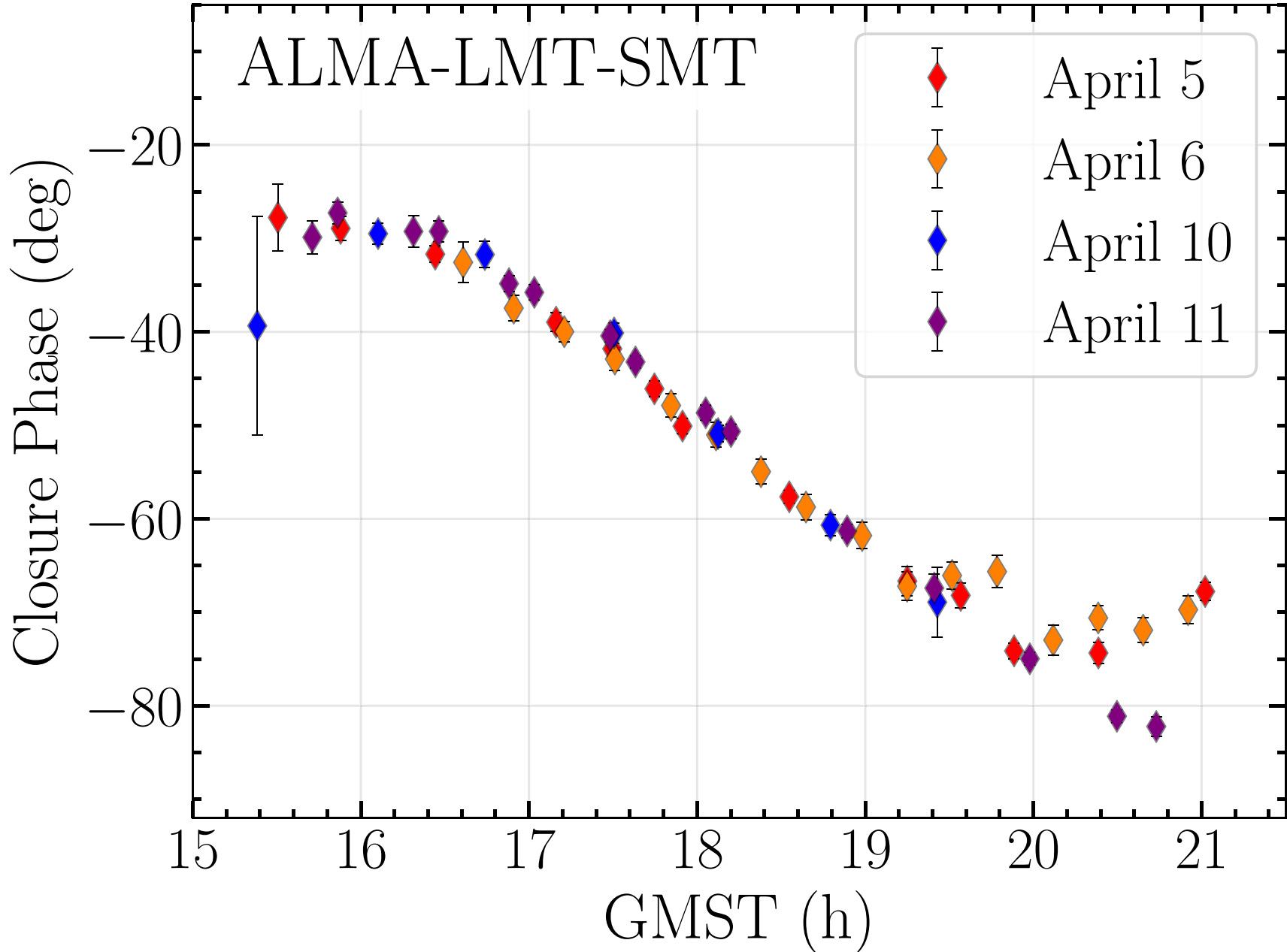
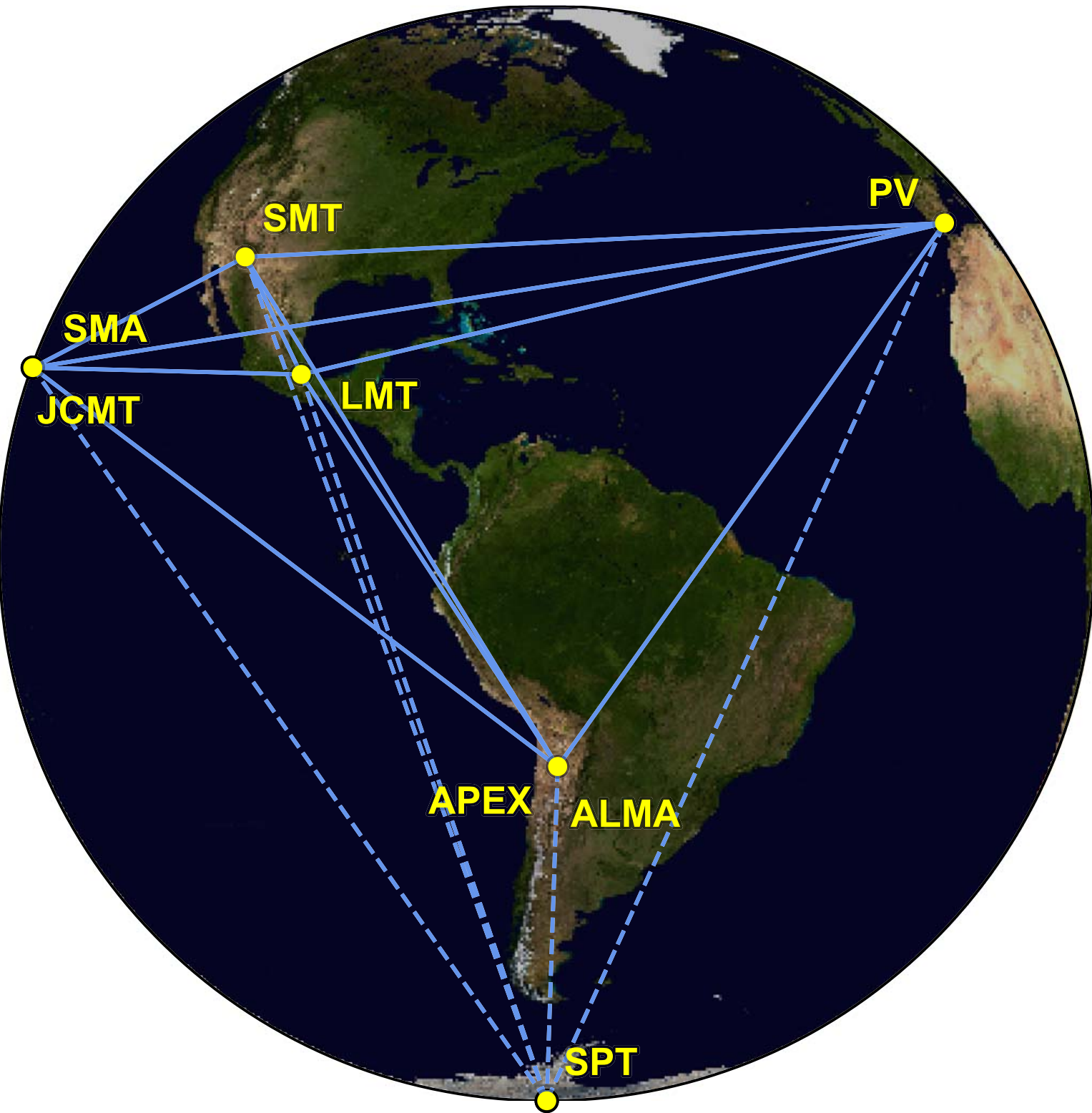
# Slowly Building Up Data

Lo-band eht-imaging on April 11





# Closure Phases: Mildly asymmetric & time-variable structure



(Paper IV)



# Challenges and Philosophy of EHT Imaging

---

## Difficulties

- Extremely sparse baseline coverage
- Large amplitude uncertainties
- No information from previous 1.3 mm images

## Major Risk:

Developing false confidence in features that may not have unambiguous support

**Agnostic:** Images should be among our most agnostic EHT outputs with the ability to reveal unexpected features and source properties

**Exploratory:** We have focused on exploring a broad space of possible algorithms and imaging algorithms to be optimal on a narrow class of images

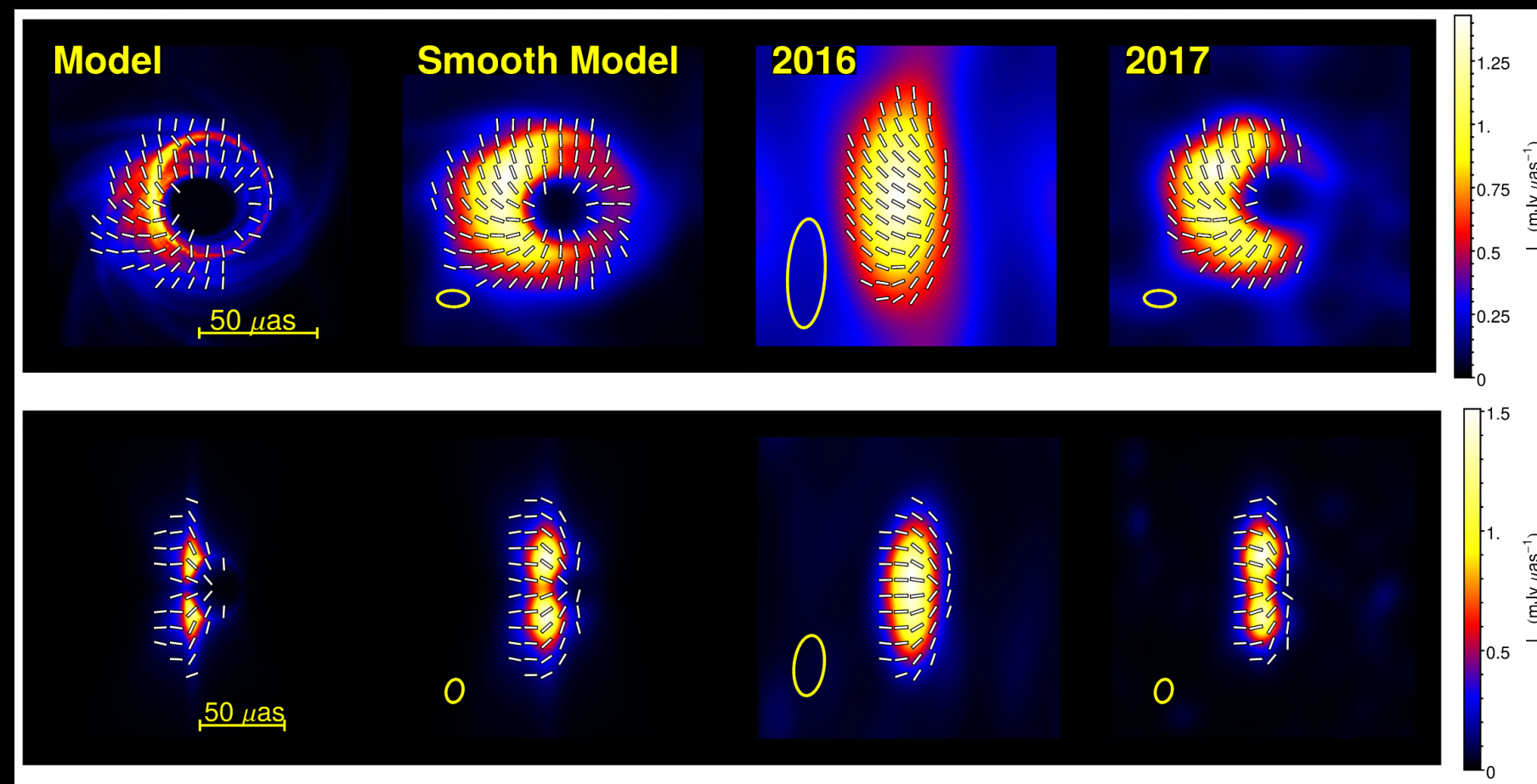
**Emphasis:** Simple algorithms over complex black boxes  
Reproducible and scriptable results



# New Imaging Methods

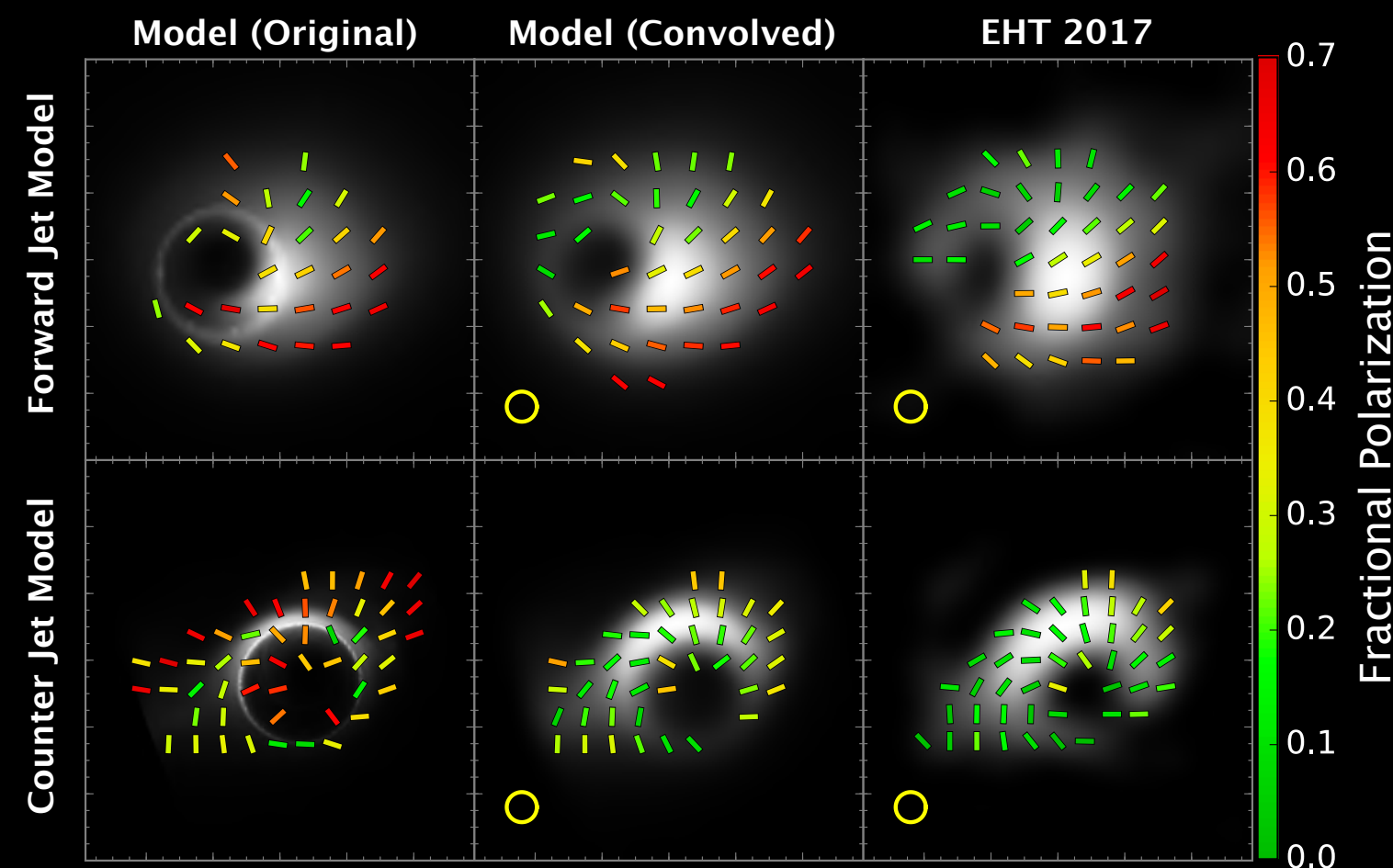
## Maximum Entropy Method (MEM)

Chael et al. 2016, Fish et al. 2014,  
Lu et al. 2014, 2016



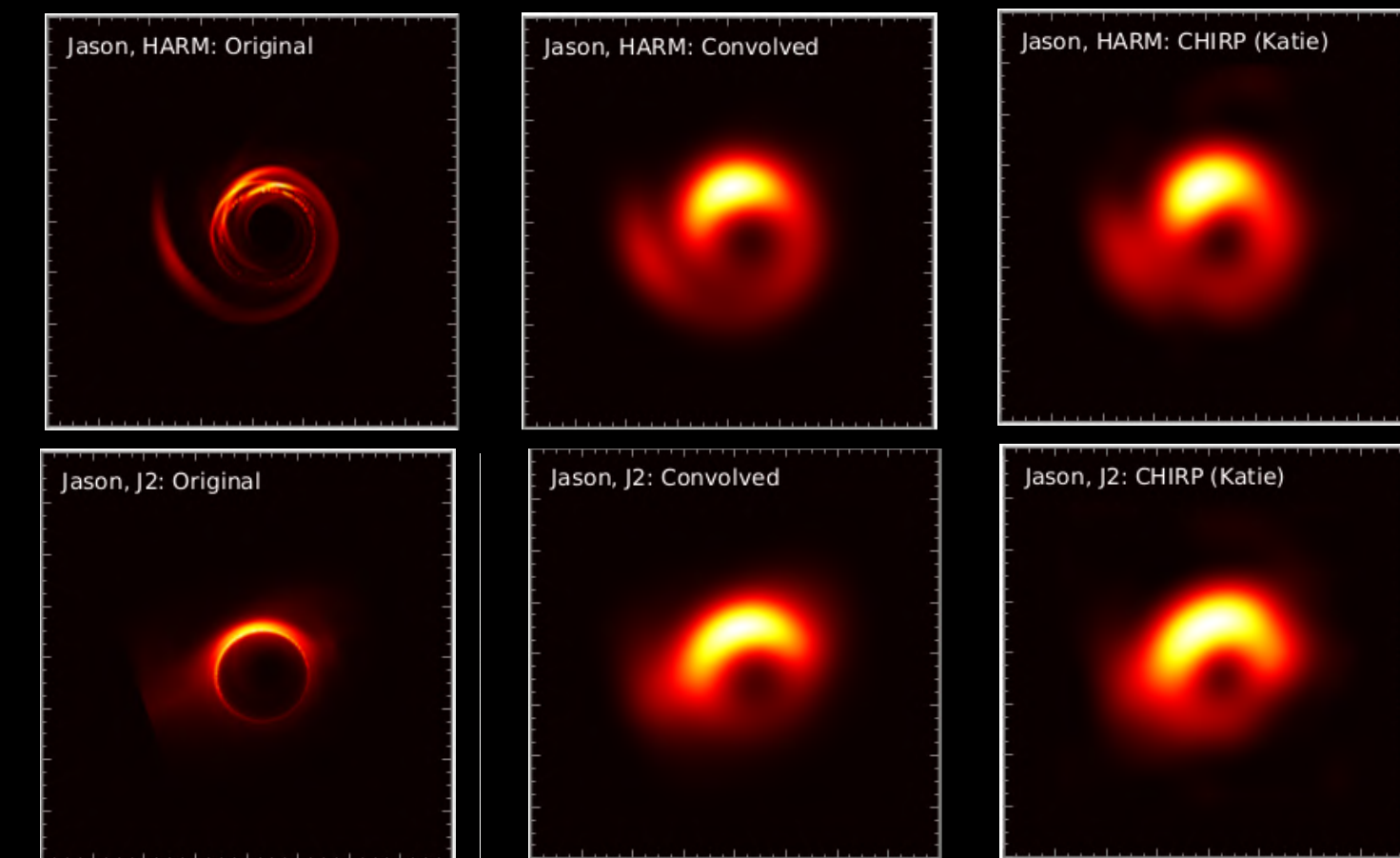
## Sparse Modeling

Akiyama et al. 2017a, 2017b  
Ikeda et al. 2016, Honma et al. 2014



## CHIRP (Machine-learning)

Bouman et al. 2016



## Two Imaging Libraries

eht-imaging (Chael+2016,2018) : <https://github.com/achael/eht-imaging>

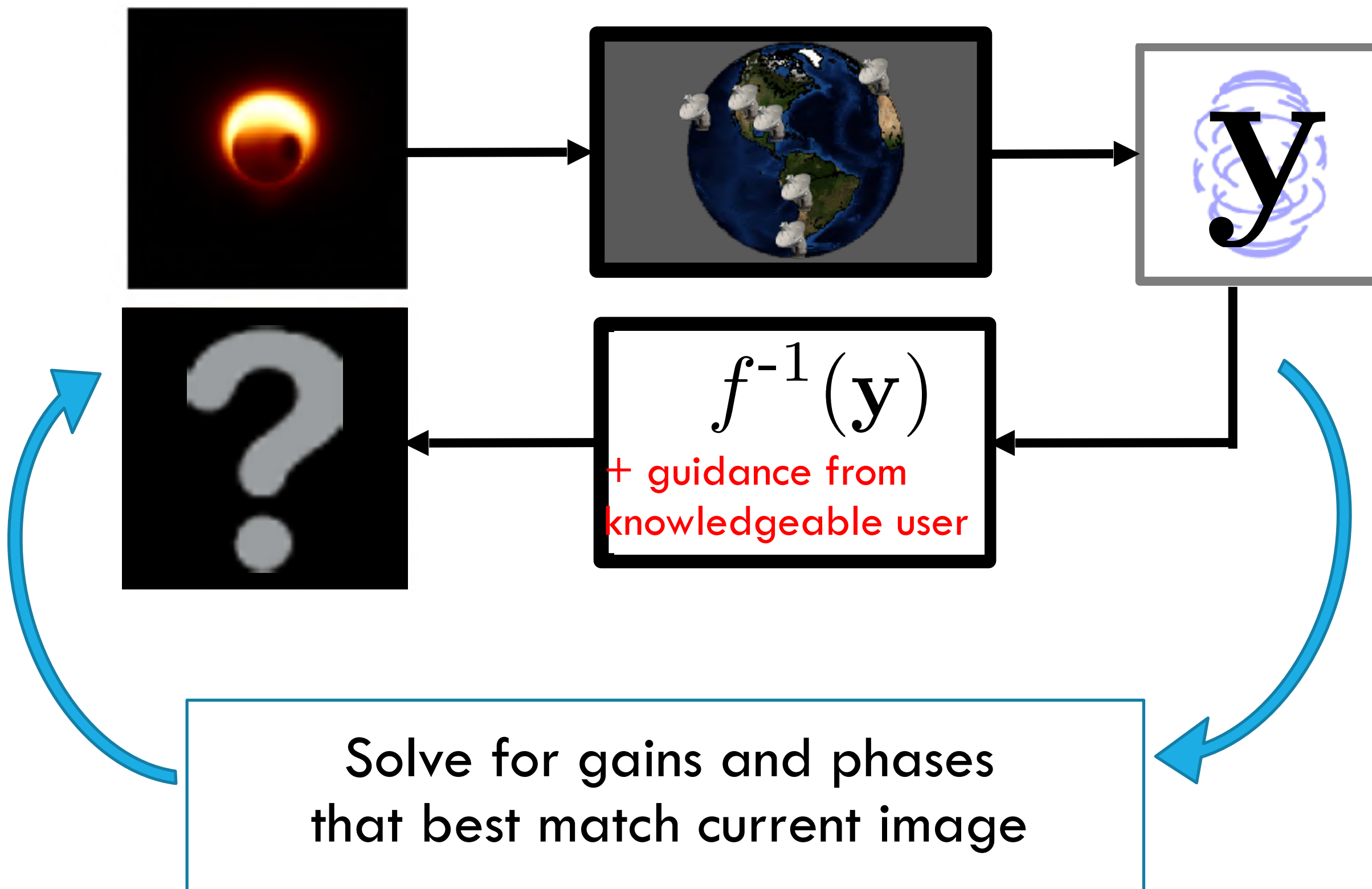
SMILI (Akiyama+2017a,b) : <https://github.com/astrosmili/smili>





# Two Classes of Imaging Algorithms

Credit: Katie Bouman

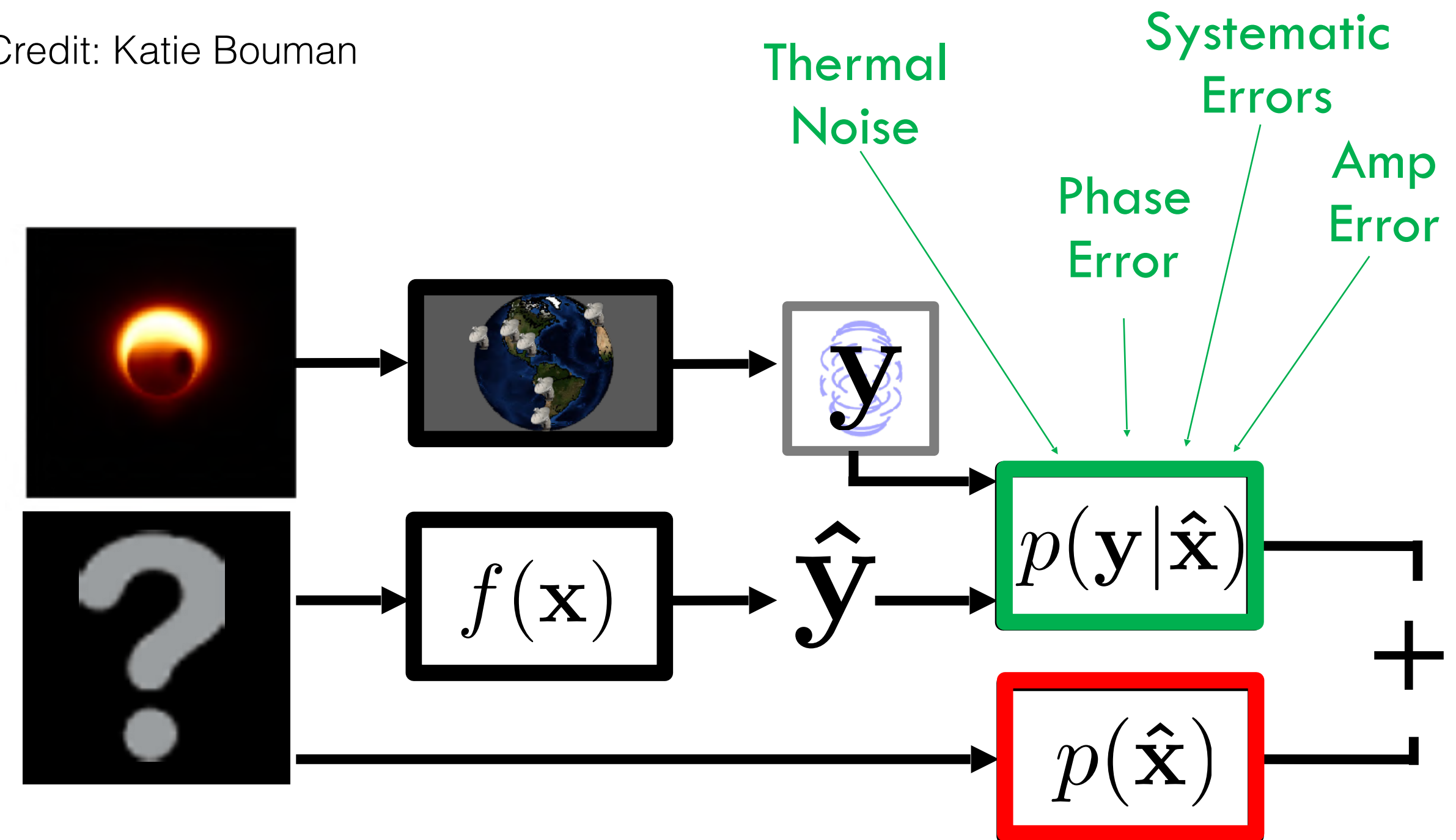


**Traditional** Inverse Modeling  
(CLEAN + Self-Calibration)



Event Horizon Telescope

Credit: Katie Bouman



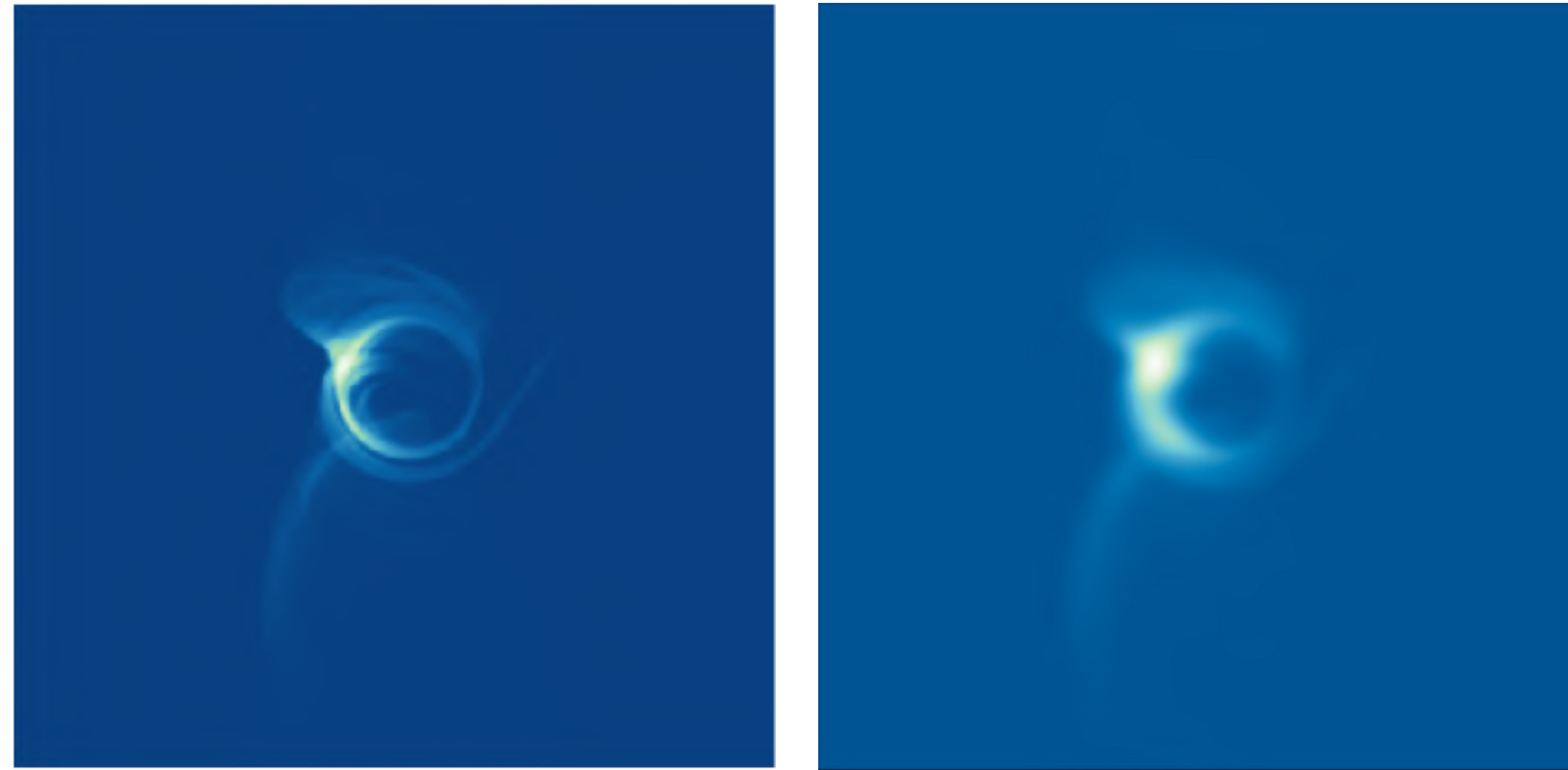
$$\hat{\mathbf{x}}_{\text{MAP}} = \operatorname{argmax}_{\mathbf{x}} [\log p(\mathbf{y}|\mathbf{x}) + \log p(\mathbf{x})]$$

Forward Modeling  
(Bayesian Inspired Optimization)



# EHT Blind Imaging Challenges (2016 -)

---



Method 1



Method 2



Method 3



Method 4



Method 5

(Katie Bouman 2016, PhD thesis; the EHT Imaging WG)





# EHT Blind Imaging Challenges (2016 -)

---



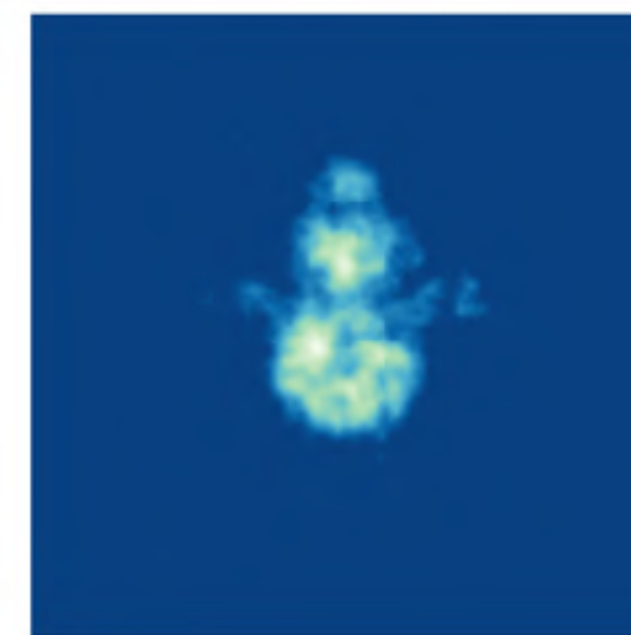
Method 1



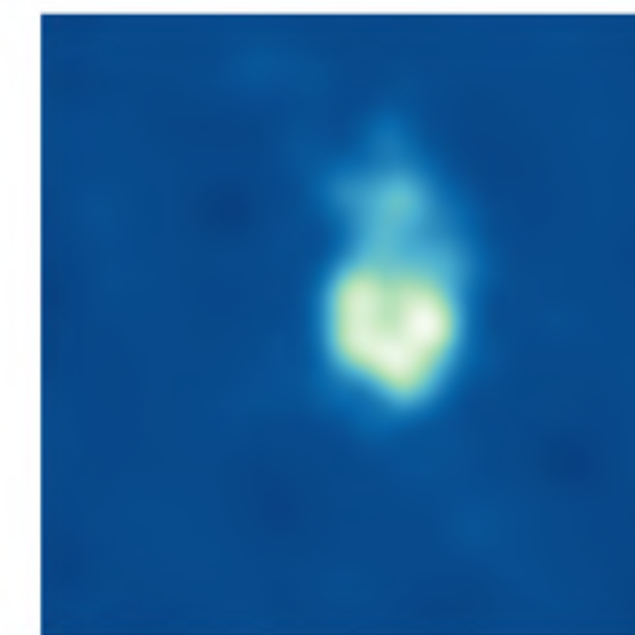
Method 2



Method 3



Method 4



Method 5





# Imaging Pipelines: Human Choices

## DIFMAP

(CLEAN + Self Calibration)

Compact Flux  
Stop Condition  
Weighting on ALMA  
Mask Size  
Data Weights

(Sheperd et al. 1997, 1998)

## eht-imaging

(Regularized Max Likelihood)

Compact Flux  
Initial Gaussian Size  
Systematic Error  
Regularizes  
MEM  
TV  
TSV  
L1

(Chael et al. 2016, 2018)

## SMILI

(Regularized Max Likelihood)

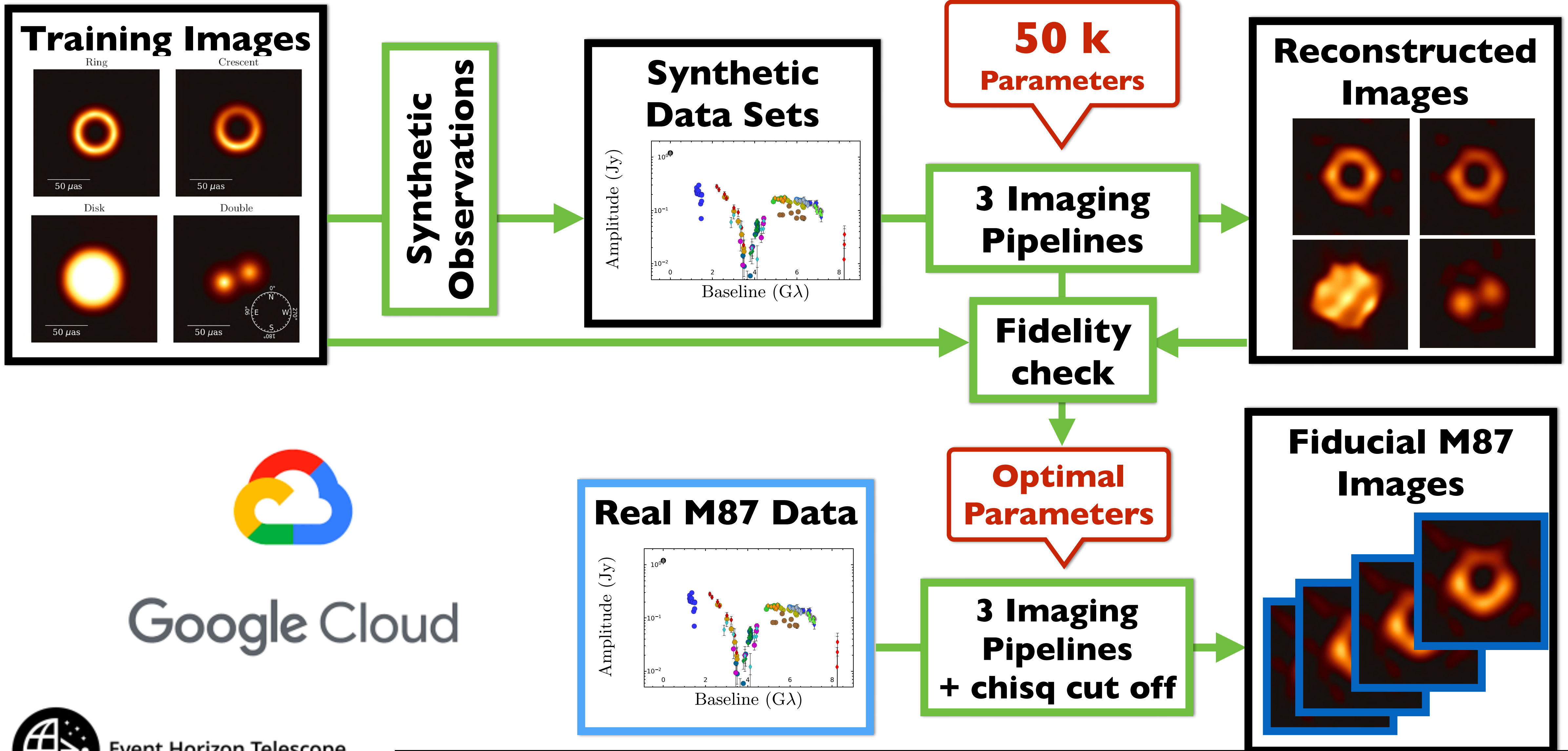
Compact Flux  
L1 Soft Mask Size  
Systematic Error  
Regularizes  
TV  
TSV  
L1

(**Akiyama** et al. 2017a,b)





# Training Imaging Process



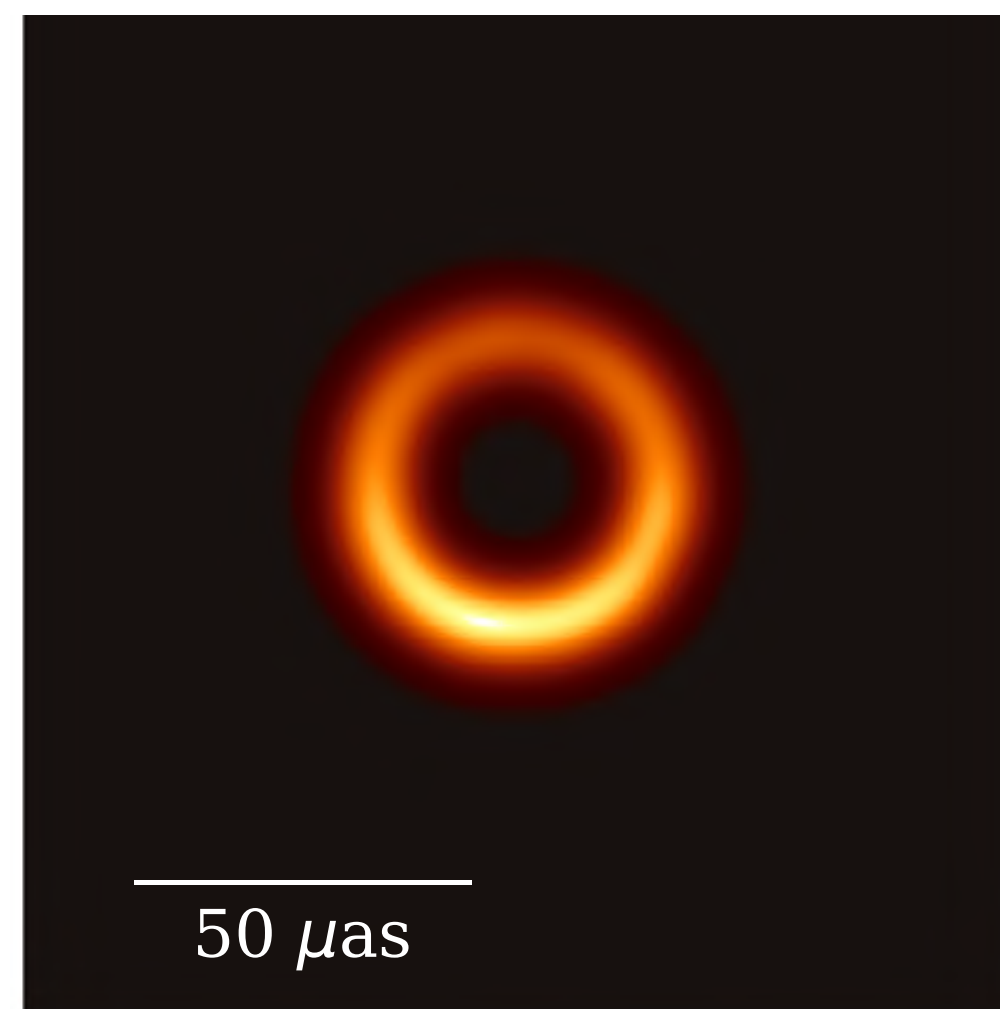
# Fiducial Reconstructions

## Massive Parameter Surveys

Total 50k parameters

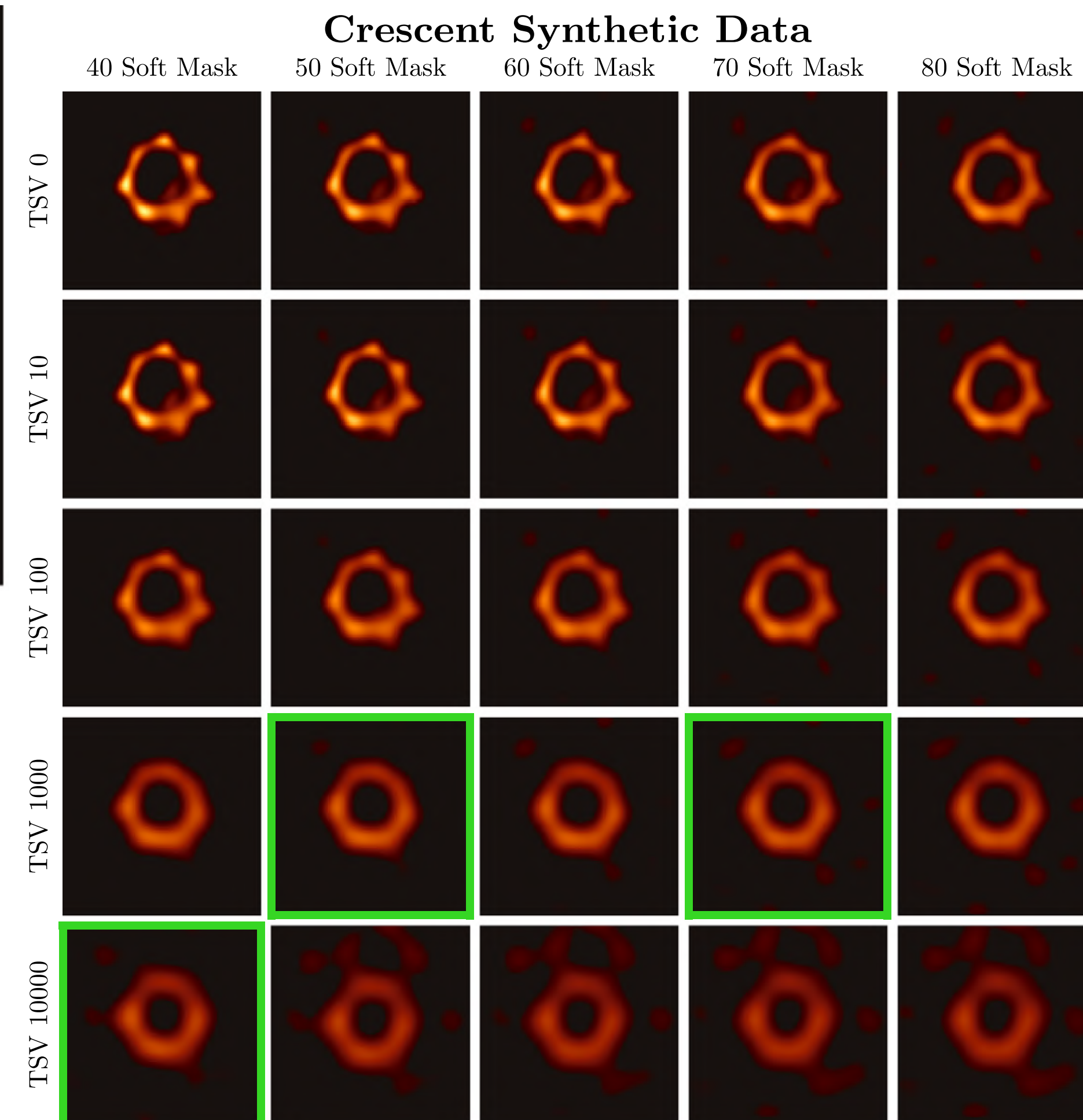


Google Cloud



Select Optimal Parameter Sets

- 1) Good fits to M87 data
- 2) Good fidelity to all of synthetic images

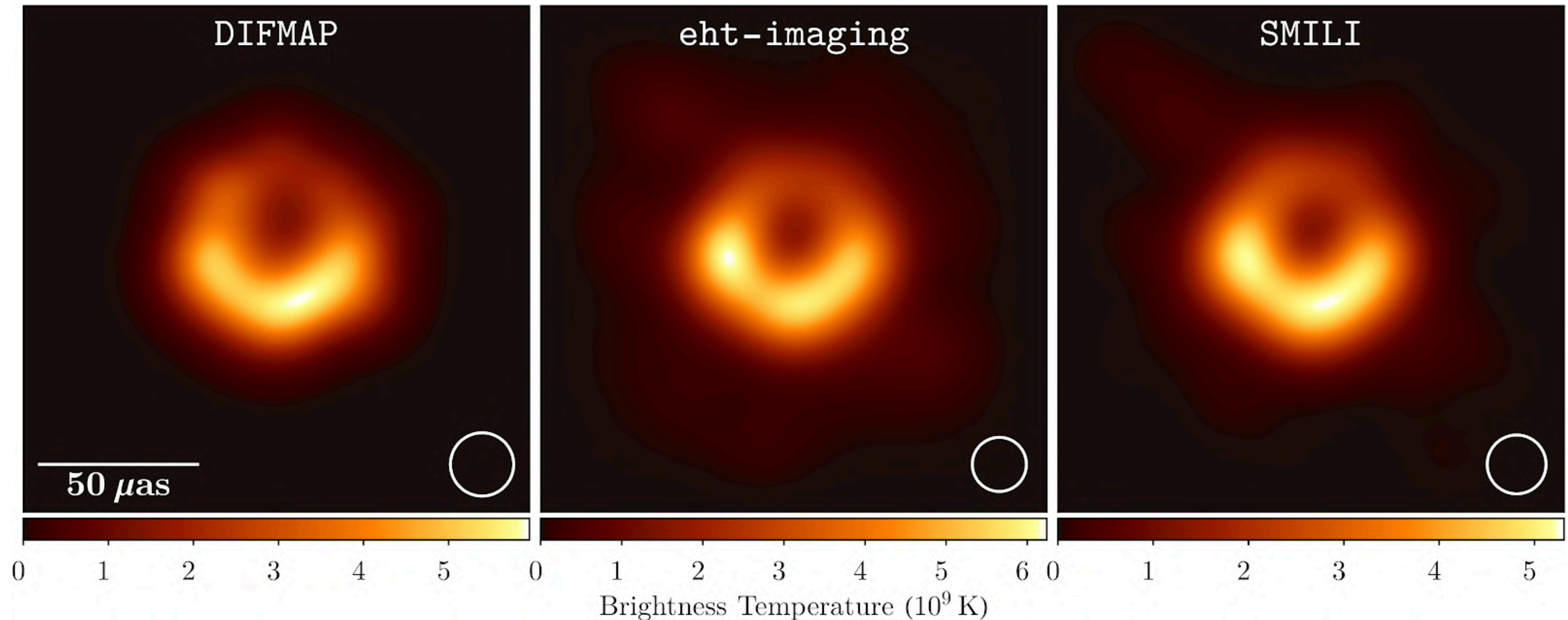


Event Horizon Telescope

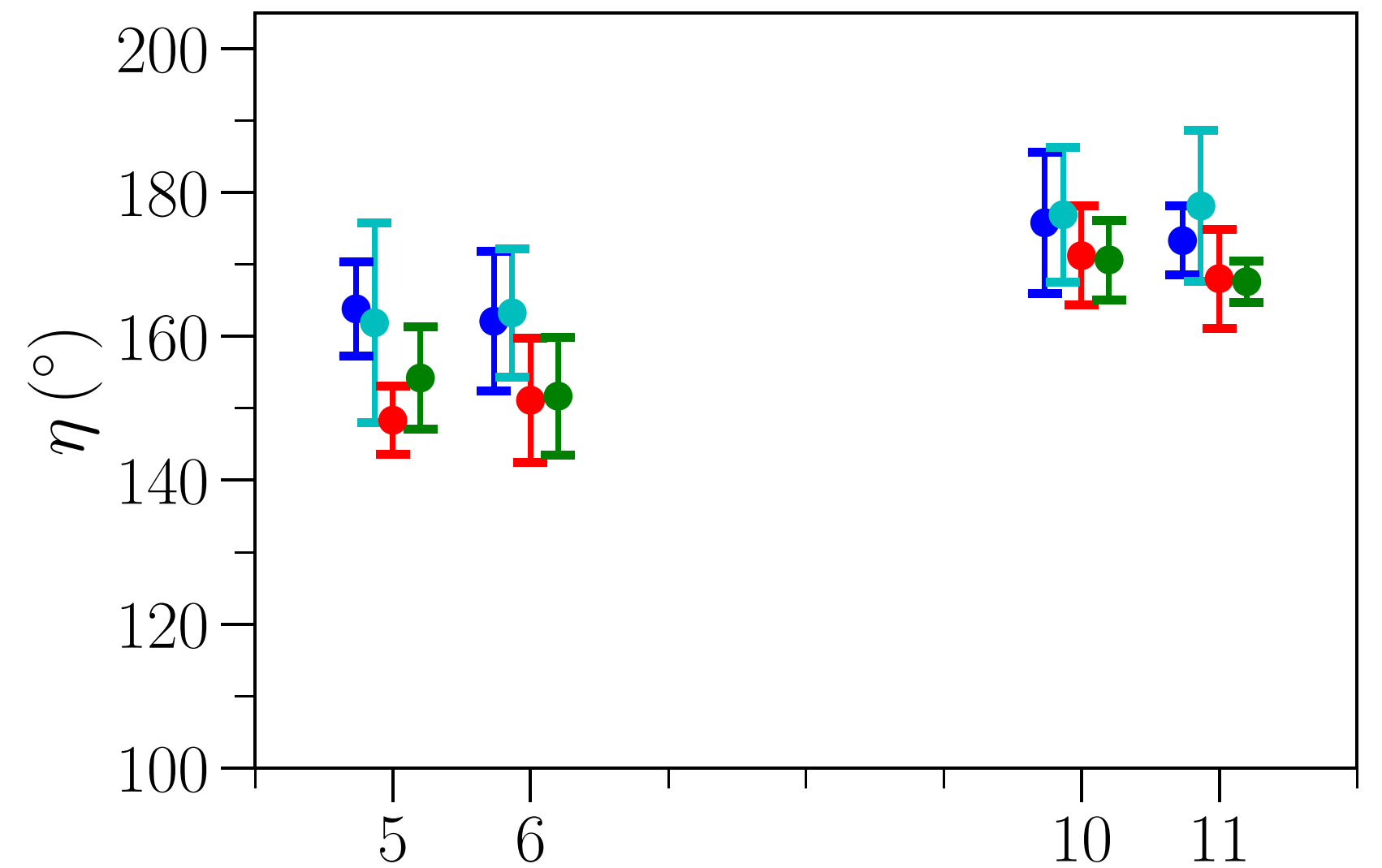
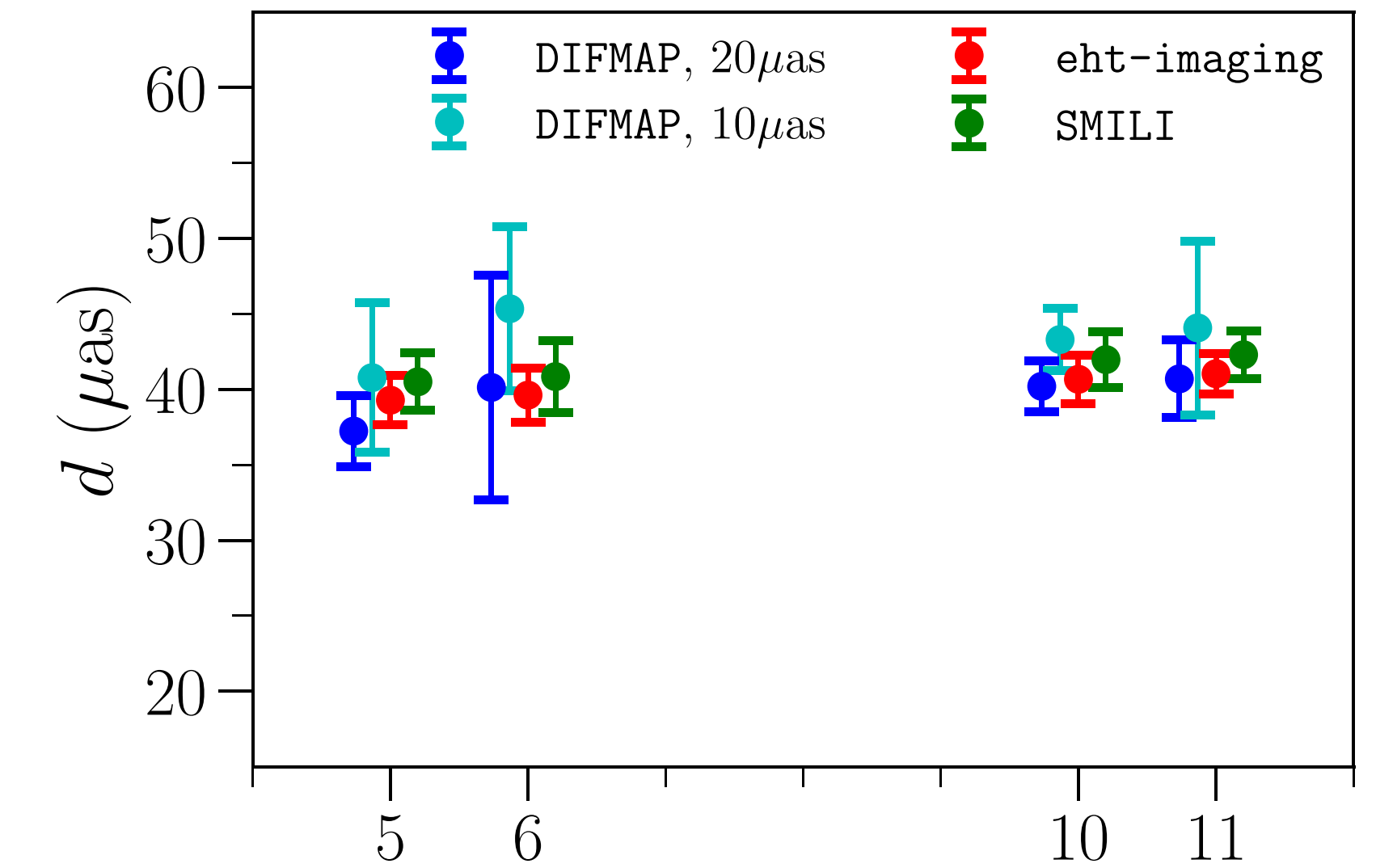
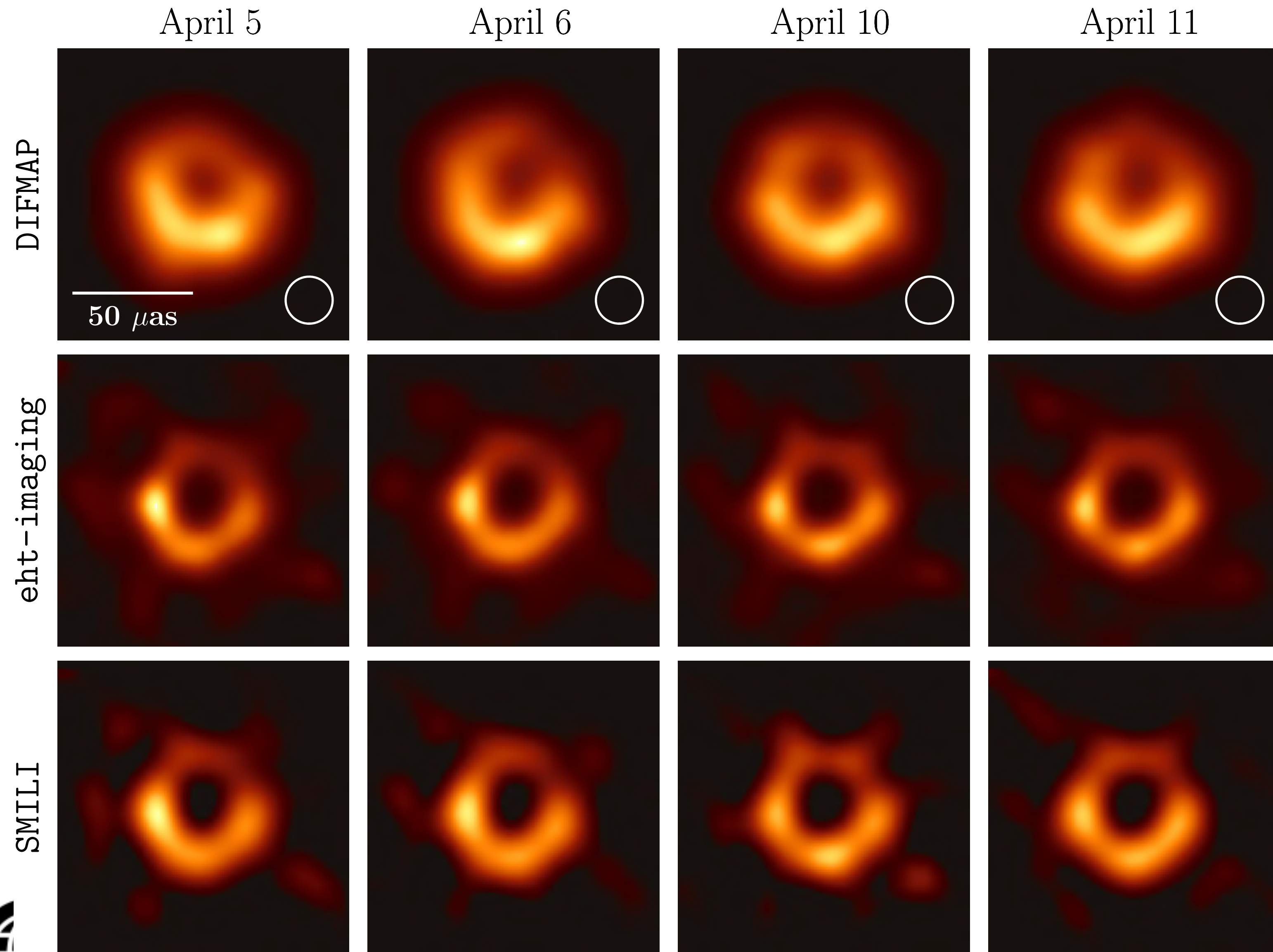


# Fiducial Images

Fiducial images of M87 for April 11 restored to an equivalent resolution show remarkably similar structure

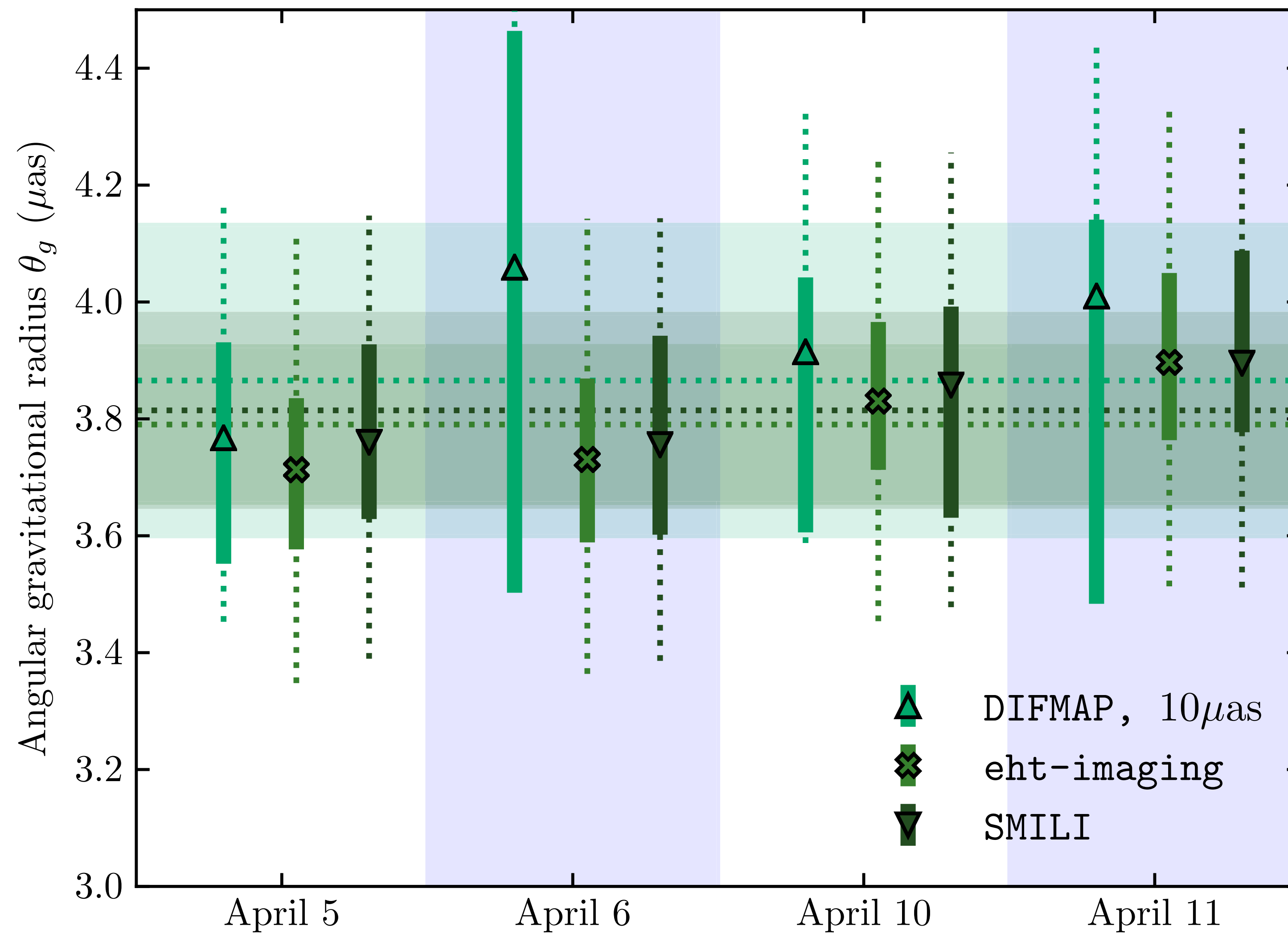


# Fiducial M87 Images





# Bias-corrected Ring diameters



(Paper VI)



---

# EHT Theory & Simulations

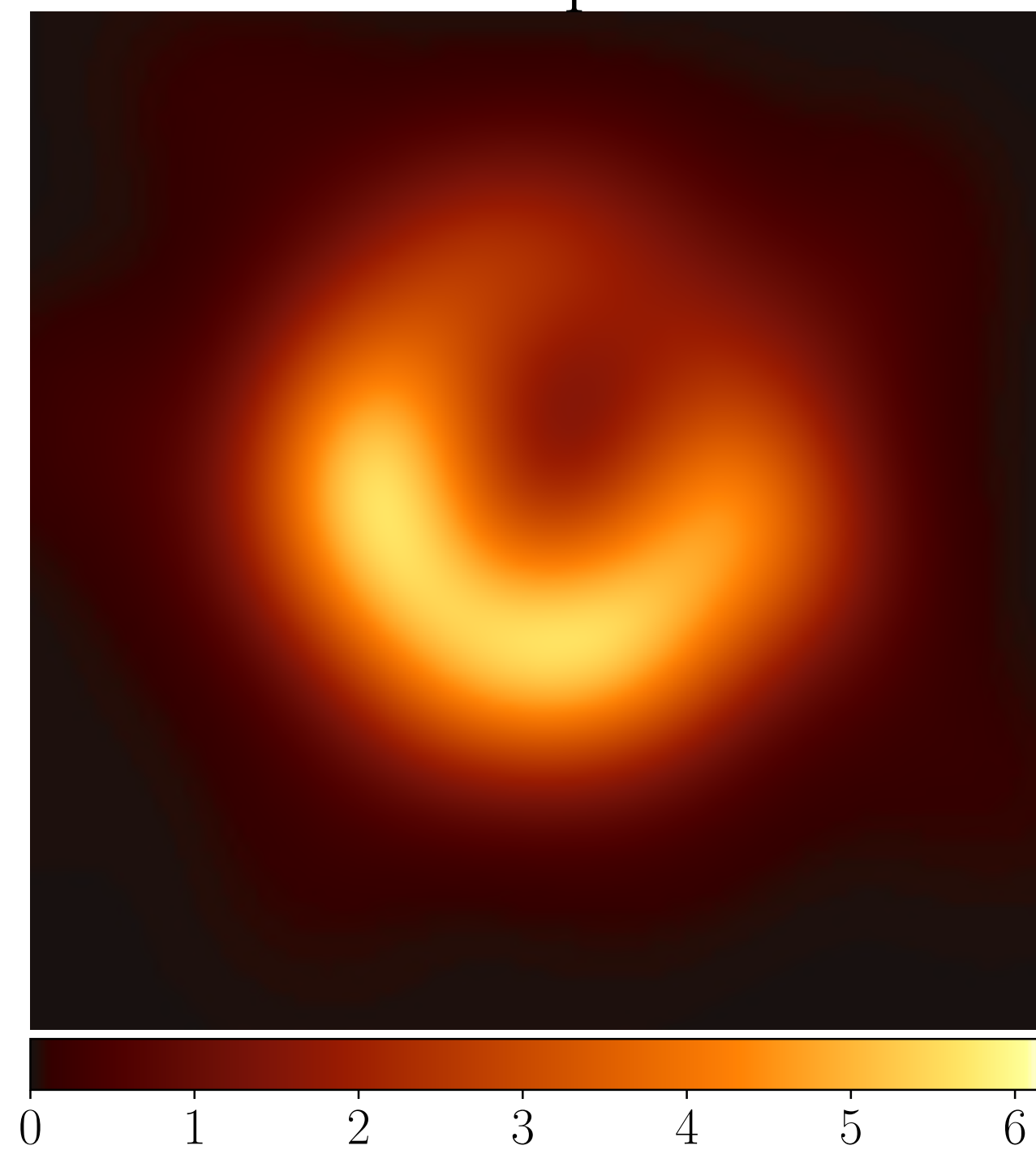




# Representative GRMHD Model Image of M87

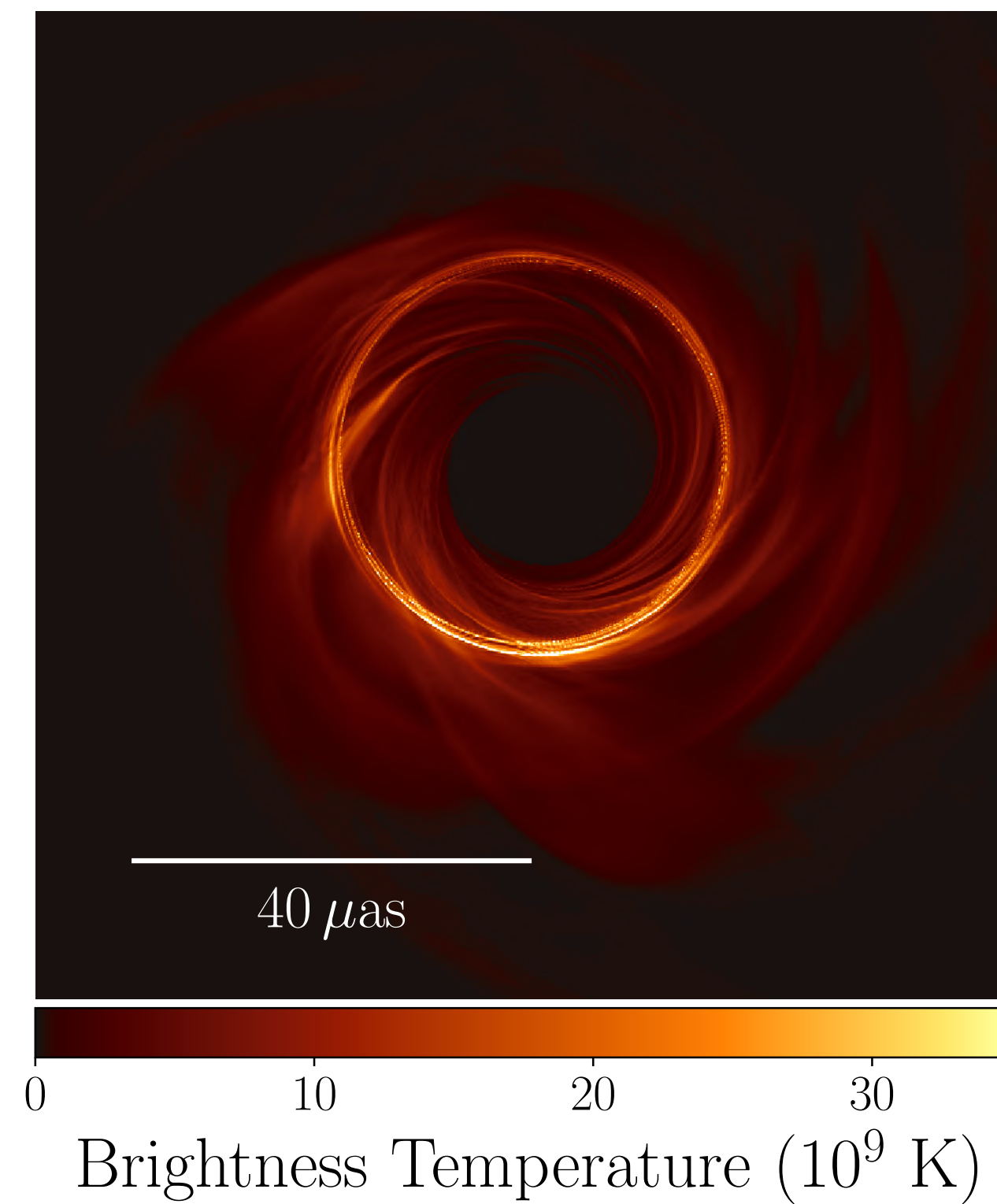
EHT2017 image

M87 April 6



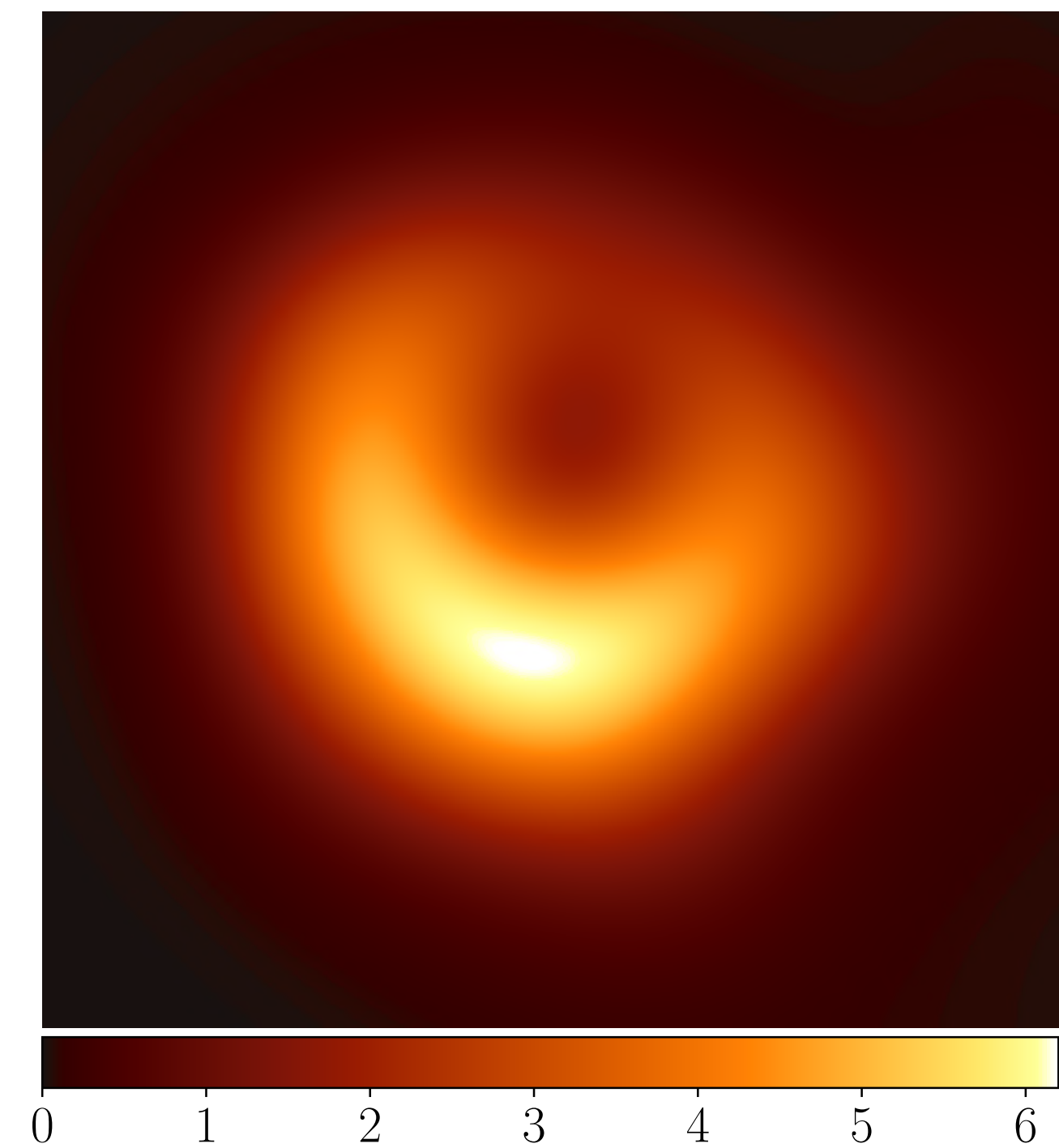
Simulated image  
from GRMHD model

GRMHD



Simulated image  
convolved with  
 $20 \mu\text{as}$  beam

Blurred GRMHD



(Paper V)



# Simulation Library

---

- 3D GRMHD simulations from: **BHAC**, iharm3d, KORAL, H-AMR
- Two accretion states according to accumulated magnetic flux on horizon:
  - SANE (Standard and Normal Evolution)
  - MAD (Magnetically Arrested Disk)
- BH spin parameter:
  - SANE: -0.94, -0.5, 0, 0.5, 0.75, 0.88, 0.94, 0.97, 0.98
  - MAD: -0.94, -0.5, 0, 0.5, 0.75, 0.94

*43 GRMHD numerical simulations*



# Image Library

---

- 1.3mm modeled images from: ipole, RAPTOR, BHOSS
- Observer inclination angles:  $i=12, 17, 22, 158, 163, 168$  deg
- Thermal electrons:  
Ion/electron temperature ratio depends on  $R_{\text{high}}=(1, 10, 20, 40, 80, 160)$ ,  
plasma beta  $\beta_p \equiv P_g/P_{\text{mag}}$ .

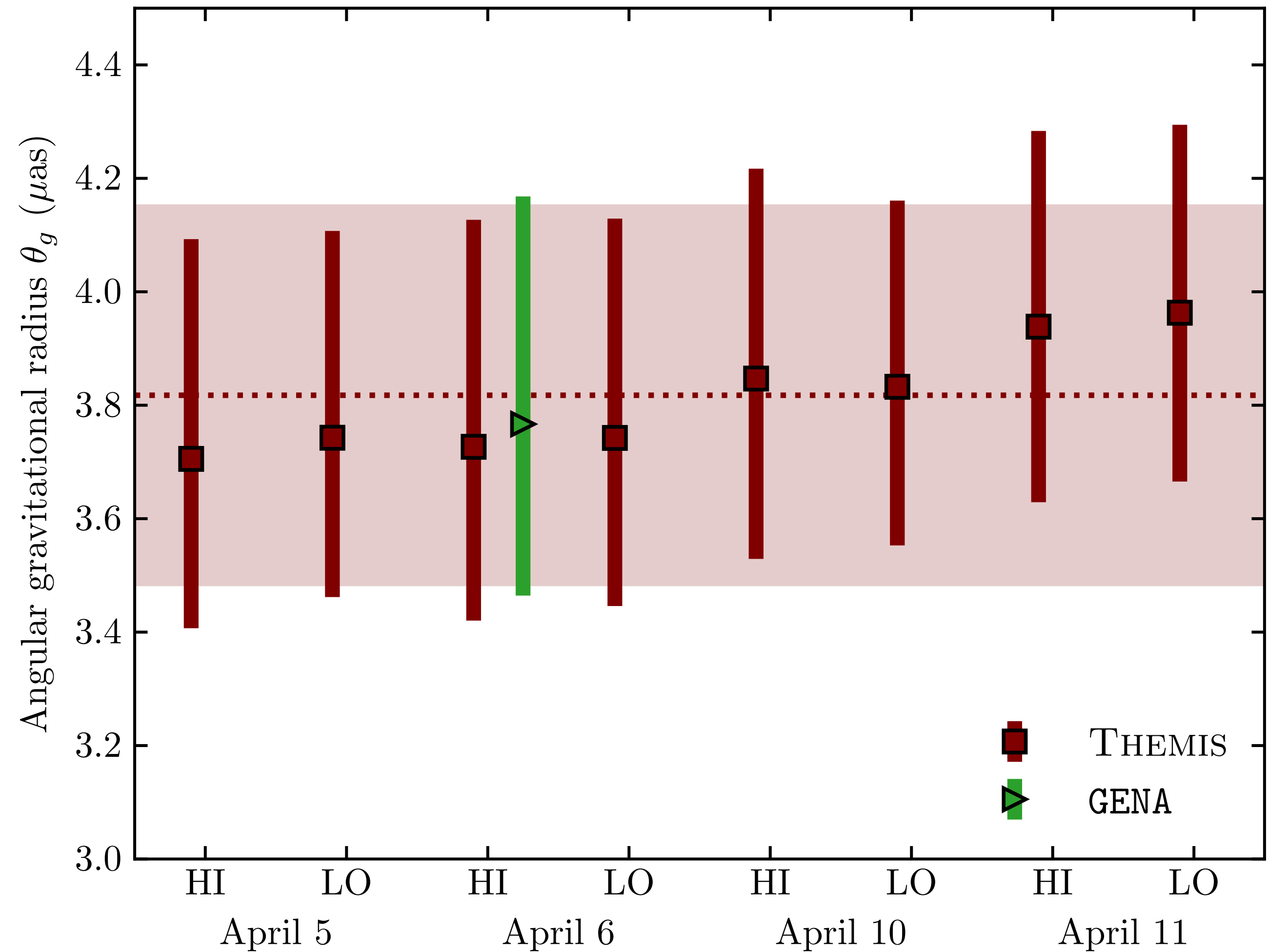
Electrons colder at high plasma beta (disk), warmer at low plasma beta (jet)

$$\frac{T_i}{T_e} = R_{\text{high}} \frac{\beta_p^2}{1 + \beta_p^2} + \frac{1}{1 + \beta_p^2}$$

*> 60,000 images*

# GRMHD model fitting: angular gravitational radius

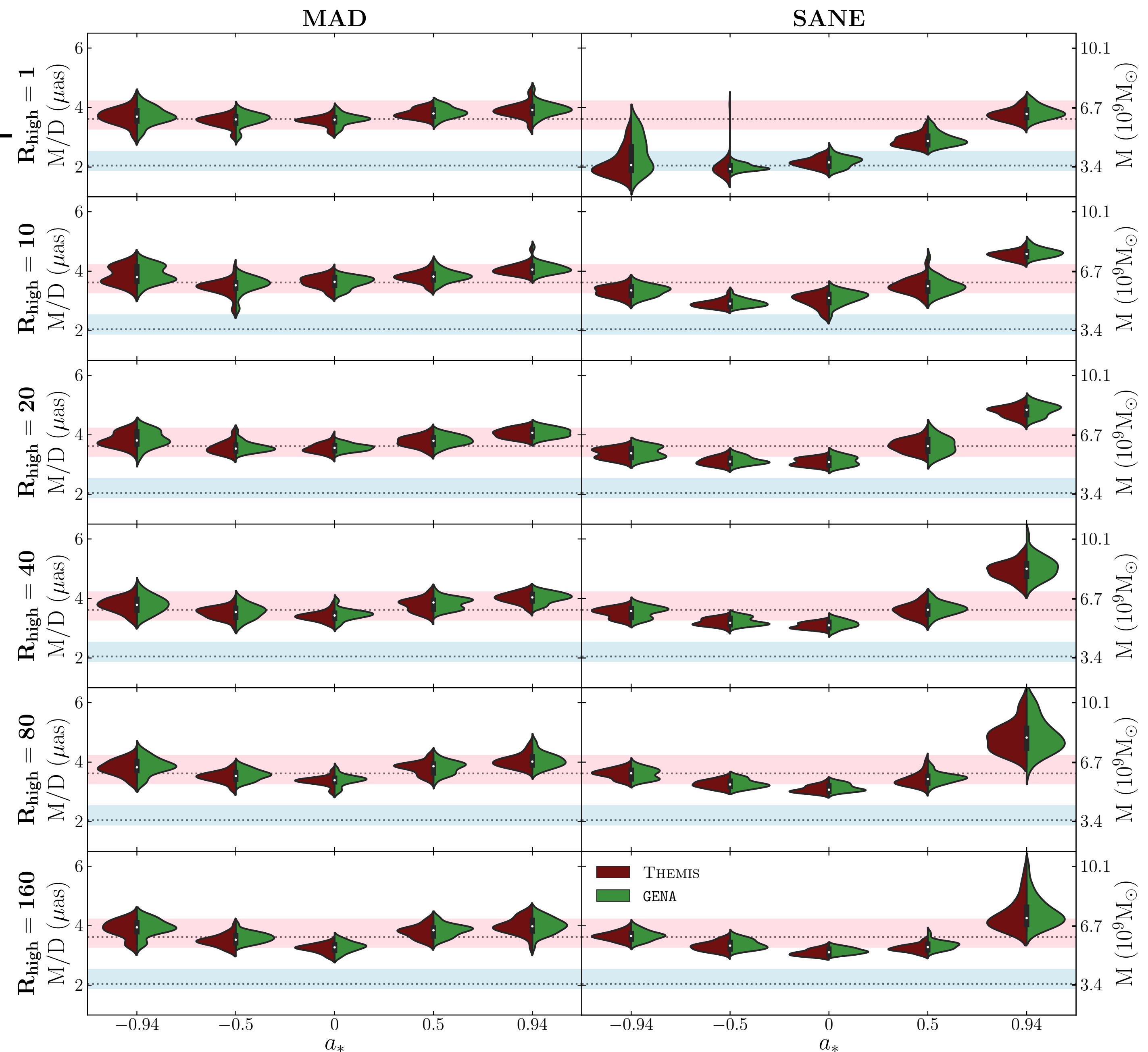
- Estimate of angular gravitational radius (M/D) using the best 10% of snapshot images from all allowed models





# Distribution of M/D

- Distribution of M/D of different BH spin and  $R_{\text{high}}$  for SANE & MAD models
- BH mass is calculated with  $D=16.9$  Mpc
- Most individual models favour M/D close to  $3.6 \mu\text{as}$
- $a < 0$ , SANE,  $R_{\text{high}}=1$  model favors  $M/D \sim 2 \mu\text{as}$  due to outer ring at scale of counterrotating disk ISCO
- $a = 0.94$ , SANE favors  $M/D > 3.6 \mu\text{as}$  due to secondary inner ring



# Average Image Scoring Summary

| Flux <sup>b</sup> | $a_*$ <sup>c</sup> | $\langle p \rangle$ <sup>d</sup> | $N_{\text{model}}$ <sup>e</sup> | MIN( $p$ ) <sup>f</sup> | MAX( $p$ ) <sup>g</sup> |
|-------------------|--------------------|----------------------------------|---------------------------------|-------------------------|-------------------------|
| SANE              | -0.94              | 0.33                             | 24                              | 0.01                    | 0.88                    |
| SANE              | -0.5               | 0.19                             | 24                              | 0.01                    | 0.73                    |
| SANE              | 0                  | 0.23                             | 24                              | 0.01                    | 0.92                    |
| SANE              | 0.5                | 0.51                             | 30                              | 0.02                    | 0.97                    |
| SANE              | 0.75               | 0.74                             | 6                               | 0.48                    | 0.98                    |
| SANE              | 0.88               | 0.65                             | 6                               | 0.26                    | 0.94                    |
| SANE              | 0.94               | 0.49                             | 24                              | 0.01                    | 0.92                    |
| SANE              | 0.97               | 0.12                             | 6                               | 0.06                    | 0.40                    |
| MAD               | -0.94              | 0.01                             | 18                              | 0.01                    | 0.04                    |
| MAD               | -0.5               | 0.75                             | 18                              | 0.34                    | 0.98                    |
| MAD               | 0                  | 0.22                             | 18                              | 0.01                    | 0.62                    |
| MAD               | 0.5                | 0.17                             | 18                              | 0.02                    | 0.54                    |
| MAD               | 0.75               | 0.28                             | 18                              | 0.01                    | 0.72                    |
| MAD               | 0.94               | 0.21                             | 18                              | 0.02                    | 0.50                    |

- Compare:  
data -  $\langle \text{model} \rangle$   
model -  $\langle \text{model} \rangle$   
using Themis-AIS
- Rejects  $a = -0.94$  MAD models
- This model exhibit highest morphological variability





# Radiative Equilibrium

---

- Calculate radiative efficiency,  $\epsilon \equiv L_{\text{bol}}/(\dot{M}c^2)$
- Reject model if  $\epsilon > \epsilon(\text{classical thin disk model})$ ; inconsistent; would cool quickly
- $L_{\text{bol}}$ : calculated by Monte Carlo code: grmonty
- Rejects MAD models with  $a \geq 0$  and  $R_{\text{high}} = 1$  (hot midplane electrons)



# X-ray constraint

---

- X-ray data: simultaneously Chandra, NuSTAR observations during EHT2017 Campaign
  - 2-10 keV luminosity:  $L_x = 4.4 \pm 0.1 \times 10^{40}$  erg/s
- Compare data to SEDs generated from simulations
  - X-ray flux is produced by inverse Compton scattering of synchrotron photons
- Reject models that consistently *overproduce* X-ray
- Overluminous model: mostly SANE with  $R_{\text{high}} \leq 20$ .
- $L_x$  is sensitive to  $R_{\text{high}}$ , very low values of  $R_{\text{high}}$  are disfavored.





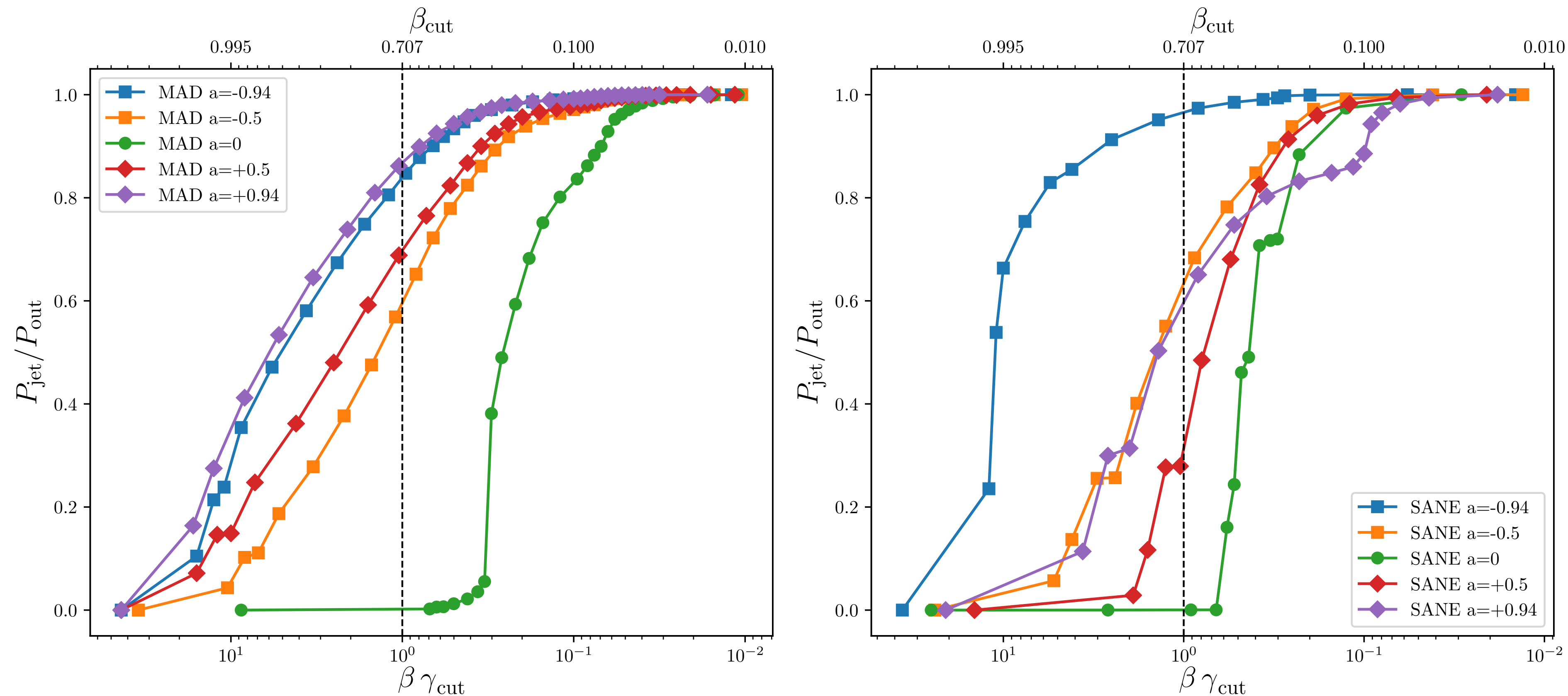
# Jet Power

---

- M87's jet power ( $P_{\text{jet}}$ ) estimates range from  $10^{42}$  to  $10^{45}$  erg/s
- Adopt conservative **lower limit** on jet power,  $P_{\text{jet,min}} = 10^{42}$  erg/s
- $P_{\text{jet}}$  defined as total energy flux in **polar regions where  $\beta\gamma > 1$**
- $P_{\text{out}}$  defined as energy flux in **all polar outflow regions** (includes wide-angle, low velocity wind)
- $P_{\text{out}}$  is *maximal* definition of jet power
- Constraint  $P_{\text{jet}} > P_{\text{jet,min}} = 10^{42}$  erg/s **rejects all  $a=0$  models** ( $P_{\text{jet}}=0$ ). These models also have  $P_{\text{out}} < 10^{42}$  erg/s
- **SANE models with  $|a| < 0.5$  rejected**
- **Most  $|a| > 0$  MAD models acceptable**
- $P_{\text{jet}}$  dominated by Poynting flux; driven by extraction of black hole spin energy through **Blandford-Znajek process**



# $P_{\text{jet}}/P_{\text{out}}$ vs $\beta\gamma_{\text{cut}}$



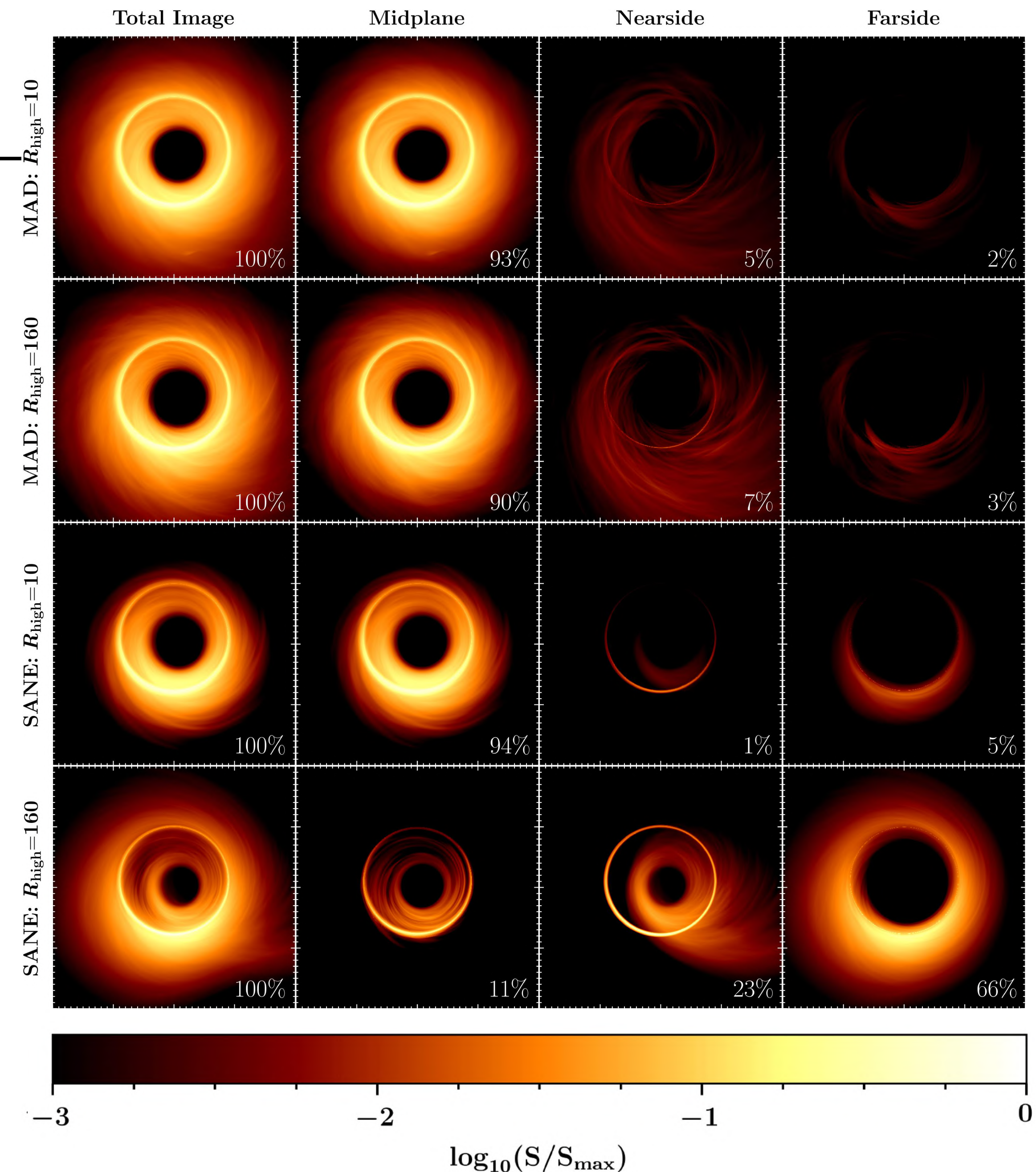
- $P_{\text{jet}}$  depends on  $\beta\gamma$  cutoff used in definition
- $P_{\text{jet}}$  small for  $a = 0$  because energy flux in relativistic outflow is small





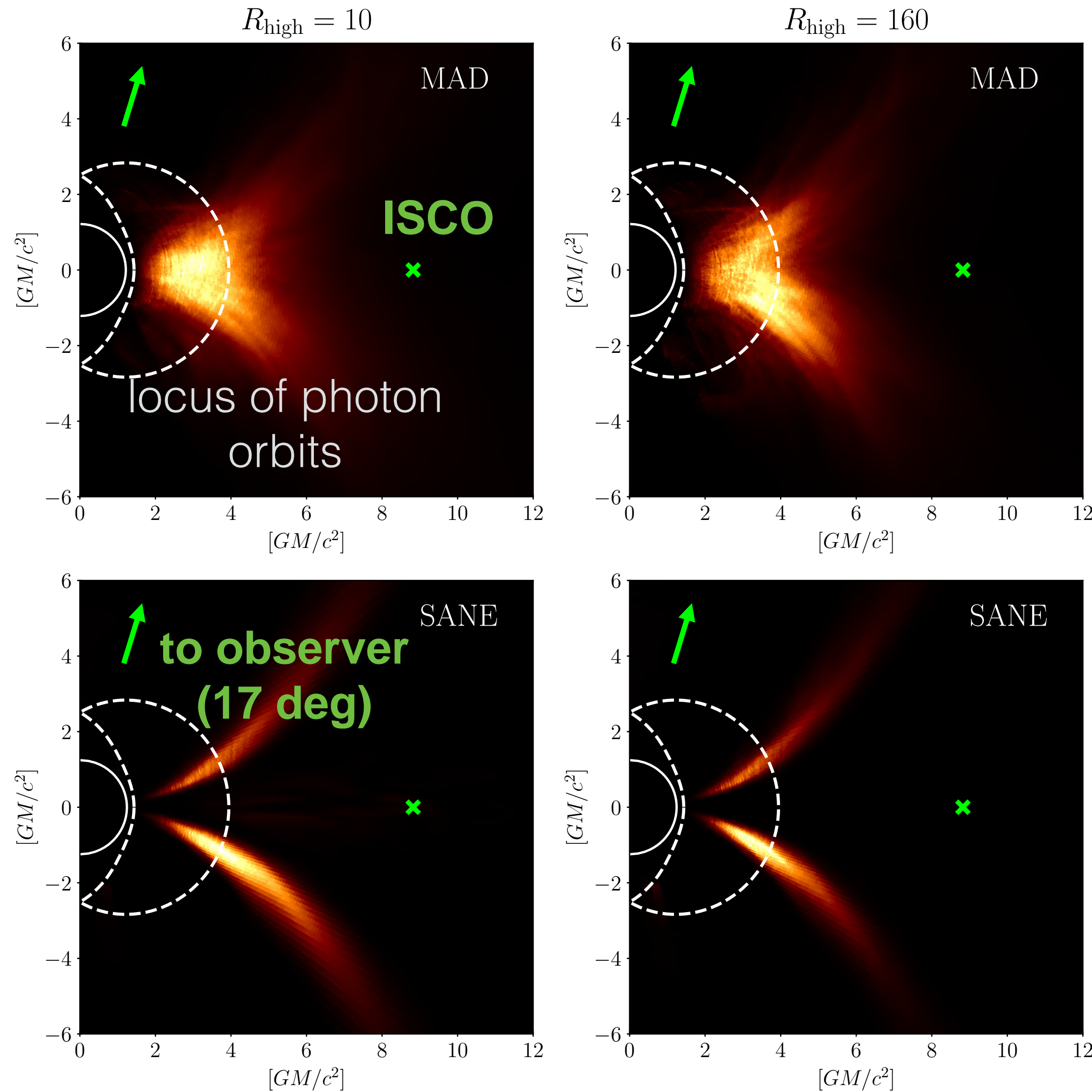
# Image decomposition

- Decompose into components: midplane, nearside (within 1 rad of polar axis nearest to the observer), and farside (within 1 rad of polar axis furthest from the observer)
- MAD, SANE at low  $R_{\text{high}}$  (hot midplane): midplane emission dominates
- SANE with high  $R_{\text{high}}$  (cold midplane): farside emission dominates





# Where do mm photons originate?



Retrograde case

MAD,  $a=-0.94$

SANE,  $a=-0.94$





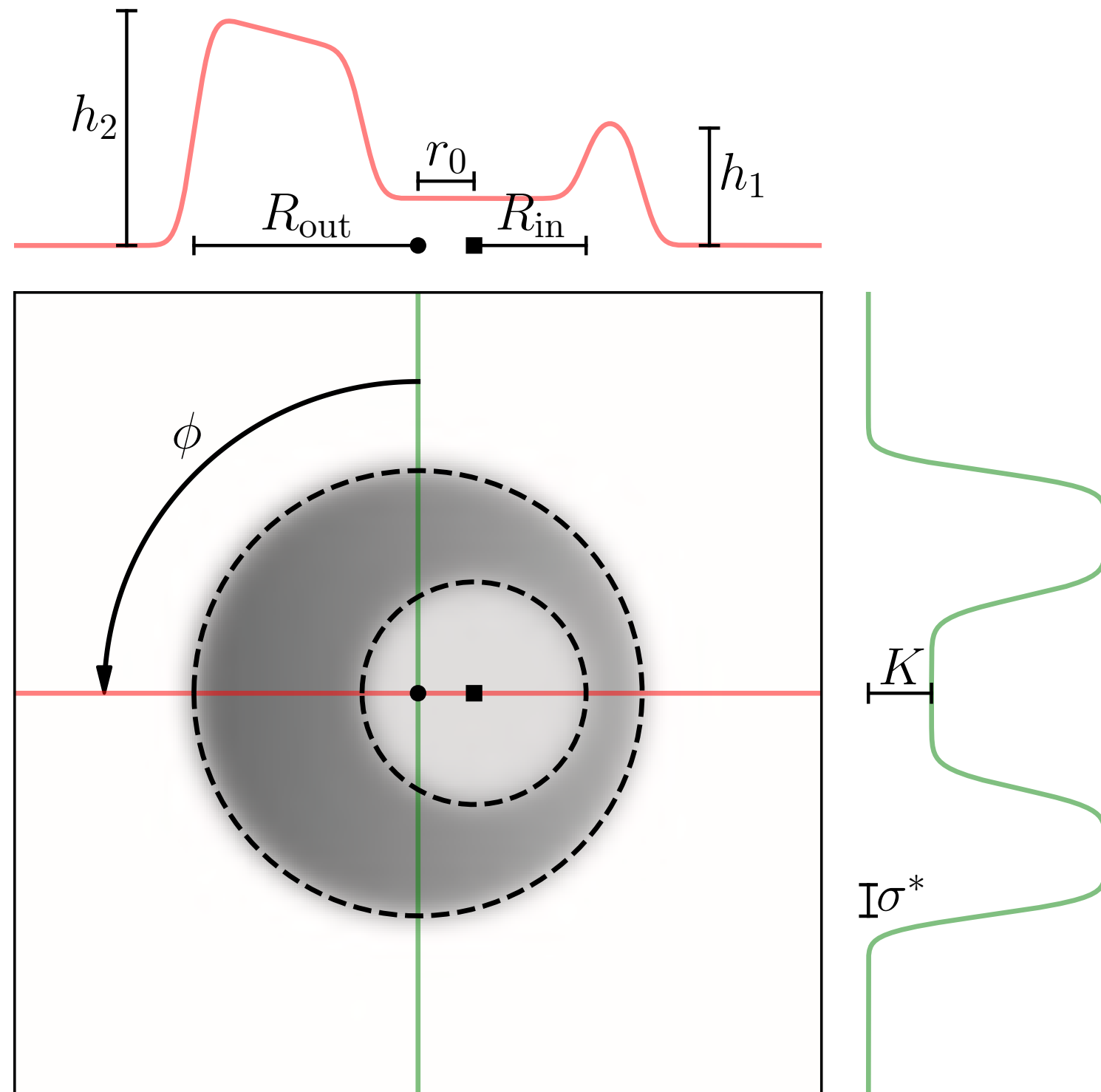
---

# EHT Model Fitting



# Quantify M87 Source Properties

Fit geometrical crescent models



Fit GRMHD models

Single Snapshot Model

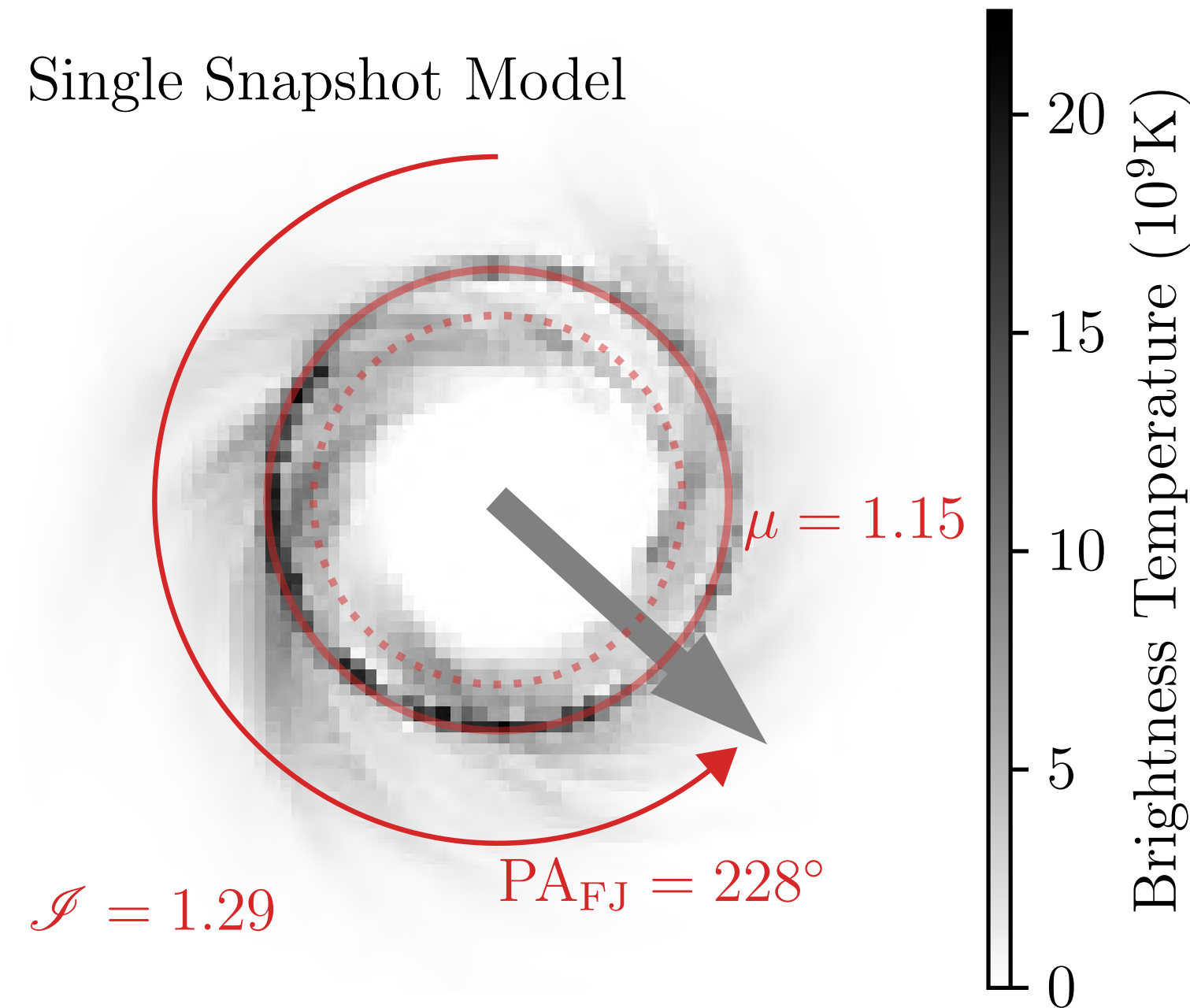
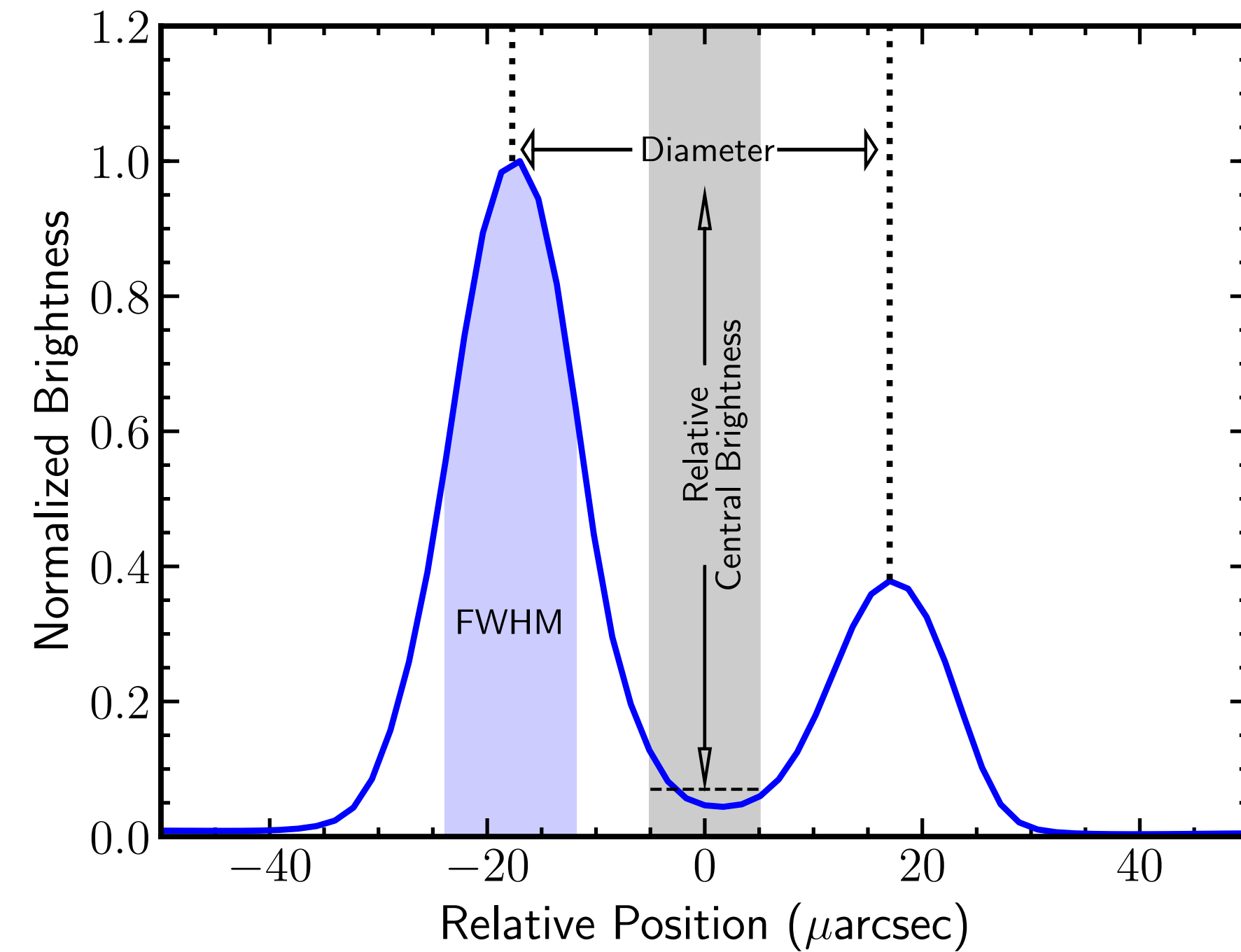


Image domain feature extraction



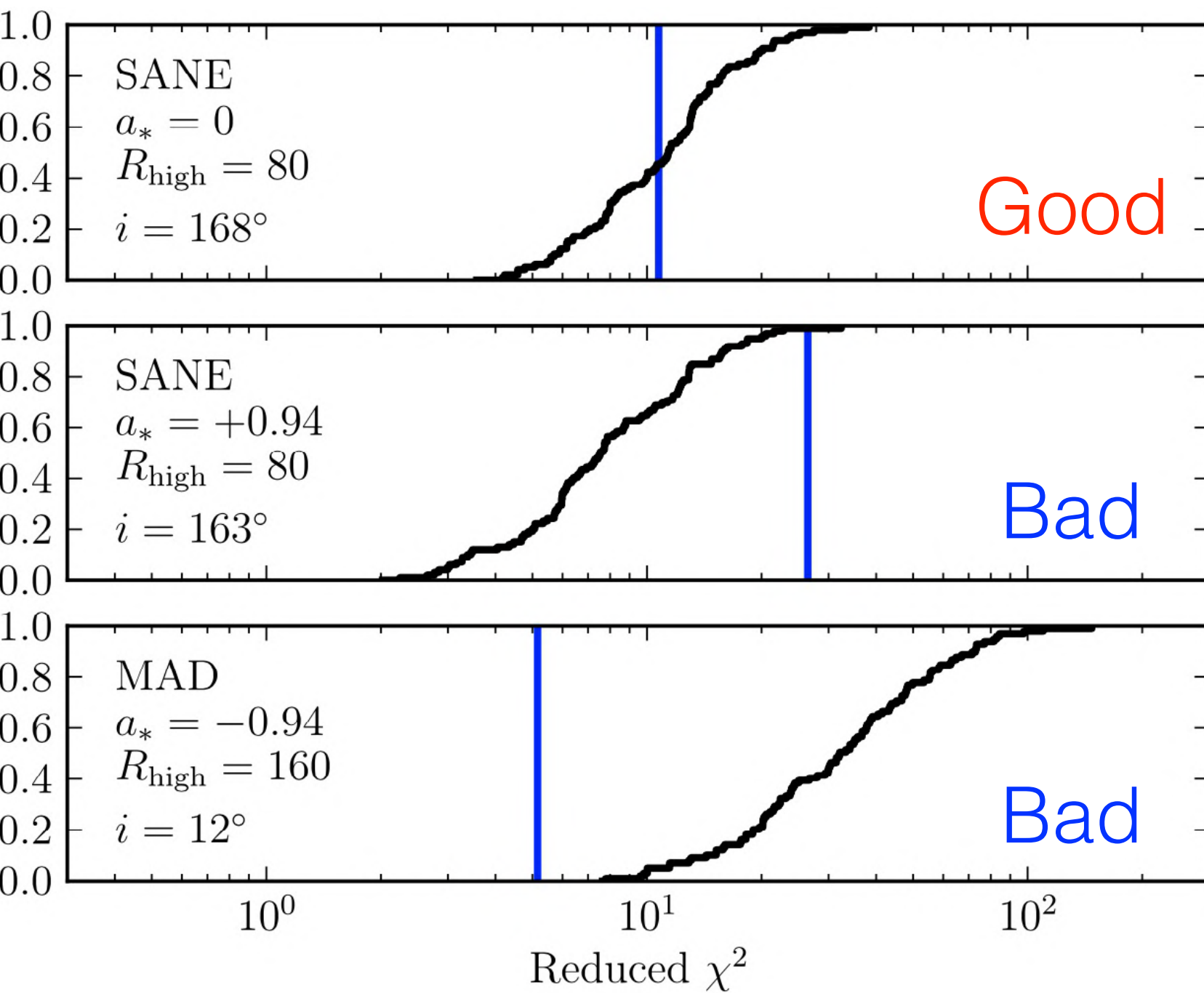
(Paper VI)



# Average Image Scoring

Themis-AIS procedure for scoring theoretical model

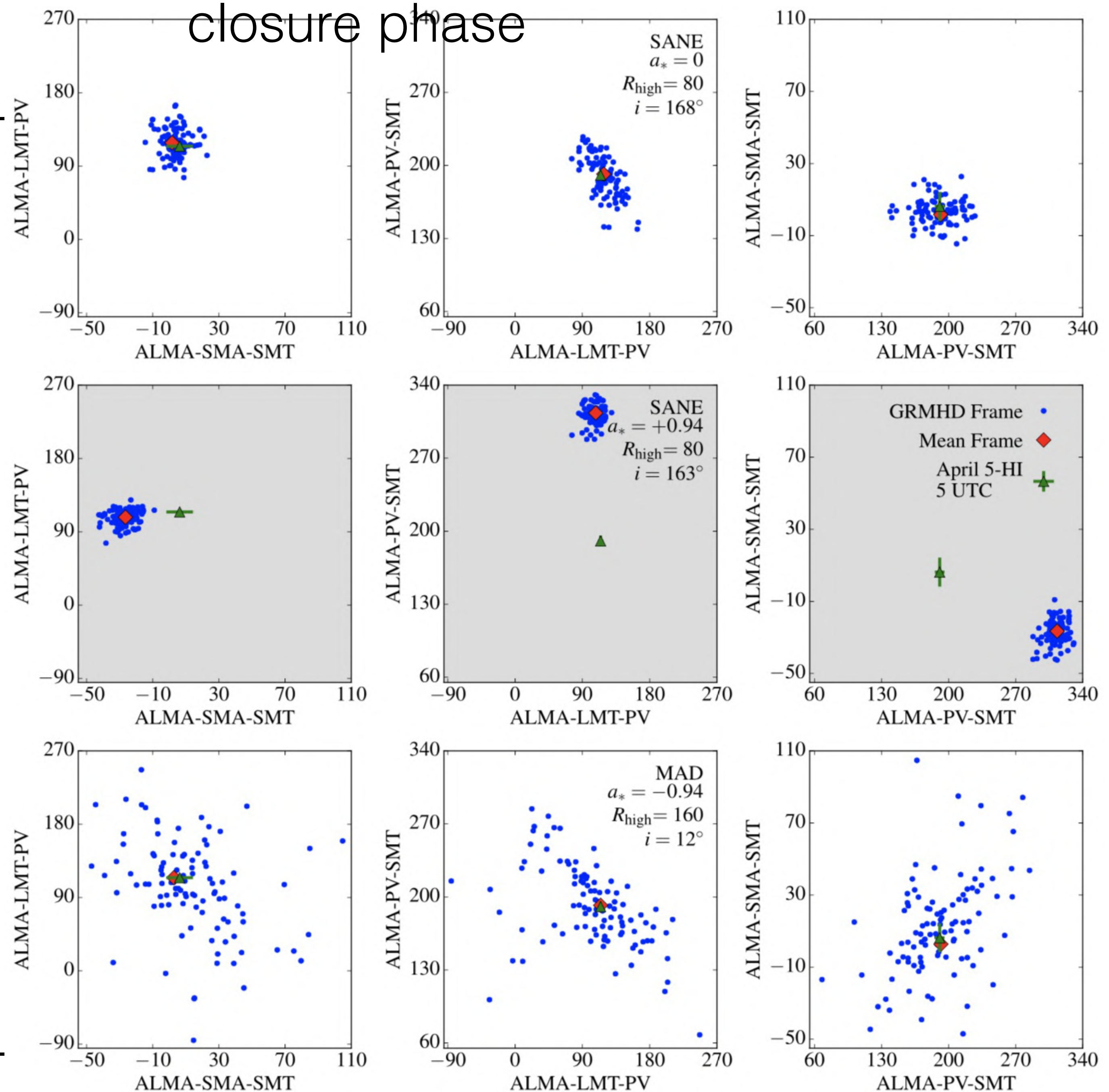
Good  
model



Bad  
model

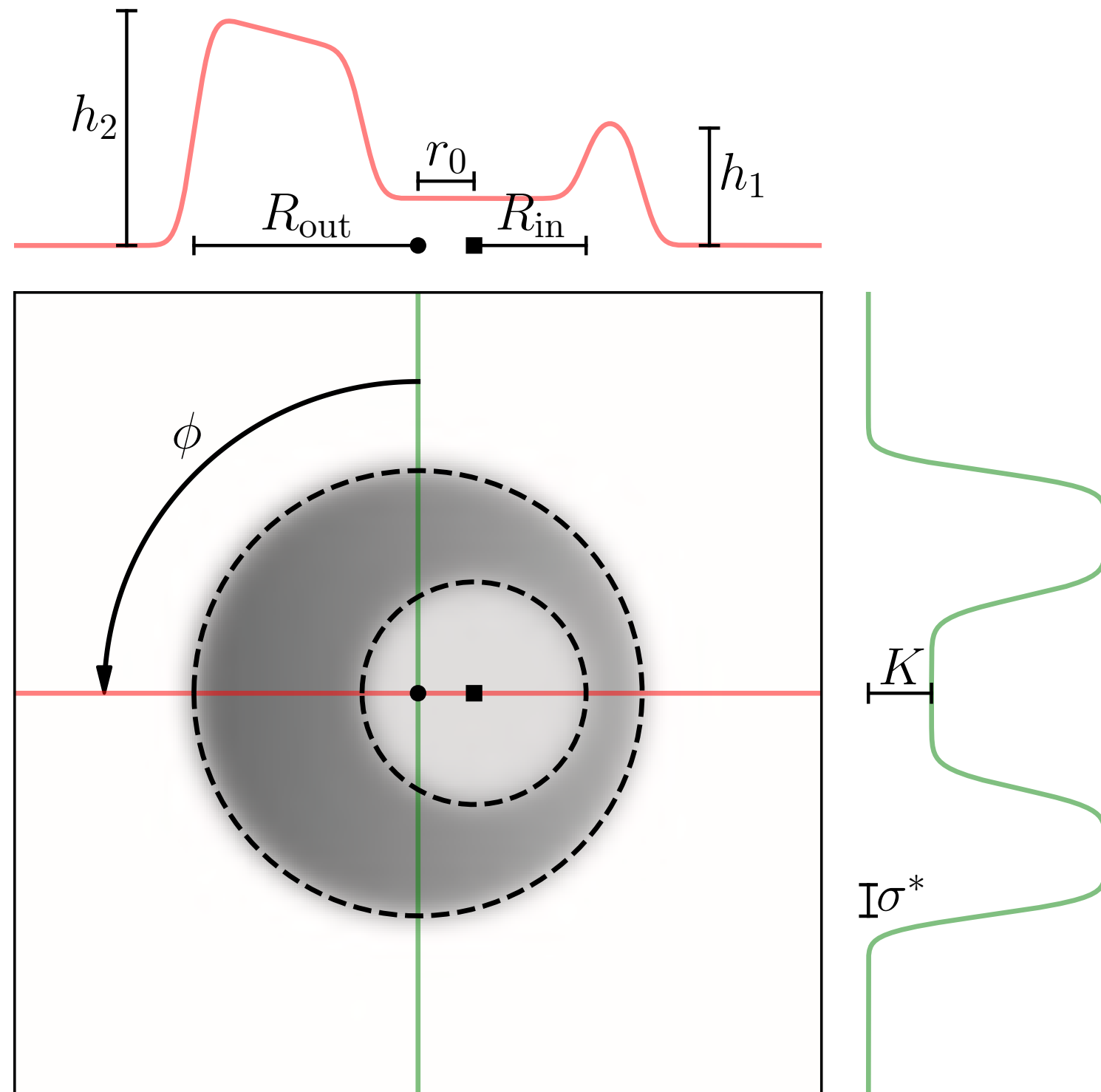
Bad  
model

closure phase



# Quantify M87 Source Properties

Fit geometrical crescent models



Fit GRMHD models

Single Snapshot Model

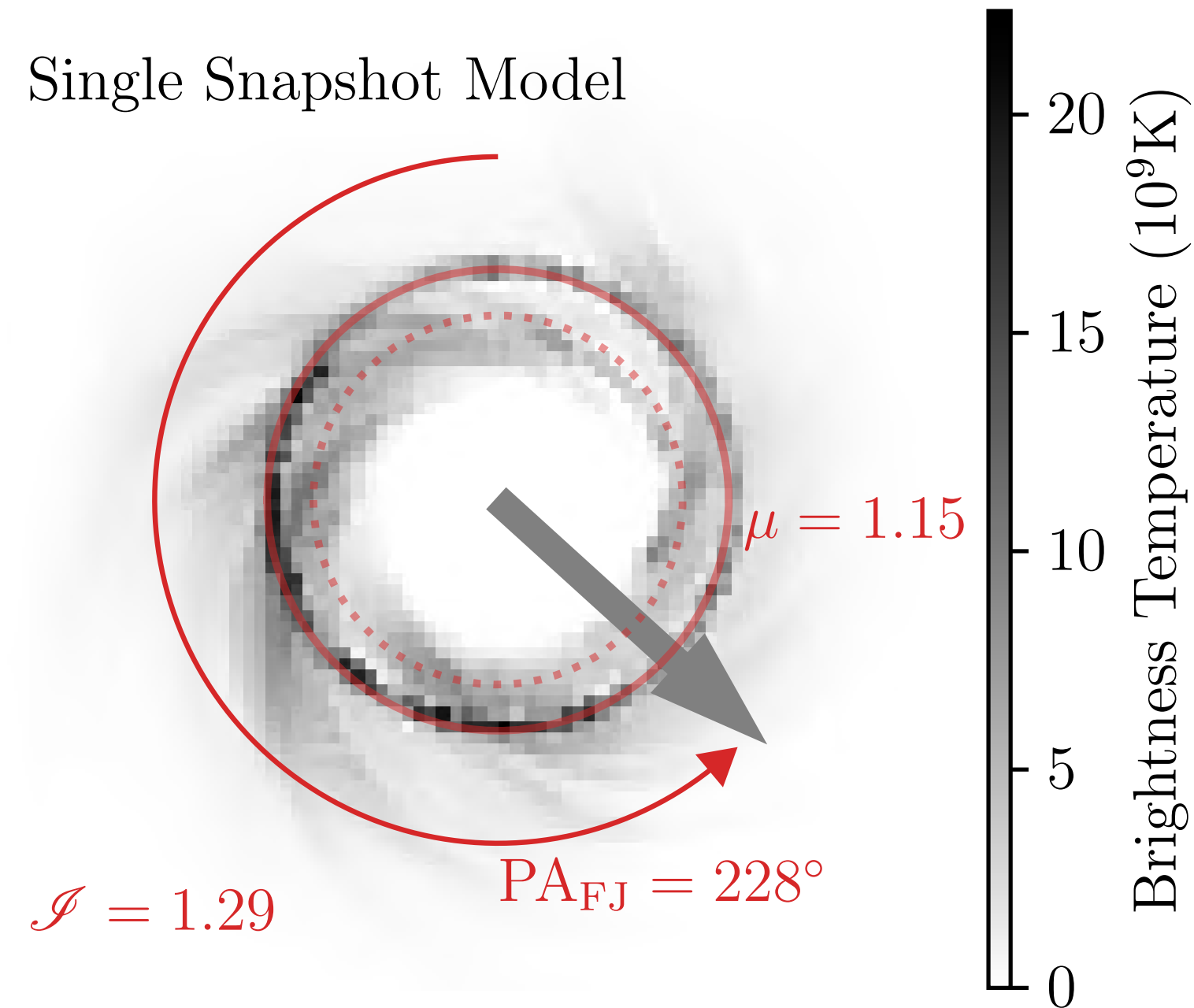
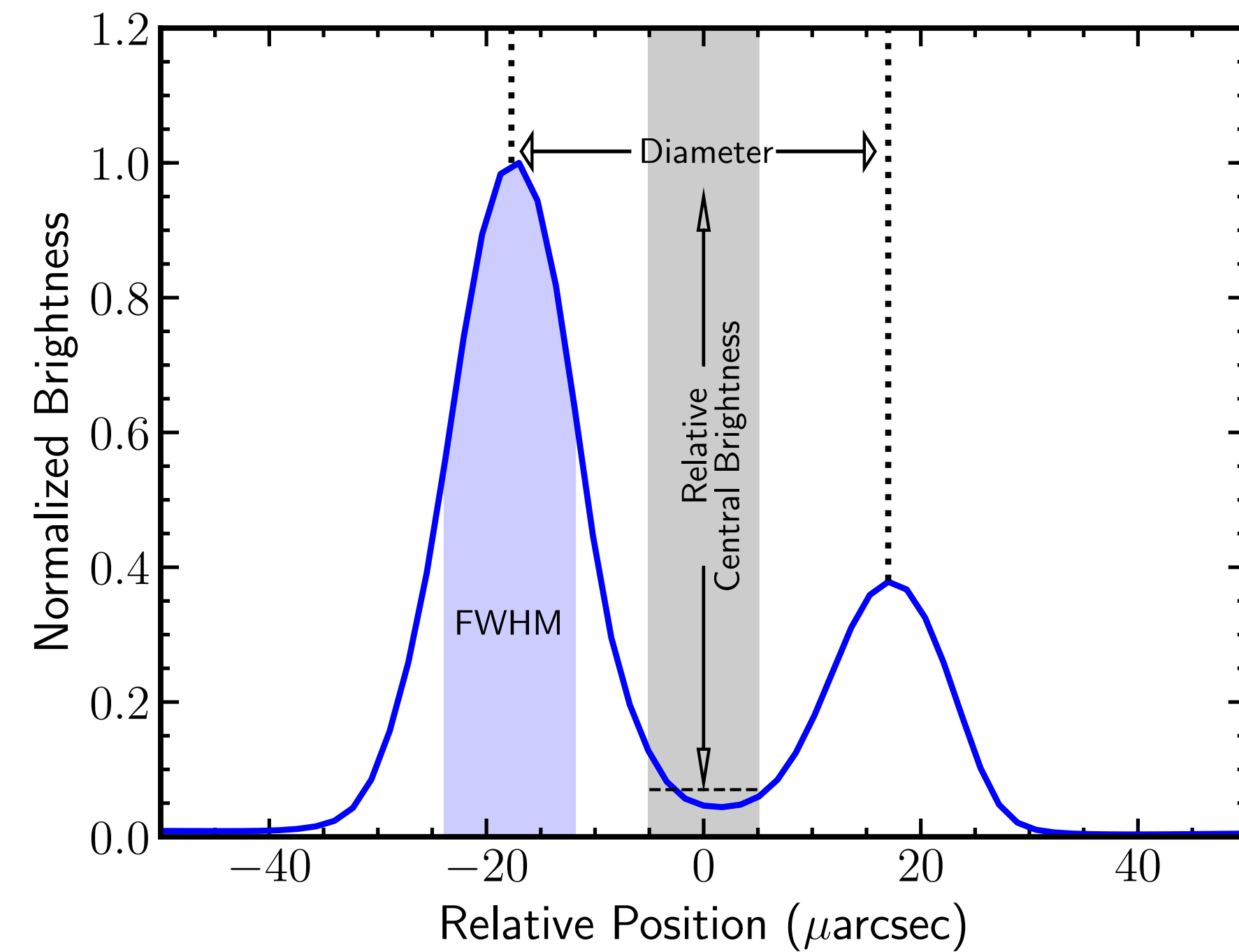


Image domain feature extraction





# Black Hole Mass Measurements

- $M = 6.5 \pm 0.7 \times 10^9 M_{\text{sun}}$   
(using  $D = 16.8 \pm 0.7$  Mpc)
- Three methods in excellent agreement
- Excellent agreement with stellar dynamics mass estimate (Gebhardt+2011)

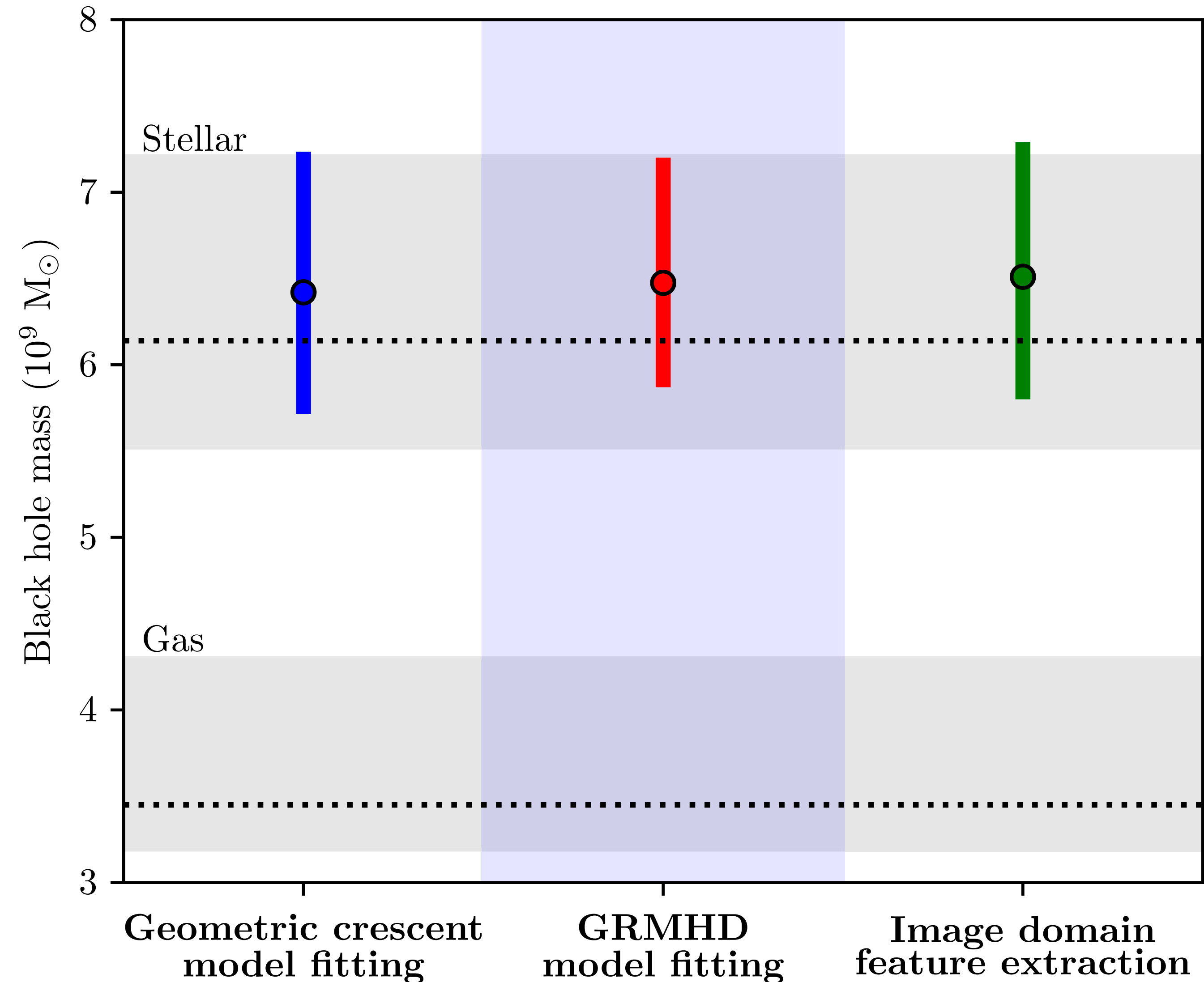


# Image Domain Feature Extraction

- Independent measurements of shadow diameter and width

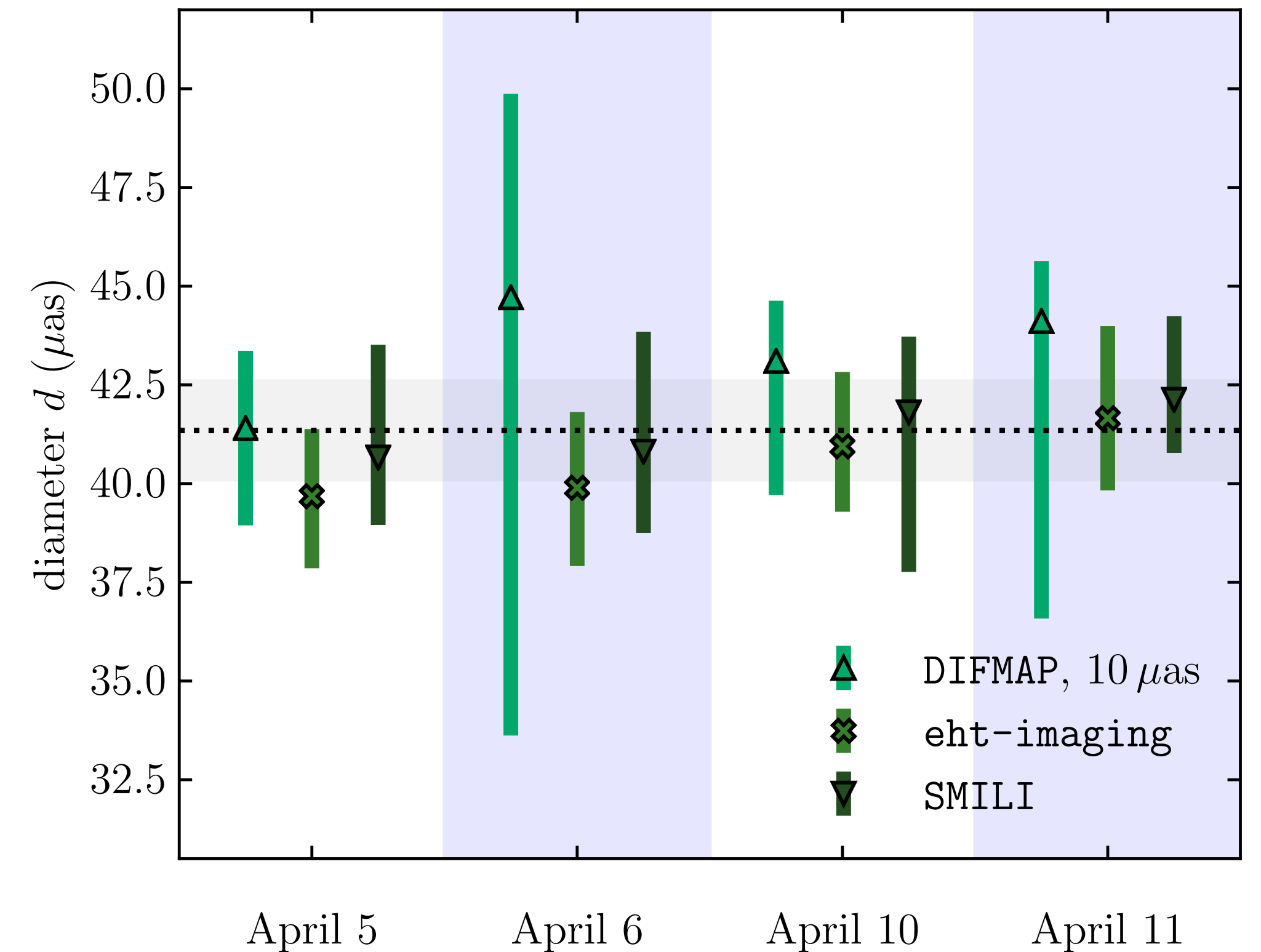
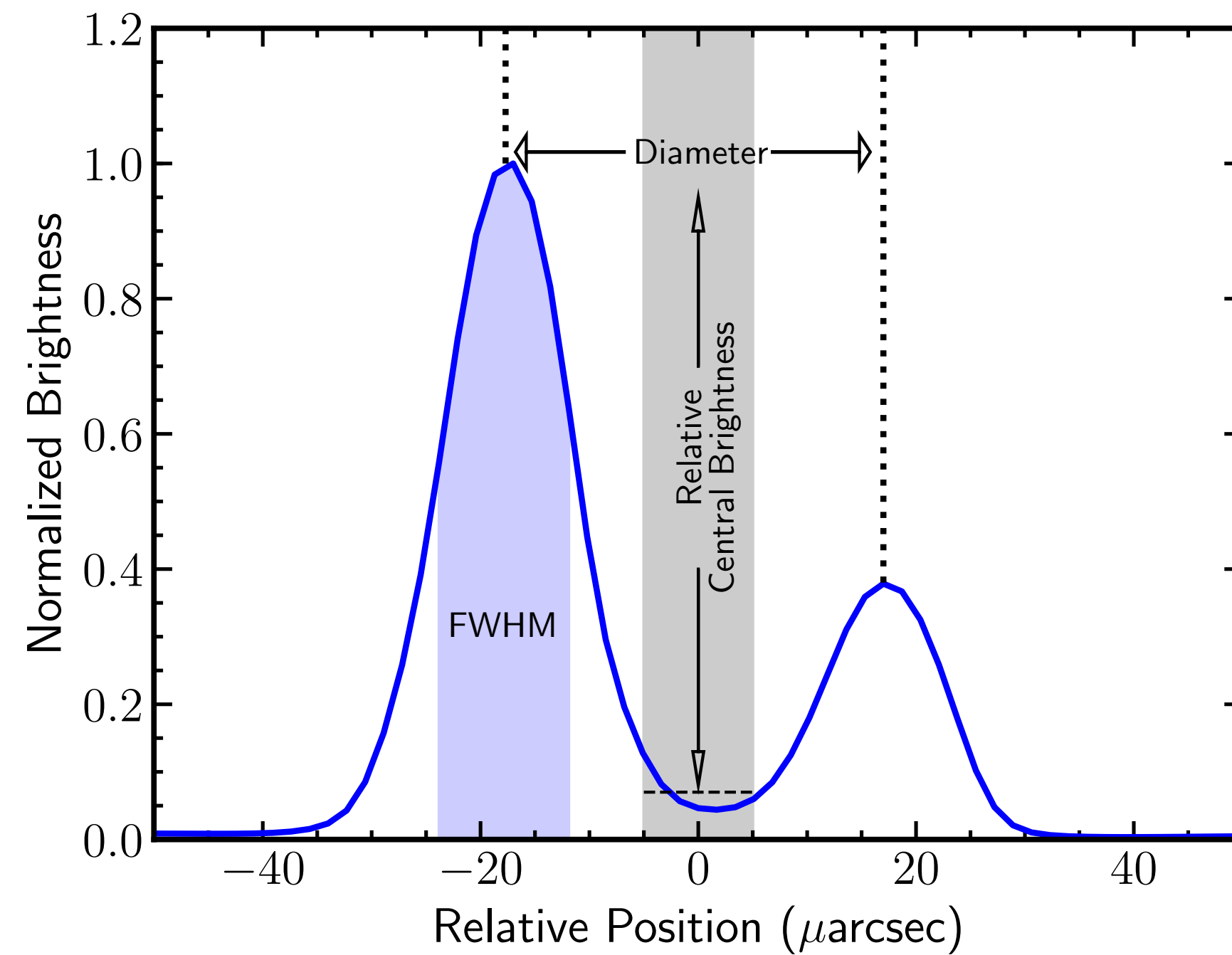
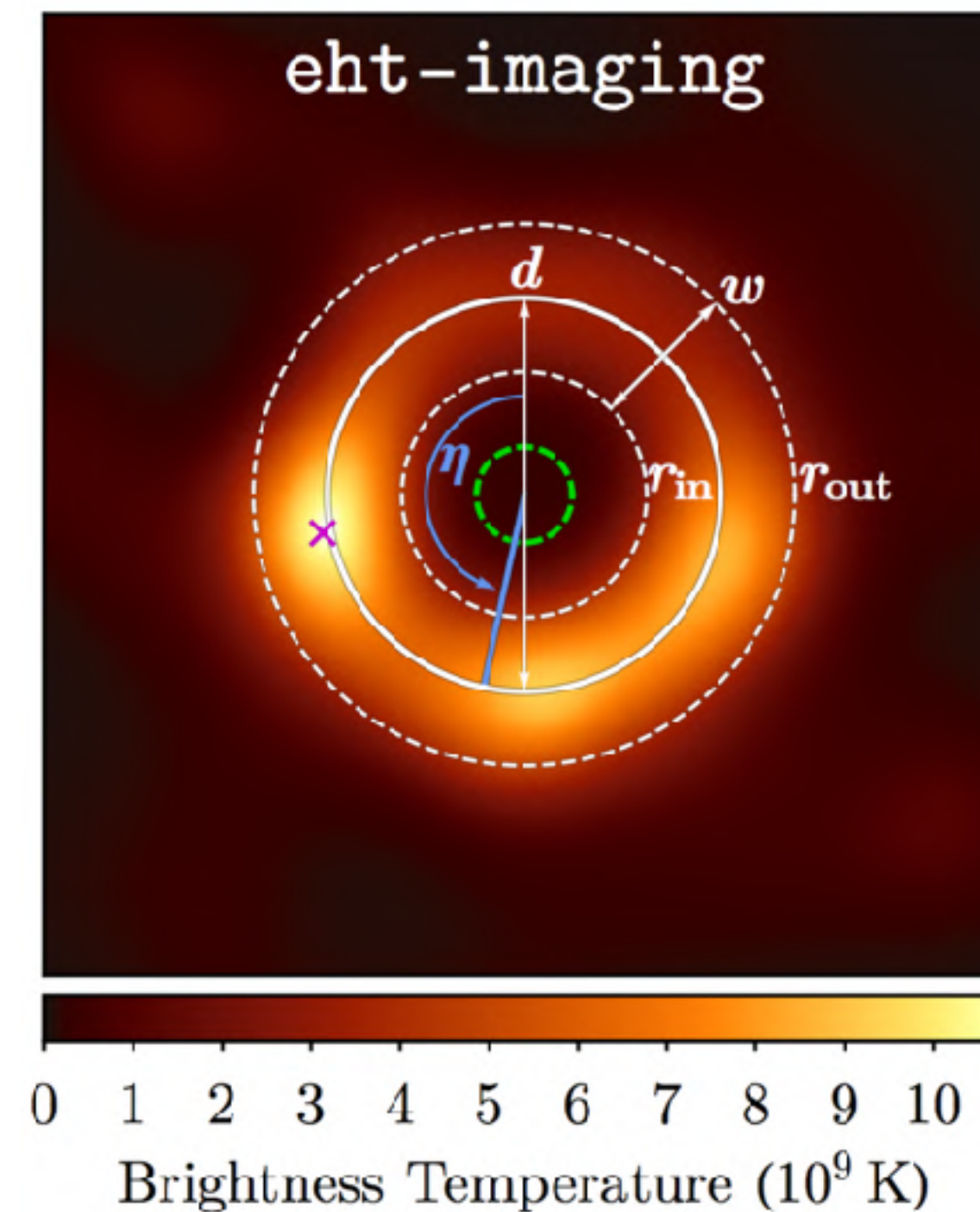




# Image Circularity

- At low inclination of M87, shadow shape should be extremely circular for all values of black hole spin (e.g. Chan+2013)
- From reconstructed images, we measure an emission region that is circular to within  $\sim 4:3$  in axis ratio
- Result is consistent with expectations from GRMHD models of M87
- Future: get to circularity of shadow and photon ring

